Universitat d'Alacant
Universidad de Alicante

DENITRIFICATION IN HALOARCHAEA: FROM GENES TO CLIMATE CHANGE

Javier Torregrosa Crespo

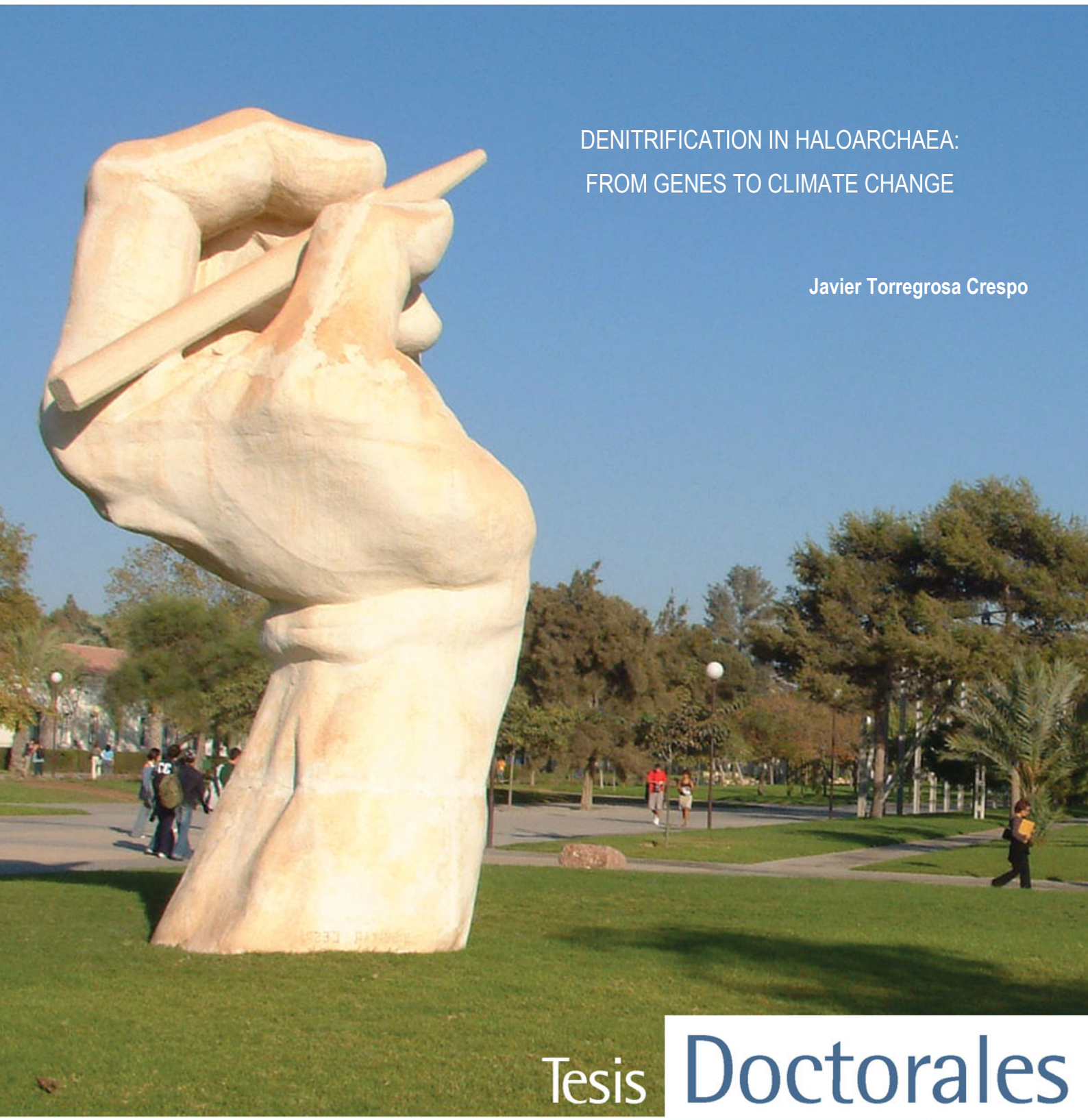

Tesis Doctorales

www.eltallerdigital.com

UNIVERSIDAD de ALICANTE

Universitat d'Alacant
Universidad de Alicante

DENITRIFICATION IN HALOARCHAEA: FROM GENES TO CLIMATE CHANGE

Javier Torregrosa Crespo

Tesis doctoral

Alicante, Septiembre 2019

DEPARTAMENTO DE AGROQUÍMICA Y BIOQUÍMICA

FACULTAD DE CIENCIAS

DENITRIFICATION IN HALOARCHAEA: FROM GENES TO CLIMATE CHANGE

JAVIER TORREGROSA CRESPO

Tesis presentada para aspirar al grado de

DOCTOR POR LA UNIVERSIDAD DE ALICANTE

MENCIÓN DE DOCTOR INTERNACIONAL

DOCTORADO EN BIOLOGÍA EXPERIMENTAL Y APLICADA

Dirigida por:

Dra. ROSA MARÍA MARTÍNEZ ESPINOSA

Dra. CARMEN PIRE GALIANA

La presente tesis doctoral ha sido financiada gracias a una subvención para la contratación de personal investigador de carácter predoctoral concedida por la Generalitat Valenciana y el Fondo Social Europeo (ACIF/2016/077). Así mismo, las dos estancias de investigación realizadas en la Norwegian University of Life Sciences (Ås, Noruega) han sido financiadas por la Escuela de Doctorado de la Universidad de Alicante, a través del programa de subvenciones para facilitar la obtención de la mención de Doctorado Internacional en el título de Doctor y por la European Molecular Biology Organization (EMBO) a través de su programa Short-term Fellowships (ASTF No 331-2016).

AGRADECIMIENTOS

AGRAÏMENTS

ACKNOWLEDGEMENTS

Com qui comença a construir una casa, pose la primera pedra del meu agraïment a la meua família. No tinc paraules per expressar l'enorme gratitud que sent per vosaltres. Gràcies. Vau deixar que fos qui sóc, vau sembrar en mi els valors amb els que ara em regeixo: el respecte, l'amor i la constància. Vaig caure, em vaig perdre, però vaig mirar cap amunt i allà estàveu. Gràcies mare pels teus sacrificis, pare per la teua visió generosa de la vida, al meu germà (Mimi) per tenir cura del seu "guellut", a la meva cunyada Vivian per portar a la nostra criatura, Ale: creix, sigues lliure i gaudeix. Al tito Manel i a Marcus, no deixeu d'agafar aquell tren per saltar de Barcelona a ací sempre que ens necessitem. Gràcies als que no hi són: us sent ben a prop, hui he aconseguit el que us vaig prometre.

Pasé mi infancia en mi pueblo, Novelda. De allí guardo grandes recuerdos, grandes amigos y personas que no olvido. Pero he de destacar a dos colegas: Carlos (sí, el guapo y alto) y Adri (no sé poner la voz grave aquí…). ¿Quién dijo que el botellón no nos llevaría lejos? ¿Y los sellos de oro? ¿Y el bakalao? ¿Quién? Hemos sobrevivido, ¡gracias cracks!

Empecé entonces la carrera de Biología. Aprendí muchas cosas de los libros, de las prácticas… bueno, no tantas… pero aprendí mucho más de un grupo de frikis por los que mereció la pena estudiar: Guille, Chechi, la meua Sapi, Gal·la, Jorge, Cuartos, Juan, Ruth, Nuria, Sandrita, Sareta, JuanCar y mi inestimable Sergio (tranquilo, luego te dedico unas líneas). Pasará el tiempo, el destino separará y unirá nuestras vidas, pero no dejéis que ese espíritu universitario que nos acompañó se esfume. Os quiero amigos.

Se cruzó por aquel entonces en mi vida un chaval de Benidorm. Ahora lo entiendo, me lo habían puesto en el camino para que fuera mi hermano de espíritu. El 12 de septiembre de 2012 la vida me dio un golpe y, a punto de caer, me recogiste. Dicen que en el mundo uno tiene un alma gemela, la mía no andaba lejos. A la tierra que ahora te acoge, Albacete, también le debo mucho: gracias a Vicen, un genio, un artista y una buena persona, a Pity y a Calvin (madre y hermana) y a Luismi. ¡Que viva Albacete… y su feria!

Ella no es de Albacete y su pueblo anda un poco difuso en la geografía, pero siempre ha estado ahí: Inma, mi nenica. Gracias por tu risa contagiosa, por llamarme (aunque yo no lo haga) y por traerme esas cositas de tu tienda que tanto me encantan. Te debo mucho.

Mi siguiente paso, el máster, me llevó a la ciudad de Madrid. Aquel año loco casi pierdo el hígado (sí, el máster era muy fácil), pero valió la pena: encontré a Freddyto, mi gorda. Amigo, ahora te casas y sé que te espera un futuro lleno de éxitos. Gósalo! No puedo marcharme de esta hermosa ciudad sin mi Diego: no he conocido persona en el mundo que se ría más veces por segundo… Bueno, no nos conocimos en Madrid capital, pero fue cerca, ¿no? Te quiero amigo, sigue sonriendo como lo haces.

Corría ya el 2013 cuando una oferta de trabajo me bajó para el sur: Sevilla. ¡Ofú! ¡Qué arte! Gracias a Noelia por abrirme las puertas de Abengoa, a Vero, a Pepe, a Maca (por su café normal), a Juanma… pero, sobre todo, gracias a tres personas muy especiales: a Luci, por ser la alegría de Sevilla, la vida no puede más que devolverte un poquito del arte que irradias; a Laurita, que siendo de Mallorca (con una elle muy intensa) es más sevillana que la Giralda y cómo no… a mi Porrita: hiciste que mi estancia en esa ciudad fuera más acogedora y reconoce que caíste a mis pies con mi disfraz de Vilma Picapiedra (Gorda Carva). La vida ya os sonríe con vuestros hijos… ¡habéis hecho tía a Carmen!

Ya, ya, ya voy… empecé esta tesis doctoral en el año 2014. Para entonces un chico perdido, sin saber si realmente quería dedicarse a esto. Para animarme estaba una de mis mentoras, Carmen Pire: gracias por ser mi primer referente científico. Ayudaste a un chico tímido e inseguro a salir del cascarón. Espero que te sientas ahora orgullosa.

En el labo recuerdo las risas de Anna y Vir, mis primeras compañeras y amigas. Ya no somos pingüinos, somo aguiluchos pero… ¡casi mejor así! Gracias por ayudarme, ya me he hecho mayor. Pero, sin duda, mi compañero de tesis, de risas, de chou business, de cenas de Layton, de vida doctoral es él… Elías. Con nuestro grito de guerra (Yuuu!) hemos sobrevivido a profesores infumables, compañeros menos fumables todavía y a diferentes tipos de alimañas que habitan las cavernas de la UA. Gracias mohón, me ayudaste cuando más lo necesitaba, eso se queda a fuego en el alma.

A los pipiolines nuevos (ahora entro en modo madre): Sandra, Vero y Gloria, mucha suerte, no desesperéis; Belencita, ánimo con esos CRISPR, todo va a salir bien (botracha); Eric y Mica, savia nueva en nuestro labo, dadle duro, sois fuertes; a mi Chemi: en ti veo mi reflejo… Chemi, trabaja,

exige y lucha, pero no pierdas ni un ápice del ánimo con el que comienzas (recuerdos a la Chemi). ¡Mucha suerte, os veo pronto en el Olimpo doctoral!

La vida suele ser más hermosa cuando sales del labo. A mí me acompañaban cuatro grandes personas: Jose Ángel, mi cuartos, siguen tus palabras grabadas en mi mente cuando me definiste como un amigo fiel. Es justo lo que pienso de ti; Sareta, gràcies per ser tan fàcil, tan lliure, tan de fotografiar les papallones vietnamites; a mi Marichocho… es que no sé qué decirte… qué te digo.. Chaíto?... Felicidades chao?... Cariña?... Mr Phu?... Mortimer? El que se queda catacrocker soy yo cada vez que te veo. Te amo. Finalmente, a mi querida Antonia (Sergio). Voy a poner aquí también que publicaste en Science, por si se borra del disco duro de la revista. En serio, eres un titán, un hombre fuerte, que mira de frente a la vida. Eres un AMIGO con todas las letras. Gracias siempre por estar ahí (al Skype también). Sois mis Mrs Phus amigos! Nos vemos en… Perú?

El sueldo durante la tesis no da para mucho… para poco… así que siempre hay que andar compartiendo piso. Para ello, os recomiendo a Miquel: collons, mira que pensava que eres un super homòfob chancli valencià… Segueix sent com eres amic, però apitxa una miqueta menys!

Acercándose la recta final de esta tesis doctoral, la vida me sorprendió con otro golpe. Uno en el que se oscurece todo y no dan ganas de nada. Me tenían otro regalo preparado: Calmaina. Apareció de la nada, me sacó de casa y me presentó a Calamardo. Entonces descubrí que yo era Patricio. Gracias trinitarios, gracias por ser personas de las que no abundan, habéis entrado en un rinconcito especial de mi corazón. No sólo eso, ambos dos me presentaron a Chuchi y Antonio (quede claro que él es menor que ella): qué pareja, qué vida, qué alegría. Juntos formamos los "Jueves Gastronómicos" (un poco de publicidad). Desde entonces, ¡el jueves es mi día favorito de la semana!

Doy gracias también por poder dedicarle un ratito de mi tiempo a mi otra pasión: el teatro. Gracias a Epidauro: Sergio, Paco Pando, Cristian, Fernando y Jose Vicente. Me abristeis las puertas de vuestra casa como uno más, eso no se olvida. Que sigamos en escena por muchos años, amigos. En especial, gracias a Paco Pando, mi cari, por soportar a Maxi… de verdad, gracias por confiar en mí. Y gracias a Cristian, mi segunda Antonia: sigue siendo quien eres, con menos whatsApps e inseguridades, pero quien eres, un tesoro.

I have to leave Spain for a moment, travel to Norway, because there are two people that I need to thank very much: thanks Linda, for hosting me in the lab and teaching me science... and thanks for believing that I could ride a horse... You are my third supervisor, this work would not have been possible without you.

Thanks to my Russian friend ... Pawel. Well, I thought you were Austrian and finally you were Polish. Thanks friend, for making me feel at home: "Life is life, life is good Javier". I think I can say it now: thanks for throwing up in the RNA lab (even if we lost that Chilean wine). Thanks friend!

Es hora de terminar y no podía olvidarme de una persona muy especial. Si a alguien le debo todo en esta etapa es a ella: no sólo enseña a medir nitratos, purificar proteínas y montar congresos (sí, ella es multitask) … a mí me ha ayudado a mucho más. A trabajar duro, a no desfallecer, a ver la luz cuando todo se había apagado, a confiar en mí mismo. Nos pusieron la zancadilla, nos cerraron las puertas y nos miraron por encima del hombro… no se dieron cuenta de nada, nos acababan de hacer más fuertes. Lo hemos logrado Rosa, no nos ha ido tan mal: "be focused, be positive and be honest", llevaré esta frase siempre en el alma.

Universitat d'Alacant
Universidad de Alicante

Gracias a todos.

Javi.

TABLE OF CONTENTS

SÍNTESIS

Antecedentes, hipótesis y objetivos.

La principal característica de los ambientes hipersalinos es la alta concentración de sales presente en sus aguas y suelos, considerablemente superior a la encontrada en el agua de mar (0,6 M o 3,5% (p/v)) (DasSarma et al., 2019). Estos ecosistemas naturales incluyen lagos, lagunas y estanques salados de superficie, depósitos salinos subsuperficiales, domos salinos submarinos o marismas (Oren, 2002; de la Haba et al., 2011; Andrei et al., 2012). Incluyen ejemplos bien conocidos como el Mar Muerto (Israel-Palestina y Jordania), el Lago Magadi (Kenia) o el Gran Lago Salado (EEUU). Otros ambientes hipersalinos han sido creados artificialmente como las balsas de precipitación usadas para producir sal, normalmente cerca del mar (DasSarma et al., 2019).

La biodiversidad de estos ambientes es mayor de la originalmente esperada, pero obviamente menor a la de los ecosistemas no salinos. En todos ellos, habitan organismos pertenecientes a los tres dominios de la vida, como *Artemia* (camarón), *Dunaliella* (alga unicelular) o *Salinibacter* (bacteria), pero cuando la concentración de sal excede del 16% (p/v), el grupo predominante de microorganismos es el de las haloarchaea (Andrei et al., 2012; Edbeid et al., 2016). Éstos, como clase dentro del dominio Archaea, son aerobios facultativos, heterótrofos/fotótrofos, caracterizados principalmente por ser halófilos obligados (DasSarma et al., 2019). Requieren altas concentraciones de sal para vivir, normalmente entre 1,5 y 4 M NaCl, que corresponde con 9-30% de sales (p/v) (Purdy et al., 2004).

En los ambientes hipersalinos, la respiración aeróbica llega a ser muy difícil porque la disponibilidad de oxígeno es muy baja debido a la presencia de altas concentraciones de sal: de hecho, a 35^{o}C, óptima temperatura para muchas haloarchaea, la solubilidad del O_2 es de 6,92

mg/L en agua destilada y cae hasta diez veces en ambientes hipersalinos (Rodríguez-Valera et al., 1985; Sherwood et al., 1991; Sherwood et al., 1992; Oren, 2013). Bajo estas condiciones, algunas haloarchaea son capaces de flotar a la interfase aire-agua, gracias a la producción de vesículas de gas (Oren, 2002). Estas estructuras incrementan la flotabilidad de las células y les permiten migrar verticalmente a regiones con mejores condiciones para sostener el crecimiento aeróbico o microaeróbico (Pfeifer, 2015). Sin embargo, esta estrategia no parece ser predominante entre las haloarchaea y, además, depende de factores medioambientales como la luz, la temperatura, la concentración de sal o la disponibilidad de O_2. De hecho, la producción de estas vesículas es inhibida en condiciones anaeróbicas (Hechler and Pfeifer, 2009). Por todo esto, los microorganismos se ven empujados a usar aceptores electrónicos alternativos. Tras la respiración de O_2, la desnitrificación es la ruta energéticamente más favorable (Zumft and Kroneck, 2006): el nitrato (NO_3^-) es secuencialmente reducido a nitrito (NO_2^-), óxido nítrico (NO), óxido nitroso (N_2O) y dinitrógeno (N_2) en una serie de cuatro reacciones catalizadas por las enzimas nitrato-(Nar), nitrito-(Nir), óxido nítrico-(Nor) y óxido nitroso-(Nos) reductasas. En las últimas décadas, debido a diversas actividades antropogénicas, las concentraciones de NO_3^- y NO_2^- en estos ecosistemas han ido incrementando, favoreciendo la desnitrificación (Martínez-Espinosa et al., 2011).

La habilidad para desnitrificar está ampliamente distribuida entre los procariotas, pero sólo ha sido estudiada en detalle en algunos organismos, principalmente bacterias mesófilas (Bakken et al., 2012; Liu et al., 2013; Bergaust et al., 2014; Borrero-de Acuña et al., 2016; Lycus et al., 2017; Olaya-Abril et al., 2018). Sin embargo, en el dominio Archaea, el conocimiento es escaso (Philippot, 2002; Yoshimatsu et al., 2002) y todavía menor en aquellos que viven en ambientes extremos, como las haloarchaea, porque sólo unos pocos géneros son capaces de crecer en condiciones de laboratorio y, de entre ellos, una minoría tiene la capacidad de desnitrificar.

En este sentido, el género *Haloferax* ha sido usado como modelo para estudiar la desnitrificación ya que algunos de sus miembros son las haloarchaea mejor conocidas en términos de ecología microbiana, bioquímica y biología molecular (Lledó et al., 2004; Martínez-Espinosa et al., 2007). En el momento en que comenzó esta tesis doctoral, el conocimiento sobre la desnitrificación en el género *Haloferax* se reducía a los siguientes hitos: en términos de análisis *in silico*, sólo los contextos génicos de *nar* (Lledó et al., 2004; Martínez-Espinosa et al., 2007) y *nir* (Esclapez et al., 2013) habían sido estudiados; a nivel bioquímico, la purificación de Nar en *H. mediterranei* (Lledó et al., 2004) y de Nar y Nir en *H. denitrificans* (Hochstein y Lang, 1991; Inatomi y Hochstein, 1996) se habían conseguido, mientras que ninguna de las otras dos enzimas (Nor y Nos) habían sido purificadas; a nivel fisiológico, ninguna especie había sido caracterizada y sólo unos pocos estudios habían medido la emisión de N_2O por parte de *H. mediterranei* usando NO_3^- como aceptor electrónico (Lledó et al., 2004; Bonete et al., 2008) y la producción de N_2O y N_2 por *H. denitrificans* (Tindall et al., 1989); así mismo, no había ningún estudio sobre la expresión de los genes involucrados en esta ruta metabólica o alguna aproximación desde otras disciplinas como la proteómica.

Con toda la información previa, la hipótesis de la presente tesis doctoral es que hay algunas especies de haloarchaea con la habilidad para reducir NO_3^-/NO_2^- a N_2 debido a que tienen la maquinaria de la desnitrificación completa y activa (desnitrificantes completos), mientras otras, si la ruta está truncada en algún punto, podrían generar como productos gases nitrogenados como NO y N_2O (desnitrificantes incompletos). El primer grupo podría actuar como sumidero de gases nitrogenados y N-aniones tóxicos en ambientes hipersalinos, mientras el segundo podría ser una fuente de gases de efecto invernadero, contribuyendo al calentamiento global y el cambio climático. De hecho, hoy en día, las actividades antropogénicas están favoreciendo la acumulación de fuentes de nitrógeno como NO_3^-, NO_2^- y NH_4^+ en los medios naturales (incluyendo los salinos e hipersalinos).

En este sentido, la tesis doctoral realizada implica un avance multidisciplinar en el conocimiento de la desnitrificación en el género *Haloferax*, sirviendo como modelo para elucidar las características de esta ruta respiratoria en ambientes extremos como los ecosistemas hipersalinos. Los objetivos de este trabajo de investigación son:

1. Revisar el conocimiento de las principales rutas respiratorias anaeróbicas en el género *Haloferax*, prestando especial atención a la desnitrificación, realizando un análisis *in silico* de la organización de las agrupaciones génicas relacionadas con ella en diferentes especies.
2. Analizar genomas completos e incompletos (borradores) de haloarchaea para identificar los genes que codifican las óxido nítrico reductasas y el su organización en el contexto génico.
3. Describir el perfil fenotípico de la desnitrificación en *H. mediterranei, H. denitrificans* y *H. volcanii* y su relación con la emisión de gases nitrogenados.
4. Describir el perfil fenotípico de la desnitrificación en *H. mediterranei* en un amplio rango de condiciones de cultivo, como diferentes concentraciones de NO_3^-, NO_2^- y valores de pH. Realización de un análisis transcripcional de los principales genes involucrados en la desnitrificación en *H. mediterranei* (*narG, nirK, norZ* y *nosZ*) acoplado a la medida en tiempo real de todos los intermediarios (NO_2^-, NO, N_2O y N_2).
5. Identificar, usando una aproximación proteómica, los componentes de la maquinaria de la desnitrificación en *H. mediterranei*: no sólo las N-reductasas, sino también otras proteínas relacionadas con el flujo de electrones y el mantenimiento de la fuerza protón motriz (algunas no descritas hasta ahora a nivel proteico).

Trabajos presentados.

Los trabajos presentados en la tesis doctoral se describen a continuación:

TRABAJOS PUBLICADOS

Capítulo 1. Metabolismo anaeróbico en el género *Haloferax*: la desnitrificación como caso de estudio.

Este capítulo repasa las características generales del género *Haloferax* y las principales rutas respiratorias anaeróbicas descritas en él, especialmente la desnitrificación. Con respecto a ésta, describe las cuatro metaloenzimas involucradas en el proceso, la organización de sus genes y las potenciales aplicaciones biotecnológicas que el metabolismo anaeróbico de las haloarchaea puede ofrecer.

Capítulo 2. El análisis de múltiples genomas de haloarchaea sugiere que la óxido nítrico reductasa respiratoria dependiente de quinona es una importante fuente de óxido nitroso en ambientes hipersalinos.

El capítulo describe un extenso análisis interespecífico de genomas de haloarqueas completos e incompletos con el fin de identificar los genes que codifican la óxido nítrico reductasa y la organización de su contexto genético. Así mismo, se presenta un modelo bioinformático de la Nor de *H. mediterranei*.

Capítulo 3. Las haloarchaea desnitrificantes del género *Haloferax* muestran fenotipos respiratorios divergentes, con implicaciones en la emisión de gases nitrogenados.

Este es el primer estudio sobre la caracterización fisiológica de la desnitrificación en haloarchaea. Tres de las especies mejor conocidas pertenecientes del género *Haloferax* (*H. mediterranei, H. denitrificans* y *H. volcanii*) son caracterizadas con respecto a su habilidad para desnitrificar. Se usan diferentes concentraciones iniciales de O_2 y de aceptores electrónicos alternativos (NO_3^-/NO_2^-) para definir el fenotipo desnitrificante, midiendo la producción de NO_2^- y la emisión de gases nitrogenados en tiempo real.

Capítulo 4. Haloarchaea desnitrificantes: fuentes y sumideros de gases nitrogenados.

Se trata de una revisión sobre el rol ecológico de las haloarchaea como fuentes o sumideros de gases nitrogenados dependiendo de si son especies desnitrificantes completas o incompletas. Se da una dimensión global de este concepto, ofreciendo información de la extensión de los ambientes semiáridos/áridos y salinos/hipersalinos donde estos microorganismos viven. Durante las últimas décadas, estos ecosistemas han incrementado en extensión y prevalencia debido a procesos de desertización favorecidos por la acción humana y el cambio climático.

TRABAJOS NO PUBLICADOS

Anexo 1. *Haloferax mediterranei,* una archaea modelo para la desnitrificación en ambientes salinos, caracterizada a través de un análisis fenotípico y transcripcional integrado.

Este trabajo profundiza en el conocimiento de la fisiología de la desnitrificación en *H. mediterranei*, estudiando su capacidad para tolerar/reducir una amplia concentración de NO_3^- /NO_2^- y diferentes valores de pH. Así mismo, se presenta el primer análisis transcripcional de los principales genes implicados en la desnitrificación (*narG, nirK, norZ* y *nosZ*) en el dominio

Archaea, combinado con una cinética detallada de los gases nitrogenados emitidos. Finalmente, la capacidad de *H. mediterranei* de actuar como sumidero de N_2O es fisiológicamente probada.

Anexo 2. Explorando la maquinaria molecular de la desnitrificación en *H. mediterranei* a través de la proteómica.

Este trabajo establece un protocolo integrado para la identificación de proteínas implicadas en esta ruta respiratoria en *H. mediterranei*. Está basado en la generación de micelas lipídicas y su subsecuente enriquecimiento a través del uso de diferentes etapas cromatográficas. Evita el uso de técnicas como el *cross-linking*, en la cual se generan interacciones artificiales entre proteínas. El protocolo pretende permitir la descripción de proteínas involucradas en la desnitrificación a todos los niveles: las N-reductasas, proteínas implicadas en el flujo electónico o en la generación de fuerza protón motriz. Algunas de ellas nunca habían sido descritas a nivel proteico hasta ahora.

Principales resultados, discusión y conclusiones.

El conocimiento sobre la desnitrificación en el género *Haloferax* estaba restringido, hasta el momento, a la caracterización bioquímica de algunas de las enzimas en unas pocas especies. Ningún trabajo sobre los genes que las codifican (excepto *nar* y *nir* en *H. mediterranei* – Lledó et al., 2004; Esclapez et al., 2013) había sido llevado a cabo. Por ello, el estudio sobre la organización de los conjuntos de genes involucrados en la desnitrificación fue el primer paso que debía ser dado.

En este sentido, los primeros resultados obtenidos mostraron que la organización del conjunto génico de *nar* fue casi idéntido en las siete especies comparadas. Principalmente, éste está constituido por genes que codifican la subunidad catalítica y la de transferencia electrónica de

Nar (*narG* y *narH,* respectivamente), un gen (*mobA*) relacionado con la síntesis del cofactor MOCO, genes que codifican proteínas relacionadas con la transferencia electrónica (*narB* y *narC*) y un gen que codifica una chaperona (*narJ*).

En segundo lugar, los genes que codifican la nitrito y la óxido nítrico reductasa (*nirK* y *norZ/norBC)* fueron localizados muy cerca uno del otro por lo que probablemente constituyan el mismo conjunto génico. En él, se identificaron también genes que codifican proteínas que podrían actuar como transportadores electrónicos durante la reducción de NO_2^- y/o NO como *hyc,* que codifica una halocianina. Las halocianinas son pequeñas proteínas azules de cobre que sirven como transportadores electrónicos.

Finalmente, la óxido nitroso reductasa también estuvo organizada en un conjunto génico. En este caso, sólo fue posible realizar el análisis *in silico* de tres especies, ya que en el resto fue imposible identificar genes que codificaran no sólo la Nos sino cualquier otra de sus proteínas accesorias. En este conjunto, pudimos identifiar: *nosL*, un gen que codifica una proteína de cobre Cu(I) que podría estar implicada en la formación de los centros de cobre de Nos; *nosY,* que codifica un transportador tipo ABC; *nosZ*, el gen de la óxido nitroso reductasa; otros genes implicados en la transferencia electrónica como *pcy*, cuyo producto parece ser una plastocianina que podría actuar como donadora electrónica de Nos.

Entre todos los genes principales que codifican las enzimas de la desnitrificación, el que codifica Nor fue de especial interés, que en la mayoría de haloarchaea estaba anotado como *norB*. Esta nomenclatura está normalmente reservada para genes que codifican la subunidad NorB de las scNor bacterianas (Nor de cadena corta), que consisten en dos monómeros (NorB y NorC). Sin embargo, una detallada inspección de las secuencias *norB* en los genomas de haloarchaea ofreció dudas sobre su anotación (por ejemplo, debido a la longitud de sus secuencias nucleotídicas).

Por ello, un estudio bioinformático extenso fue llevado a cabo sobre las Nor en haloarchaea, que reveló que la versión de esta enzima que predomina en este grupo de microorganismos es la óxido nítrico reductasa dependiente de quinona, conocida como qNor (o Nor de cadena larga – lcNor) codificada por el gen *norZ*. Se concluyó, por tanto, que la Nor de haloarchaea no es de tipo cNor (scNor). La evidencia fue demostrada usando la Nor respiratoria de *H. mediterranei* como modelo para el alineamiento con los genomas de 141 especies de haloarchaea. Aunque este gen está ampliamente distribuido en haloarchaea, la organización de las ORFs de su entorno génico varió considerablemente entre especies. De hecho, hubo sólo una característica comunes a todos los estudiados: la proximidad a *norZ* de *nirK* (nitrito reductasa) y *hyc* (halocianina periplásmica). La alta variabilidad observada en estas regiones génicas, junto con la presencia de algunos genes cerca de *norZ* que codifican XerD (proteína implicada en procesos de recombinación), podría indicar una reciente adquisición de *norZ* por las haloarchaea a través de eventos de transferencia horizontal de genes y recombinación. Aunque no está claro por qué las haloarchaea expresan qNor más que cNor, podría haber dos importantes implicaciones bioenergéticas en este sentido: por una parte, *norZ* produce una proteína más sencilla comparada con la expresada por el gen *norB*, que implica la formación y maduración de un complejo NorBC; por otra parte, aunque qNor no es electrogénica (Salomonsson et al., 2012), esta limitación podría ser subsanada por las haloarchaea mediante la expresión de una pNar que conserva energía (Martínez-Espinosa et al., 2007).

Todos estos resultados obtenidos mediante la bioinformática demostraron la capacidad para desnitrificar (parcial o total) de numerosos miembros del género *Haloferax*. Sin embargo, fue necesario dar un paso más para conocer la implicación real de estos microorganismos en la reducción de N oxianiones y la emisión de gases nitrogenados. Por esta razón, una serie de estudios fisiológicos fueron llevados a cabo, en los cuales el perfil fenotípico de tres especies de haloarchaea (*H. mediterranei, H. denitrificans* y *H. volcanii*) fue definido bajo condiciones desnitrificantes.

Entre ellas, *H. mediterranei* fue capaz de reducir todo el NO_3^-/NO_2^- disponible a N_2 en las condiciones definidas como estándar (5 mM KNO_3 o 1 mM KNO_2 con 1% O_2 (v/v)), con una mínima y temporal acumulación de los intermediarios (NO_2^-, NO, N_2O). Mostró, además, una rápida y efectiva transición a la desnitrificación tras el consumo de O_2, sin un aparente retraso o caída en el flujo electrónico total hacia los aceptores terminales. *H. mediterranei* sólo tuvo dificultades para desnitrificar cuando la concentración inicial de O_2 fue aproximadamente de O%, donde sólo el 50% de los cultivos pudo consumir prácticamente todo el NO_3^- disponible y ninguno de ellos fue capaz de desnitrificar cuando el NO_2^- fue usado como aceptor electrónico inicial.

Por su parte, *H. denitrificans* mostró un fenotipo desnitrificante variable: en el caso del NO_3^-, sólo una pequeña fracción de los cultivos (1/3) fue capaz de desnitrificar, siendo una mezcla de N_2O y N_2 el producto final; en el caso del NO_2^-, el exceso de NO acumulado durante la incubación pareció producir un cese general de la respiración. La ineficiencia en la desnitrificación de *H. denitrificans* fue evidente al observar la transición del flujo electrónico entre las fases aeróbica y anaeróbica, con un aparente período de latencia de unas doce horas aproximadamente. Esto podría indicar una lenta y gradual expresión de Nar en la población celular, que retrasa el inicio de la desnitrificación. Si hay una inducción débil inicial del aparato de la desnitrificación a través de sensores de O_2, esto explicaría que la probabilidad de producir N_2 como único producto final incrementa cuando la concentración inicial de O_2 lo hace. Por otra parte, cuando el NO_2^- se usó como aceptor terminal electrónico alternativo, hubo un rápido incremento de NO, llegando a concentraciones micromolares, que produjo un cese general de la respiración con independencia de la concentración inicial de O_2.

Finalmente, *H. volcanii* fue incapaz de reducir NO_3^- a NO_2^- y, cuando se usó este último como aceptor electrónico, hubo un incremento de NO y N_2O hasta concentraciones micromolares, que provocó que la respiración se detuviera. Aunque *H. volcanii* ha sido descrita como desnitrificante

(Hattori et al., 2016), en estos experimentos no pudo reducir NO_3^- a NO_2^-. Si bien es cierto que las aproximaciones experimentales usadas diferían entre los estudios (por ejemplo, con respecto a las concentraciones de NO_3^- o las condiciones de agitación), las discrepancias fenotípicas fueron principalmente debidas a las diferencias entre las cepas utilizadas.

Por lo tanto, *H. mediterranei* mostró las mejores características como desnitrificante entre las especies estudiadas, ya que redujo todo el NO_3^-/NO_2^- disponible a N_2 a partir de una concentración inicial de O_2 de 1% (v/v), con una baja y temporal acumulación de gases nitrogenados. Además, esta especie mostró ratios de crecimiento aeróbico:anaeróbico similares a los de organismos modelo en la desnitrificación como *Paracoccus denitrificans* (Bergaust et al., 2010) u otros desnitrificantes recientemente aislados de muestras de suelo (Rocco et al., 2017). Con todos estos datos, *H. mediterranei* fue presentada como un modelo eficiente y reproducible para el estudio de la desnitrificación en ambientes hipersalinos y como candidata para su estudio en futuras aplicaciones en biorremediación.

La evaluación del perfil fenotípico de las haloarchaea estudiadas es un claro ejemplo de que debemos ser cuidadosos cuando describimos la capacidad desnitrificante de los microorganismos. La génetica, la filogenia y la bioinformática son pobres predictores de la tendencia de un organismo desnitrificante a liberar N óxidos (Lycus et al., 2017; Rocco et al., 2017). Para saber si un organismo puede actuar como fuente o sumidero de intermediarios tóxicos (como NO y N_2O), es necesario llevar a cabo análisis fenotípicos detallados como el aquí presentado: *H. volcanii* era potencialmente un desnitrificante capaz de reducir NO_3^- (en su genoma está anotado un gen que codifica una nitrato reductasa respiratoria) pero su incapacidad fue demostrada, al menos en las condiciones estudiadas; *H. mediterranei* y *H. denitrificans* poseen todos los genes para la expresión de las metaloenzimas implicadas en la desnitrificación, pero su fenotipo fue claramente diferente, siendo la primera una especie que

podría actuar como sumidero de N-oxianiones, mientras la segunda emitió cantidades significativas de gases nitrogenados a la atmósfera de los cultivos.

Hoy en día, no existen datos precisos sobre la prevalencia y el área total de los ambientes salinos/hipersalinos. Como ejemplo, las mejores estimaciones realizadas sobre el área de marismas salinas van desde 2,2 a 40 Mha (Pendleton et al., 2012). Considerando que estos ambientes no son los ecosistemas hipersalinos predominantes, su extensión debe ser significativamente mayor. De hecho, las zonas salinas e hipersalinas son concomitantes con las áridas y semiáridas, que cubren alrededor del 41% de la superficie de la Tierra (Delgado-Baquerizo et al., 2013) y que están viéndose incrementadas debido a los efectos del cambio climático. Por lo tanto, el rol de las haloarchaea como fuentes o sumideros de gases nitrogenados debería ser entendido desde una perspectiva global.

Considerando todos estos hechos, y una vez demostrada la capacidad desnitrificante de *H. mediterranei* por encima de las otras especies, ésta fue seleccionada para llevar a cabo estudios más detallados sobre su fisiología, así como otros centrados en el análisis transcripcional de los principales genes implicados en la desnitrificación: *narG, nirK, norZ* y *nosZ*.

H. mediterranei fue expuesta a diferentes concentraciones iniciales de NO_3^- (en un rango de 2 mM a 2 M KNO_3) y NO_2^- (entre 1 y 40 mM KNO_2) con 1% de O_2 inicial (v/v), midiendo la producción de todos los intermediarios en tiempo real (NO_2^-, NO, N_2O y N_2). La adición de altas cantidades de NO_3^- debería permitir múltiples generaciones de crecimiento exponencial anaeróbico, proporcionalmente a la concentración inicial de NO_3^-. Sin embargo, con independencia de la cantidad de NO_3^- disponible, *H. mediterranei* fue incapaz de mantener el crecimiento exponencial por desnitrificación por encima de 1,5 a 2 generaciones. Esto principalmente reflejaría la falta de síntesis *de novo* de las enzimas de la desnitrificación y su consecuente dilución por el número de células durante las siguientes divisiones celulares. Parece que, en caso de *H. mediterranei*, las condiciones microóxicas fueron requeridas para la síntesis

de novo de las N reductasas ya que en cultivos crecidos en las mismas condiciones (5 mM KNO_3) pero con 7% de O_2 inicial (v/v), no se observó la prematura disminución en la velocidad del crecimiento exponencial y el O_2 permaneció en concentraciones cercanas a 5 µM cuando los N óxidos se agotaron.

En caso de NO_2^-, este fenómeno también ocurrió cuando *H. mediterranei* fue incubada con 5 mM KNO_2: el crecimiento exponencial cesó prematuramente mientras más de la mitad del NO_2^- inicial permanecía en el medio de cultivo. A menores concentraciones de KNO_2 (1 y 2 mM), *H. mediterranei* mostró una buena capacidad desnitrificante, siendo capaz de reducir todo el NO_2^- disponible a N_2 con una baja y temporal acumulación de NO y N_2O. Para las mayores concentraciones de KNO_2 probadas (10 y 40 mM), el exceso de NO provocó el cese del funcionamiento de la maquinaria de la desnitrificación.

En los experimentos, también se evaluó la habilidad de respirar NO_3^-/NO_2^- por parte de *H. mediterranei* a diferentes valores de pH: entre 7,3 (óptimo para este microorganismo) y 5,7. Con independencia del N oxianion usado, por debajo de 6,5 las células no fueron capaces de comenzar la desnitrificación. En el caso del NO_3^-, hubo una aparente inhibición generalizada de todas las N reductasas. Esto contrasta con otros desnitrificantes, como *P. denitrificans*, donde la acidificación del medio afecta principalmente a la función de Nos más que al resto de enzimas (Bergaust et al., 2010); en el caso de NO_2^-, las células no pudieron ni siquiera consumir el O_2 inicial como aceptor electrónico. Esto podría haber sido debido a la formación de algunas sustancias tóxicas como el ácido nitroso (HNO_2), producto de la protonación de NO_2^- a bajo pH (Almeida et al., 1995; Reddy et al., 1983).

El análisis transcripcional llevado a cabo incluyó la monitorización de la expresión de los genes *narG, nirK, norZ* y *nosZ* acoplada a la cinética de gases nitrogenados y la acumulación de NO_2^- durante la incubación, usando 1% O_2 (v/v) y 5 mM KNO_3 como aceptores electrónicos

terminales. Los resultados se pueden resumir en los siguientes tres eventos principales de expresión:

i) Los niveles transcripcionales de *narG* y *nosZ* incrementaron en un orden de magnitud inmediatamente antes de la aparición de los picos de NO y N_2O (cerca de las 10 horas de incubación). La transcripción de *narG* decayó después y se mantuvo en un nivel bajo constante durante la fase anóxica.

ii) El segundo evento ocurrió justo después del pico máximo alcanzado por NO: *nosZ* llegó a su máximo de expresión, que coincidió con una alta expresión de *nirK* y *nosZ* (que se habían mantenido en niveles muy bajos hasta entonces). Tras este evento, los niveles transcripcionales de los tres genes fueron gradualmente disminuyendo en un orden de magnitud.

iii) Finalmente, cuando la velocidad del crecimiento aparente por desnitrificación comenzó a caer (cerca de las 40 horas de incubación), los niveles de transcripción de *nirK, norZ* y *nosZ* volvieron a incrementarse, especialmente los del primero.

La caída en la velocidad de crecimiento aparente bajo condiciones anóxicas fue debida al mismo fenómeno descrito anteriormente (la falta de síntesis *de novo* de las enzimas de la desnitrificación): cerca de las 40 horas de incubación, el flujo electrónico hacia Nir llegó a una fase de meseta, que coincidió con la acumulación de NO_2^- en el medio de cultivo y el comienzo de un nuevo evento de expresión de *nirK*, que permitió la reducción de los N oxianiones restantes a N_2.

Combinando los datos transcripcionales con los de cinética de gases, parece que: primero, *narG* y *nosZ* fueron ambos inducidos via un sensor de O_2 (y posiblemente, de NO_3^-), debido a su temprana transcripción; segundo, *nirK* y *norZ* no fueron inducidos sólo por la hipoxia, sino que aparentemente requirieron la presencia de NO (y probablemente NO_2^-), ya que ambos genes

mantuvieron sus niveles de expresión muy bajos hasta que NO llegó a su máxima concentración. Probablemente, ambos podrían estar bajo el control de un sensor(s) desconocido de NO/NO_2^-. Así mismo, *nosZ* pareció también estar positivamente regulado por NO, debido a que su acumulación también coincidió con un segundo pico de expresión de este gen, junto con los de *nirK* y *norZ*.

La temprana expresión de *nosZ* abrió la cuestión de si Nos podría ser una enzima activa en presencia de concentraciones micromolares de O_2. Para evaluar este esto, se incubaron células de *H. mediterranei* con 1% (v/v) tanto de O_2 como de N_2O, con 5 mM KNO_3 en el medio. Durante las primeras horas de incubación (8), las células usaron principalmente el O_2 como aceptor electrónico. Sin embargo, a medida que la concentración de éste llegó aproximadamente al 50% de la inicial, N_2O fue rápidamente reducido, coincidiendo su agotamiento con la aparición de NO. El flujo electrónico calculado hacia los diferentes aceptores electrónicos mostró una respiración paralela de O_2 y N_2O durante varias horas.

La maquinaria de la desnitrificación consiste en un conjunto de proteínas que va más allá de las enzimas estructurales (Nar, Nir, Nor y Nos). Esto incluye, por ejemplo, aquellas que participan en el plegamiento y la conformación estructural de las enzimas o aquellas que actúan como donadores/transportadores electrónicos. Las aproximaciones basadas en la fisiología, el análisis transcripcional o la bioinformática no pueden ofrecer una perspectiva global sobre la síntesis de las proteínas relacionadas con la desnitrificación. Por ello, con el fin de obtener una completa visión de esta ruta respiratoria, se llevó a cabo una aproximación proteómica para identificar los componentes implicados en la desnitrificación en *H. mediterranei*. Los resultados mostraron que el uso de detergentes combinado con diferentes pasos cromatográficos para el enriquecimiento en proteínas desnitrificantes es una buena aproximación para su estudio en condiciones nativas. De hecho, fue demostrado que la actividad Nar permitió la selección de las micelas de interés, siendo una herramienta útil, rápida y barata para la copurificación de todas las N reductasas

junto con sus proteínas accesorias, esenciales para sostener la fuerza protón motriz y el flujo electrónico. Entre ellas, es remarcable la identificación de donadores electrónicos potenciales como las halocianinas o las azurinas, que podría actuar como proveedores de electrones para Nir y Nor, respectivamente, Así mismo, se identificaron diferentes errores de anotación génica o en las bases de datos de proteínas: un ejemplo fue la "segunda copia" de la nitrito reductasa codificada en el entorno génico de *nirK*, que fue en realidad una oxidorreductasa de cobre sin ninguna similitud con la enzima.

Justificación de la unidad temática durante la tesis.

La presente tesis doctoral versa sobre la misma unidad temática: la desnitrificación en haloarchaea. A partir del conocimiento previo obtenido, diferentes aproximaciones y disciplinas científicas fueron usadas para avanzar en el conocimiento de esta ruta respiratoria en ambientes hipersalinos. Específicamente, el capítulo 1 ofreció las bases de conocimiento para el resto de estudios y experimentos, describiendo con detalle las agrupaciones génicas implicadas en la desnitrificación, obteniendo así una idea general sobre la capacidad desnitrificante de las haloarchaea. Además, usando la bioinformática, se probó que la óxido nítrico reductasa en estos microorganismos es de tipo qNor (capítulo 2). Esto supuso un avance en el conocimiento de Nor ya que no había estudios previos en haloarchaea sobre esta enzima. Todo el trabajo realizado *in silico* permitió la subsecuente evaluación fenotípica, describiendo la fisiología de la desnitrificación de tres miembros del género *Haloferax* (capítulo 3). Algunos de ellos fueron identificados como desnitrificantes completos (reduciendo NO_3^- a N_2) mientras otros como parciales, emitiendo gases nitrogenados durante la respiración de NO_3^-/NO_2^-. Las diferencias fenotípicas tienen importantes implicaciones ecológicas, por lo que la desnitrificación debe ser entendida desde una perspectiva global (capítulo 4). Entre las especies evaluadas, *H. mediterranei* mostró el perfil más óptimo como organismo modelo para la desnitrificación en halófilos. Por ello, los siguientes estudios se centraron en este microorganismo: primero, en el

Anexo 1, fue evaluada su capacidad para tolerar/reducir altas concentraciones de N oxianiones y variaciones de pH; en segundo lugar, fue realizado un análisis transcripcional de los cuatro principales genes de la desnitrificación (*narG, nirK, norZ* y *nosZ*) junto con la cinética de los gases nitrogenados en tiempo real, elucidando así potenciales mecanismos regulatorios de la desnitrificación en haloarchaea por primera vez (apéndice 1); finalmente, la aproximación proteómica fue usada como herramienta para describir nuevos agentes implicados en esta ruta respiratoria que no hubieran podido ser identificadas previamente por otras disciplinas, como potenciales donadores electrónicos en haloarchaea (apéndice 2).

Referencias.

Andrei, A.S., Banciu, H.L., Oren, A. (2012) Living with salt: metabolic and phylogenetic diversity of archaea inhabiting saline ecosystems. *FEMS Microbiol Lett* 330: 1-9.

Almeida, J.S., Júlio, S.M., Reis, M.A.M., Carrondo, M.J.T. (1995) Nitrite inhibition of denitrification by *Pseudomonas fluorescens. Biotech Bioeng* 46: 194-201.

Bakken, L.R., Bergaust, L., Liu, B., Frostegård, A. (2012) Regulation of denitrification at the cellular level: a clue to the understanding of N_2O emissions from soils. *Philos Trans R Soc Lond B Biol Sci* 367: 1226-1234.

Bergaust, L., Mao, Y., Bakken, L.R., Frostegård, A. (2010) Denitrification response patterns during the transition to anoxic respiration and posttranscriptional effects. *Appl Environ Microbiol* 76: 6387-6396.

Bergaust, L., Hartsock, A., Liu, B., Bakken, L.R., Shapleigh, J.P. (2014) Role of norEF in denitrification, elucidated by physiological experiments with *Rhodobacter sphaeroides*. *J Bacteriol* 196: 2190-2200.

Bonete, M.J., Martínez-Espinosa, R.M., Pire, C., Zafrilla, B., Richardson, D.J. (2008) Nitrogen metabolism in haloarchaea. *Saline systems* 4:9.

Borrero-de Acuña, J.M., Rohde, M., Wissing, J., Jänsch, L., Schobert, M., Molinari, G., Timmis, K.N., Jahn, M., Jahn, D. (2016) Protein network of the *Pseudomonas aeruginosa* denitrification apparatus. *J Bacteriol* 198: 1401-1413.

DasSarma, P., Capes, M.D., DasSarma, S. (2019) Comparative genomics of *Halobacterium* strains from diverse locations in *Microbial diversity in the genomic era*, Das, S., and Dash, H.R. (eds). London: Elsevier, pp. 285-322.

de la Haba, R.R., Sánchez-Porro, C., Márquez, M.C., Ventosa, A. (2011) Taxonomy of halophiles, in *Extremophile Handbook,* Horikoshi, K. (ed). Tokyo, Japan: Springer Science & Business Media, pp. 256-283.

Delgado-Baquerizo, M., Maestre, F.T., Gallardo, A., et al. (2013) Decoupling of soil nutrient cycles as a function of aridity in global drylands. *Nature* 502: 672-676.

Edbeib, M.F., Wahab, R.A., Huyop, F. (2016) Halophiles: biology, adaptation, and their role in decontamination of hypersaline environments. *World J Microbiol Biotechnol* 32: 1-23.

Esclapez, J., Zafrilla, B., Martínez-Espinosa, R.M., Bonete, M.J. (2013). Cu-NirK from *Haloferax mediterranei* is an example of metalloprotein maturation and exportation via Tat system. *Biochim. Biophys. Acta.* 1834: 1003-1009. doi: 10.1016/j.bbapap.2013.03.002.

Hattori, T., Shiba, H., Ashiki, K., Araki, T., Nagashima, Y., Yoshimatsu, K., Fujiwara, T. (2016) Anaerobic growth of haloarchaeon *Haloferax volcanii* by denitrification is controlled by the transcription regulator NarO. *J Bacteriol* 198: 1077-1086.

Hechler, T., Pfeifer, F. (2009) Anaerobiosis inhibits gas vesicle formation in halophilic archaea. *Mol Microbiol* 71: 132-145.

Hochstein, L.I., Lang, F. (1991) Purification and properties of dissimilatory nitrate reductase from *Haloferax denitrificans*. *Arch Biochem Biophys* 288: 380-385.

Inatomi, K., and Hocstein, L.I. (1996) The purification and properties of a copper nitrite reductase from *Haloferax denitrificans*. *Curr Microbiol* 32: 72-76.

Liu, B., Mao, Y., Bergaust, L., Bakken, L.R., Frostegård, A. (2013) Strains in the genus *Thaurea* exhibit remarkably different denitrification regulatory phenotypes. *Environ Microbiol* 15: 2816-2828.

LLedó, B., Martínez-Espinosa, R.M., Marhuenda-Egea, F.C., Bonete, M.J. (2004) Respiratory nitrate reductase from haloarchaeon *Haloferax mediterranei*: biochemical and genetic analysis. *Biochim Biophys Acta* 1674: 50-59.

Martínez-Espinosa, R.M., Dridge, E.J., Bonete, M.J., Butt, J.N., Butler, C.S., Sargent, F., Richardson, D.J. (2007) Look on the positive site! The orientation, identification and bioenergetics of 'Archaeal' membrane-bound nitrate reductases. *FEMS Microbiol Lett* 276: 129-139.

Martínez-Espinosa, R.M., Cole, J.A., Richardson, D.J., et al. (2011) Enzimology and ecology of the nitrogen cycle. *Biochem Soc Trans* 39: 175-178.

Lycus, P., Bothun, K.L., Bergaust, L., Shapleigh, J.P., Bakken, L.R., Frostegård, A. (2017) Phenotypic and genotypic richness of denitrifiers revealed by a novel isolation strategy. *ISME J* 11: 2219-2232.

Olaya-Abril, A., Hidalgo-Carrillo, J., Luque-Almagro, V.M., Fuentes-Almagro, C., Urbano, F.J., Moreno-Vivián, C., Richardson, D.J., Roldán, M.D. (2018) Exploring the denitrification proteome of *Paracoccus denitrificans* PD1222. *Front Microbiol* 9:1137.

Oren, A. (2002) Diversity of halophilic microorganisms: environments, phylogeny, physiology and applications. *J Ind Microbiol Biotechnol* 28: 56-63.

Oren, A. (2013) Life at high salt concentrations, intracellular KCl concentrations and acidic proteomes. *Front Microbiol* 4: 1-6.

Pendleton, L., Donato D.C., Murray, B.C., et al. (2012) Estimating global blue carbon emissions from conversion and degradation of vegetated coastal ecosystems. *PLoS One* 7:e43542.

Pfeifer, F. (2015) Haloarchaea and the formation of gas vesicles. *Life* 5: 385-402.

Philippot, L. (2002) Denitrifying genes in bacterial and archaeal genomes. *Biochim Biophys Acta* 1577: 355-376.

Purdy, K.J., Cresswell-Maynard, T.D., Nedwell, D.B., McGenity, T.J., Grant, W.D., Timmis, K.N., Embley, T.M. (2004) Isolation of haloarchaea that grow at low salinities. *Environ Microbiol* 6: 591-595.

Reddy, D., Lancaster, J.R., Cornforth, D.P. (1983) Nitrite inhibition of *Clostridium botulinum*: electron spin resonance detection of iron-nitric oxide complexes. *Science* 221: 769-770.

Roco, C.A., Bergaust, L., Bakken, L.R., Yavitt, J.B., Shapleigh, J.P. (2017) Modularity of nitrogen-oxide reducing soil bacteria: linking phenotype to genotype. *Environ Microbiol* 19: 2507-2519.

Rodríguez-Valera, F., Ventosa, A., Juez, G., Imhoff, J.F. (1985) Variation of environmental features and microbial populations with salt concentration in a multi-pond saltern. *Microb Ecol* 11: 107-115.

Salomonsson, L., Reimann, J., Tosha, T., Krause, N., Gonska, N., Shiro, Y., Adelroth, P. (2012) Proton transfer in the quinol-dependent nitric oxide reductase from *Geobacillus stearothermophilus* during the reduction of oxygen. *Biochim Biophys Acta* 1817: 1914-1920.

Sherwood, J.E., Stagnitti, F., Kokkinn, M.J., Williams, W.D. (1991) Dissolved oxygen concentrations in hypersaline waters. *Limnol Oceanogr* 36: 235-250.

Sherwood, J.E., Stagnitti, F., Kokkinn, M.J., Williams, W.D. (1992) A standard table for predicting equilibrium dissolved oxygen concentrations in salt lakes dominated by sodium chloride. *Int J Salt Lake Res* 1: 1-6.

Tindall, B.J., Tomlinson, G.A., Hochstein, L.I. (1989) Transfer to *Halobacterium denitrificans* (Tomlinson, Jahnke and Hocstein) to the genus *Haloferax* as *Haloferax denitrificans* comb nov. *Int J Syst Bacteriol* 39: 359-360.

Yoshimatsu, K., Iwasaki, T., Fujiwara, T. (2002) Sequence and electron paramagnetic resonance analyses of nitrate reductase NarGH from a denitrifying halophilic euryarchaeote *Haloarcula marismortui*. *FEBS Lett* 516: 145-150.

Zumft, W.G, Kroneck, P.M. (2006) Respiratory transformation of nitrous oxide (N_2O) to dinitrogen by Bacteria and Archaea. *Adv Microb Physiol* 52: 107-227.

SYNTHESIS

State of the art, hypothesis and objectives.

The main characteristic of hypersaline environments is the high concentration of salts present in waters and soils, which is considerably higher than that found in seawater (0.6 M or 3.5% (w/v)) (DasSarma et al., 2019). These natural ecosystems include lakes, lagoons and salty surface ponds, subsurface salt deposits, submarine salt domes and salt marshes (Oren, 2002; de la Haba et al., 2011; Andrei et al., 2012). Among them, some well-known examples are the Dead Sea (Israel-Palestine and Jordan), The Magadi Lake (Kenya) or The Great Salt Lake (United States). Other hypersaline environments have been made by human action such as the artificial solar salterns used to produce salt, usually near the sea side (DasSarma et al., 2019).

The biodiversity of these environments is higher than initially expected, but obviously lower than that of non-saline ecosystems. In all of them, there are organisms belonging to the three domains of Life, as *Artemia* (shrimp), *Dunaliella* (unicellular algae) or *Salinibacter* (red bacteria), but when the salt concentration exceeds 16% (w/v), the predominant group of microorganisms is the haloarchaea (Andrei et al., 2012; Edbeid et al., 2016). These microorganisms, as a class within the Archaea domain, are facultative aerobes, heterotrophic/phototrophic, characterised mainly by being obligate halophiles (DasSarma et al., 2019). They require high salt concentrations to live, usually between 1.5 and 4 M NaCl, which corresponds to 9-30% salts (w/v) (Purdy et al., 2004).

In hypersaline environments, aerobic respiration becomes difficult because the availability of oxygen is very low due to the presence of high salt concentrations: in fact, at 35ºC, the optimum temperature for many haloarchaea, the solubility of O_2 is 6.92 mg/L in distilled water and drops ten folds in hypersaline environments (Rodríguez-Valera et al., 1985; Sherwood et al., 1991;

Sherwood et al., 1992; Oren, 2013). Under these conditions, some haloarchaea can float to the air-water interface, thanks to the production of gas vesicles (Oren, 2002). These structures increase the buoyancy of cells and allow them to migrate vertically to regions with better conditions to sustain microaerobic or aerobic growth (Pfeifer, 2015). However, this strategy does not seem to be predominant among the haloarchaea and, in addition, it depends on environmental factors, such as light, temperature, salt concentration and O_2 availability. In fact, the production of these vesicles is inhibited in anaerobic conditions (Hechler and Pfeifer, 2009). Because of all these factors, microorganisms are pushed towards the use of alternative electron acceptors. Apart from O_2 respiration, denitrification is the most energetically profitable pathway (Zumft and Kroneck, 2006): nitrate (NO_3^-) is sequentially reduced to nitrite (NO_2^-), nitric oxide (NO), nitrous oxide (N_2O) and dinitrogen (N_2) in a series of four reactions catalysed by the enzymes nitrate- (Nar), nitrite- (Nir), nitric oxide- (Nor) and nitrous oxide- (Nos) reductases. In the last decades, due to various anthropogenic activities, the concentrations of NO_3^- and NO_2^- in these ecosystems have been increasing, thus favouring denitrification (Martínez-Espinosa et al., 2011).

The ability to denitrify is widely distributed in prokaryotes, but it has only been studied in detail in some organisms, mainly mesophilic bacteria (Bakken et al., 2012; Liu et al., 2013; Bergaust et al., 2014; Borrero-de Acuña et al., 2016; Lycus et al., 2017; Olaya-Abril et al., 2018). However, in the Archaea domain, knowledge is scarce (Philippot, 2002; Yoshimatsu et al., 2002) and even lower in those that live in extreme environments, such as haloarchaea, because only a few genera can grow under laboratory conditions and out of those, a minority is able to denitrify.

In this sense, the genus *Haloferax* has been used as model to study denitrification since some of the members are the best-known haloarchaea in terms of microbial ecology, biochemistry and molecular biology (Lledó et al., 2004; Martínez-Espinosa et al., 2007). At the beginning of this thesis, knowledge about denitrification in the genus *Haloferax* was reduced to the following

achievements: in terms of *in silico* analyses, only the *nar* (Lledó et al., 2004; Martínez-Espinosa et al., 2007) and *nir* gene contexts had been explored (Esclapez et al., 2013); at biochemical level, the purification of Nar in *H. mediterranei* (Lledó et al., 2004) and Nar and Nir *H. denitrificans* (Hochstein and Lang, 1991; Inatomi and Hochstein, 1996) had been achieved. None of the other two enzymes (Nor and Nos) had been purified; at physiological level, no species had been characterized and only a few studies had measured the emission of N_2O by *H. mediterranei* using NO_3^- as electron acceptor (Lledó et al., 2004; Bonete et al., 2008) and the production of N_2O and N_2 by *H. denitrificans* (Tindall et al., 1989); likewise, there was not any study on the expression of the genes involved in this metabolic pathway or any approach from other disciplines such as proteomics.

With all the previous information, the hypothesis of the present doctoral thesis is that there are some species of haloarchaea with the ability to reduce NO_3^-/NO_2^- to N_2 because they have the complete and active machinery of denitrification (complete denitrifiers), while others, because the route is truncated at some point, would generate as products NO and N_2O (incomplete denitrifiers). The first group could act as sink of nitrogenous gases and toxic N anions in hypersaline environments, while the latter would be a source of greenhouse gases, thus contributing to global warming and climate change. In fact, nowadays, the anthropogenic activities are favouring the accumulation of N-sources as NO_3^-, NO_2^- and NH_4^+ in media (including saline/hypersaline media).

In this sense, the doctoral thesis means a multidisciplinary advance in the knowledge of denitrification in the genus *Haloferax*, serving as a model to elucidate the characteristics of this respiratory route in extreme environments such as hypersaline ecosystems. The objectives of this research work are:

1. To review the knowledge of the main respiratory anaerobic pathways in *Haloferax* genus, paying special attention to denitrification. To achieve this aim, an *in silico* analysis

of the organization of the gene clusters related to denitrification in different species has been carried out.

2. To analyse both, complete and draft haloarchaeal genomes, in order to identify the genes that encode the nitric oxide reductases as well as to study the organization of the coding sequences belonging to its genetic context.

3. To describe of the phenotypic profile of denitrification in *H. mediterranei, H. denitrificans* and *H. volcanii* and their relationship with the emission of nitrogenous gases.

4. To analyse the denitrifying profile of *H. mediterranei* in a wide range of culture conditions, such as different concentrations of NO_3^-, NO_2^- and pH values. Transcriptional analysis of the main genes involved in denitrification in *H. mediterranei* (*narG, nirK, norZ* and *nosZ*) coupled with real-time measurements of all the intermediates (NO_2^-, NO, N_2O and N_2) has also been explored.

5. To identify, using a proteomic approach, the components of the machinery of dentrification in *H. mediterranei*: not only the N-reductases, but also other proteins related to electron flow and proton motive force (some of them not described at protein level so far).

Presented works.

The works presented in the doctoral thesis are described below:

PUBLISHED WORKS

Chapter 1. Anaerobic metabolism in *Haloferax* genus: denitrification as case of study.

This chapter reviews the general characteristics of *Haloferax* genus and the main anaerobic respiratory pathways described from it, focusing on denitrification. Regarding this topic, it describes the four metalloenzymes involved in the process, the organization of their genes and clusters and the potential biotechnological applications that the anaerobic metabolism of haloarchaea can offer.

Chapter 2. Analysis of multiple haloarchaeal genomes suggests that the quinone-dependent respiratory nitric oxide reductase is an important source of nitrous oxide in hypersaline environments.

The chapter describes an extensive interspecific analysis of both complete and incomplete haloarchaeal genomes in order to identify the genes coding for the enzyme nitric oxide reductase and the organization of the genetic context. Likewise, a bioinformatic model of Nor in *H. mediterranei* is designed.

Chapter 3. Denitrifying haloarchaea within the genus *Haloferax* display divergent respiratory phenotypes, with implications for their release of nitrogenous gases.

This is the first study on the physiological characterization of denitrification in haloarchaea. Three of the best-known species belonging to the genus *Haloferax* (*H. mediterranei, H. denitrificans* and *H. volcanii*) are characterized with respect to their ability to denitrify. Different

initial O_2 concentrations and alternative electron acceptors (NO_3^-/NO_2^-) are used to define the denitrification phenotype, measuring the production of NO_2^- and the emission of nitrogenous gases in real time.

Chapter 4. Denitrifying haloarchaea: sources and sinks of nitrogenous gases.

This is a review of the ecological role of haloarchaea as sources or sinks of nitrogenous gases depending on whether they are complete or incomplete denitrifying species. A global dimension of this concept is given, by offering information on the extent of semi-arid/arid and saline/ hypersaline environments where these microorganisms inhabit. During the last decades, these ecosystems have increased in extent and prevalence due to the processes of desertification favoured by human action and climate change.

UNPUBLISHED WORKS

Appendix 1. *Haloferax mediterranei,* an archaeal model for denitrification in saline systems, characterised through integrated phenotypic and transcriptional analyses.

This work deepens in the knowledge of denitrification physiology in *H. mediterranei*, testing its capacity to tolerate/reduce a wide range of NO_3^-/NO_2^- concentrations and different pH values. Likewise, the first transcriptional analysis of the main genes involved in denitrification (*narG, nirK, norZ* and *nosZ*) is presented in Archaea, combined with a detailed kinetics of the nitrogenous gases emitted. Finally, the capacity of *H. mediterranei* to act as an N_2O sink is physiologically tested.

Appendix 2. Exploring the molecular machinery of denitrification in *H. mediterranei* through proteomics.

This work establishes an integrated protocol for the identification of proteins involved in this denitrification in *H. mediterranei*. It is based on the generation of lipid micelles and their subsequent enrichment using different chromatographic steps. This approach avoids techniques such as cross-linking, in which artificial interactions between proteins are generated. The protocol aims to describe proteins involved in denitrification at all levels: N-reductases, proteins involved in electron flow or in the generation of the proton motive force. Some of them have never been described at protein level so far.

Main results, discussion and conclusions.

Knowledge about denitrification in *Haloferax* genus was restricted, until now, to the biochemical characterization of some of the enzymes in a few species. No study of the genes that encode these proteins (except for the *nar* and *nir* in *H. Mediterranei* - Lledó et al., 2004; Esclapez et al., 2013) was carried out before the research here presented. Therefore, the analysis of the organization of gene clusters involved in denitrification was the first step to be taken.

In this sense, the first results obtained showed that the organization of *nar* cluster was almost the same in the seven species compared. Mainly, it is constituted by the genes coding for the catalytic subunit and the electron transfer subunit of Nar (*narG* and *narH*, respectively), a gene (*mobA*) involved in the synthesis of the MOCO cofactor, genes coding for proteins involved in electron transfer (*narB* and *narC*) and a gene that encode a chaperone (narJ).

Second, genes coding for nitrite and nitric oxide reductases (*nirK* and *norZ*/*norBC*) were located very close to each other so they could constitute the same gene cluster. It also contains genes that encode proteins that could act as electron carrier during the reduction of NO_2^- and/or NO

as *hyc*, coding for a halocyanin. It is a small blue copper protein which serves as a mobile electron carrier.

Finally, nitrous oxide reductase was also organized in a gene cluster. In this case, it was only possible to make the *in silico* analysis of three species, since in the rest it was impossible to identify genes that encoded either Nos or any of the accessory proteins. In this cluster, we identified: *nosL*, a gene coding for a Cu(I) protein that could be involved in the formation of Cu centers of Nos; *nosY*, which encodes an ABC-type transporter; *nosZ*, the nitrous oxide reductase gene; other genes involved in electron transfer such as *pcy*, a plastocyanin that could act as Nos electron donor.

Among all the main genes coding for denitrification enzymes, the one that encode Nor was of the special interest, which was annotated as *norB* in most haloarchaea. This annotation is usually reserved for genes that encode the NorB subunit of bacterial scNor (short chain Nor), consisting of two monomers (NorB and NorC). However, a detailed inspection of *norB* sequences in the haloarchaeal genomes raised doubts about their annotation (for example, the length of their nucleotide sequence).

Therefore, an extensive bioinformatic study was carried out on Nor in haloarchaea, which revealed that the version of the enzyme that predominates in this group of microorganisms is the quinone-dependent nitric oxide reductase, known as qNor (or long chain Nor - lcNor) encoded by the *norZ* gene. It was concluded, therefore, that the haloarchaeal Nor is not the cNOR (scNOR)-type. The evidence was demonstrated using the respiratory Nor of *H. mediterranei* as model for the alignment with genomes of 141 species of haloarchaea. Although this gene is widely distributed in haloarchaea, the organization of the ORFs around it varied considerably between species. In fact, there were only one common feature to all those studied: the proximity of *nirK* (nitrite reductase) and *hyc* (periplasmic halocyanin) genes to *norZ*. The high variability observed in these gene regions, together with some genes close to *norZ* as those that

encode XerD (involved in recombination processes), could indicate a recent acquisition of *norZ* by haloarchaea through horizontal gene transfer and subsequent recombination events. Although it is not clear why haloarchaea express qNor more than cNor, there could be two important bioenergetic considerations in this sense: on one hand, *norZ* produces a discrete protein compared the derived from the expression of *norB*, which implies the formation and maturation of a NorBC complex; on the other hand, although qNor is not electrogenic (Salomonsson et al., 2012), this limitation could be overcome by haloarchaea through expression of the energy conserving pNar (Martínez-Espinosa et al., 2007).

All these results obtained using bioinformatics demonstrated the denitrifying capacity (partial or total) of many members of the *Haloferax* genus. However, it was necessary to take a step further to know real implications of these microorganisms in the reduction of N-oxyanions and nitrogenous gases emission. For this reason, a series of physiological studies were carried out in which the phenotypic profile of three species of haloarchaea (*H. mediterranei, H. denitificans* and *H. volcanii*) was defined under denitrifying conditions.

Among them, *H. mediterranei* was able to reduce all the available of NO_3^-/NO_2^- to N_2 in the standard conditions (5 mM KNO_3 or 1 mM KNO_2 with 1% O_2 (v/v)), with minimal and transient accumulation of the intermediates (NO_2^-, NO, N_2O). It showed a rapid and effective transition to denitrification after O_2 consumption, with no apparent delay or decrease in total electron flow towards terminal electron acceptors. *H. mediterranei* only had difficulties to denitrify when the O_2 initial concentration was approximately 0%, where only 50% of the cultures managed to consume practically all NO_3^- available, and none of them was able to denitrify when NO_2^- was used as electron acceptor.

Moreover, *H. denitrificans* showed a variable denitrifying phenotype: in case of NO_3^-, only a minor fraction of the cultures (1/3) was able to denitrify, being a mixture of N_2O and N_2 the final products; in case of NO_2^-, the excess of NO accumulated during the incubation seemed to

produce a general arrest in respiration. The inefficiency in denitrification of *H. denitrificans* was evident when looking at the transition of the electron flow between aerobic and anaerobic phases, with an apparent lag phase of approximately twelve hours. This could indicate a slow and gradual onset of Nar expression in the cell population, which slows down the beginning of denitrification. If there were an initial weak induction of denitrification apparatus through O_2 sensors, this would explain that the probability of producing N_2 as the only final product increases as the initial concentration of O_2 does. Moreover, when NO_2^- was used as alternative electron acceptor, there was a rapid increase in NO, reaching micromolar concentrations, that produced a general arrest in respiration irrespective of initial O_2 concentration.

Finally, *H. volcanii* was unable to reduce NO_3^- to NO_2^- and, when using the latter as alternative electron acceptor, there was an increase of NO and N_2O up to micromolar concentrations, after which respiration came to a halt. Although *H. volcanii* has been described as denitrifier (Hattori et al., 2016), in these experiments it did not reduce NO_3^- to NO_2^-. Despite the experimental approaches used differed between studies (for example, with respect to NO_3^- concentrations and stirring conditions), the phenotypic discrepancies were more likely due to inter-strain differences.

Therefore, *H. mediterranei* showed the best features as denitrifier between the species tested, since it reduced all the available NO_3^-/NO_2^- to N_2 from 1% of initial O_2 (v/v), with low and transient accumulation of nitrogenous gases. In addition, it showed ratios of aerobic: anaerobic growth similar to model organisms for denitrification such as *Paracoccus denitrificans* (Bergaust et al., 2010) or other denitrifiers recently isolated from soil samples (Roco et al., 2017). Considering all these data, *H. mediterranei* was presented as efficient and reproducible model for the study of denitrification in hypersaline environments and as a candidate for future applications in bioremediation.

The evaluation of the phenotypic profile of the haloarchaea tested is a clear example of how cautious researchers must be when describing the denitrifying capacity of microorganisms. Genetic make-up, phylogeny and bioinformatics are poor predictors of a denitrifying organism's propensity to release N oxides (Lycus et al., 2017; Roco et al., 2017). In order to know if an organism can act as source or sink of toxic intermediates (such as NO and N_2O), it is necessary to carry out a detailed phenotypic analysis like the one presented: *H. volcanii* was potentially a denitrifier able to reduce NO_3^- (its genome contains a gene coding for a respiratory nitrate reductase) but its inability was demonstrated, at least, in the culture conditions tested; *H. mediterranei* and *H. denitrificans* possess all the genes for the expression of the metalloenzymes involved in denitrification, but their phenotype were clearly different: the first one acted as a sink for N-oxyanions, while the second emitted significant amounts of nitrogenous gases to the atmosphere.

Nowadays, there are no accurate data of the prevalence and total area of saline/hypersaline environments. As an example, some best estimates of the area of salt marshes range from 2.2 to 40 Mha (Pendleton et al., 2012). Considering that these environments are not the predominant hypersaline ecosystems, their extension is significantly larger. In fact, saline and hypersaline zones are concomitant with arid and semi-arid areas, which cover about 41% of the Earth's land surface (Delgado-Baquerizo et al., 2013) and which are being increased, due to the effects of climate change. Therefore, the role of haloarchaea as sources or sinks of nitrogen gases should be understood from a global perspective.

Considering all these facts, and once demonstrated the denitrifying capacity of *H. mediterranei* above the other tested species, it was selected to carry out more detailed studies on its physiology as well as others focused on the transcriptional analysis of the main genes involved in denitrification*: narG, nirK, norZ, nosZ*.

H. mediterranei was then exposed to different initial concentrations of NO_3^- (in a range between 2 mM and 2 M KNO_3) and NO_2^- (between 1 and 40 mM KNO_2) with 1% initial O_2 (v/v), measuring the production of all the intermediates in real time (NO_2^-, NO, N_2O, N_2). The addition of high amounts of NO_3^- should support multiple generations of exponential anaerobic growth, in proportion to initial NO_3^- concentration. However, regardless of the amount of NO_3^- available, *H. mediterranei* was unable to maintain exponential growth by denitrification beyond 1.5 to 2 generations. This likely reflected lack of *de novo* synthesis of denitrification enzymes and thus dilution of per cell concentrations of the reductases during subsequent cell division. It seems that, in case of *H. mediterranei*, micro-oxic conditions were required for *de novo* synthesis of N-reductases since in cultures grown under the same conditions (5 mM KNO_3), but with 7% initial O_2 (v/v), the premature decline in the exponential growth rate was not observed and O_2 remained in concentrations around 5 µM when the N oxides were exhausted.

In case of NO_2^-, this phenomenon also occurred when *H. mediterranei* was incubated with 5 mM KNO_2: the exponential growth ceased prematurely while more than half of the initial NO_2^- remained. At lower concentrations of KNO_2 (1 and 2 mM), *H. mediterranei* showed a significant denitrifying capacity, being able to reduce all the available NO_2^- to N_2 with a discrete and transient accumulation of the intermediates NO and N_2O. At the highest concentrations explored (10 and 40 mM), the excess of NO caused the arrest of denitrifying machinery.

In the experiments, the ability to respire NO_3^-/NO_2^- by *H. mediterranei* at different pH values was also tested: between 7.3 (optimum for this microorganism) and 5.7. Irrespective of the N oxyanion used, below 6.5, the cells were not able to start denitrification. In case of NO_3^-, there was an apparent generalized inhibition of all the N-oxide reductases. This contrasts with other denitrifiers, such as *P. denitrificans*, where the acidification affects mainly the function of Nos more than the rest of the enzymes (Bergaust et al., 2010); in case of NO_2^-, the cells could not even consume the initial O_2 as final electron acceptor. This may have been due to the formation

of toxic substances, such as nitrous acid (HNO_2) derived from the protonation of NO_2^- at low pH (Almedia et al., 1995; Reddy et al., 1983).

The transcriptional analysis carried out involved the monitoring of the expression of the genes *narG, nirK, norZ* and *nosZ* coupled with the kinetics of nitrogenous gases and the accumulation of NO_2^- during the incubation, using 1% O_2 (v/v) and 5 mM KNO_3 as terminal electron acceptors. It can be summarized in three main expression events:

i) The transcriptional levels of *narG* and *nosZ* increased by an order of magnitude immediately before the transient NO and N_2O peaks (close to 10 hours of incubation). Transcription of *narG* subsequently decreased and remained at a constant level during the anoxic phase.

ii) The second expression event occurred just after NO peaked: *nosZ* reached a maximum expression, which coincided with high expression of *nirK* and *norZ* from the background levels. Next, the transcription of the three genes gradually dropped by an order of magnitude.

iii) Finally, when the apparent growth rate by denitrification began to fall (approximately at 40 hours of incubation), the transcription levels of *nirK, norZ* and *nosZ* increased again (specially the first one).

The decrease in the apparent growth rate under anoxic conditions was due to the same phenomenon described above (lack of *de novo* synthesis of denitrification enzymes): around 40 hours of incubation, the electron flow towards Nir reached a plateau, which coincided with the accumulation of NO_2^- in the medium and the beginning of a new expression event of *nirK*, which deal with the reduction of all of the remained N-oxyianions to N_2.

Combining transcriptional data with gas kinetics, it seemed that: first, *narG* and *nosZ* were both activated via an O_2 (and possibly NO_3^-) sensor, due to its early transcription; second, *nirK* and *norZ* were not induced by hypoxia alone, but apparently required the presence of NO (and possibly NO_2^-), since both genes maintained their expression levels very low until NO reached

the maximum concentration. Probably, both genes would be under the control of unknown NO/NO_2^- sensor(s). Likewise, *nosZ* seemed to be also positively regulated by NO, because its appearance also coincided with a second peak of this gene, which was observed along with *nirk* and *norZ* expressions.

The early expression of *nosZ* raised the question whether Nos would be active in the presence of micromolar concentrations of O_2. To test this, incubations of *H. mediterranei* cells were carried out with 1% (v/v) each of O_2 and N_2O, containing 5 mM KNO_3 in the medium. During the first hours of incubation (8 h) the cells mainly used O_2 as the electron acceptor. However, as O_2 concentration reached approximately 50% of the initial concentration, N_2O was rapidly reduced, coinciding its exhaustion with the appearance of NO. The electron flow calculated towards the different acceptors showed a parallel respiration of O_2 and N_2O for several hours.

The denitrification machinery consists of a set of proteins beyond the structural enzymes (Nar, Nir, Nor and Nos). This includes, for example, those that participate in folding and structural conformation of enzymes or those that act as electron donors/carriers. Approaches based on physiology, transcriptional analysis or bioinformatics cannot get a global perspective on protein synthesis related to denitrification. Therefore, in order to have a holistic picture of this respiratory route, a proteomic approach was carried out to identify the components involved in denitrification in *H. mediterranei*. The results showed that the use of detergents combined with different chromatographic steps for the enrichment of proteins related to denitrification is a good approach for their study in native conditions. In fact, it was demonstrated that Nar activity allowed the selection of the micelles of interest, being a useful, fast and cheap tool for the co-purification of all the N-reductases together with their accessory proteins, which could be essential to sustain the proton motive force and electron flow. Between them, it is remarkably the identification of potential electron donors like halocyanins or azurins, that could act as electron suppliers for Nir and Nor, respectively. Likewise, different potential errors were

identified in gene and protein annotations in databases: an example was a “second copy” of the nitrite reductase encoded in the *nir-nor* cluster, which turned out to be a copper oxidoreductase without any resemblance to the Nir enzyme.

Justification of the thematic coherence throughout the doctoral thesis.

This doctoral thesis is focused on the following thematic unit: denitrification in haloarchaea, and all the manuscripts included (already published or submitted) belongs to this topic being robustly interconnected. From the background that was had, different approaches and scientific disciplines were used to advance in the knowledge of this respiratory pathway in hypersaline environments. Specifically, chapter 1 provided the basis for the rest of the experiments and studies, describing in detail the gene clusters involved in denitrification and thus obtaining a general idea of the denitrifying capacity of haloarchaea. Moreover, using bioinformatics, it was proved that nitric oxide reductase in haloarchaea is of qNor type (chapter 2). This supposed an advance in the knowledge of Nor since there were no previous studies in this group of microorganisms about this enzyme. All the *in silico* research allowed the subsequent phenotypic evaluation by describing the physiology of denitrification of three members of *Haloferax* genus (chapter 3). Some of them were identified as complete denitrifiers (reducing NO_3^- to N_2) while others as partial denitrifiers, thus emitting nitrogenous gases. The phenotypic differences have important ecological implications, so denitrification in haloarchaea should be understood from a global perspective (chapter 4). Among the species tested, *H. mediterranei* showed the most optimal profile as model organism for denitrification in halophiles. Therefore, the following studies focused on this microorganism: first, in Appendix 1, it was evaluated its ability to tolerate/reduce high NO_3^-/NO_2^- concentrations and pH variations; secondly, a transcriptional analysis of the main denitrification genes (*narG, nirK, norZ* and *nosZ*) was made coupled with gas

kinetics in real time, thus elucidating the potential regulatory mechanisms involved in denitrification in haloarchaea for the first time (Appendix 1); finally, the proteomic approach was used as tool to describe new agents involved in this respiratory pathway that could not be identified by the previous disciplines, as potential specific electron donors in haloarchaea (Appendix 2).

References.

Andrei, A.S., Banciu, H.L., Oren, A. (2012) Living with salt: metabolic and phylogenetic diversity of archaea inhabiting saline ecosystems. *FEMS Microbiol Lett* 330: 1-9.

Almeida, J.S., Júlio, S.M., Reis, M.A.M., Carrondo, M.J.T. (1995) Nitrite inhibition of denitrification by *Pseudomonas fluorescens. Biotech Bioeng* 46: 194-201.

Bakken, L.R., Bergaust, L., Liu, B., Frostegård, A. (2012) Regulation of denitrification at the cellular level: a clue to the understanding of N_2O emissions from soils. *Philos Trans R Soc Lond B Biol Sci* 367: 1226-1234.

Bergaust, L., Mao, Y., Bakken, L.R., Frostegård, A. (2010) Denitrification response patterns during the transition to anoxic respiration and posttranscriptional effects. *Appl Environ Microbiol* 76: 6387-6396.

Bergaust, L., Hartsock, A., Liu, B., Bakken, L.R., Shapleigh, J.P. (2014) Role of norEF in denitrification, elucidated by physiological experiments with *Rhodobacter sphaeroides*. *J Bacteriol* 196: 2190-2200.

Bonete, M.J., Martínez-Espinosa, R.M., Pire, C., Zafrilla, B., Richardson, D.J. (2008) Nitrogen metabolism in haloarchaea. *Saline systems* 4:9.

Borrero-de Acuña, J.M., Rohde, M., Wissing, J., Jänsch, L., Schobert, M., Molinari, G., Timmis, K.N., Jahn, M., Jahn, D. (2016) Protein network of the *Pseudomonas aeruginosa* denitrification apparatus. *J Bacteriol* 198: 1401-1413.

DasSarma, P., Capes, M.D., DasSarma, S. (2019) Comparative genomics of *Halobacterium* strains from diverse locations in *Microbial diversity in the genomic era*, Das, S., and Dash, H.R. (eds). London: Elsevier, pp. 285-322.

de la Haba, R.R., Sánchez-Porro, C., Márquez, M.C., Ventosa, A. (2011) Taxonomy of halophiles, in *Extremophile Handbook,* Horikoshi, K. (ed). Tokyo, Japan: Springer Science & Business Media, pp. 256-283.

Delgado-Baquerizo, M., Maestre, F.T., Gallardo, A., et al. (2013) Decoupling of soil nutrient cycles as a function of aridity in global drylands. *Nature* 502: 672-676.

Edbeib, M.F., Wahab, R.A., Huyop, F. (2016) Halophiles: biology, adaptation, and their role in decontamination of hypersaline environments. *World J Microbiol Biotechnol* 32: 1-23.

Esclapez, J., Zafrilla, B., Martínez-Espinosa, R.M., Bonete, M.J. (2013). Cu-NirK from *Haloferax mediterranei* is an example of metalloprotein maturation and exportation via Tat system. *Biochim. Biophys. Acta.* 1834: 1003-1009. doi: 10.1016/j.bbapap.2013.03.002.

Hattori, T., Shiba, H., Ashiki, K., Araki, T., Nagashima, Y., Yoshimatsu, K., Fujiwara, T. (2016) Anaerobic growth of haloarchaeon *Haloferax volcanii* by denitrification is controlled by the transcription regulator NarO. *J Bacteriol* 198: 1077-1086.

Hechler, T., Pfeifer, F. (2009) Anaerobiosis inhibits gas vesicle formation in halophilic archaea. *Mol Microbiol* 71: 132-145.

Hochstein, L.I., Lang, F. (1991) Purification and properties of dissimilatory nitrate reductase from *Haloferax denitrificans*. *Arch Biochem Biophys* 288: 380-385.

Inatomi, K., and Hocstein, L.I. (1996) The purification and properties of a copper nitrite reductase from *Haloferax denitrificans*. *Curr Microbiol* 32: 72-76.

Liu, B., Mao, Y., Bergaust, L., Bakken, L.R., Frostegård, A. (2013) Strains in the genus *Thaurea* exhibit remarkably different denitrification regulatory phenotypes. *Environ Microbiol* 15: 2816-2828.

LLedó, B., Martínez-Espinosa, R.M., Marhuenda-Egea, F.C., Bonete, M.J. (2004) Respiratory nitrate reductase from haloarchaeon *Haloferax mediterranei*: biochemical and genetic analysis. *Biochim Biophys Acta* 1674: 50-59.

Martínez-Espinosa, R.M., Dridge, E.J., Bonete, M.J., Butt, J.N., Butler, C.S., Sargent, F., Richardson, D.J. (2007) Look on the positive site! The orientation, identification and bioenergetics of 'Archaeal' membrane-bound nitrate reductases. *FEMS Microbiol Lett* 276: 129-139.

Martínez-Espinosa, R.M., Cole, J.A., Richardson, D.J., et al. (2011) Enzimology and ecology of the nitrogen cycle. *Biochem Soc Trans* 39: 175-178.

Lycus, P., Bothun, K.L., Bergaust, L., Shapleigh, J.P., Bakken, L.R., Frostegård, A. (2017) Phenotypic and genotypic richness of denitrifiers revealed by a novel isolation strategy. *ISME J* 11: 2219-2232.

Olaya-Abril, A., Hidalgo-Carrillo, J., Luque-Almagro, V.M., Fuentes-Almagro, C., Urbano, F.J., Moreno-Vivián, C., Richardson, D.J., Roldán, M.D. (2018) Exploring the denitrification proteome of *Paracoccus denitrificans* PD1222. *Front Microbiol* 9:1137.

Oren, A. (2002) Diversity of halophilic microorganisms: environments, phylogeny, physiology and applications. *J Ind Microbiol Biotechnol* 28: 56-63.

Oren, A. (2013) Life at high salt concentrations, intracellular KCl concentrations and acidic proteomes. *Front Microbiol* 4: 1-6.

Pendleton, L., Donato D.C., Murray, B.C., et al. (2012) Estimating global blue carbon emissions from conversion and degradation of vegetated coastal ecosystems. *PLoS One* 7:e43542.

Pfeifer, F. (2015) Haloarchaea and the formation of gas vesicles. *Life* 5: 385-402.

Philippot, L. (2002) Denitrifying genes in bacterial and archaeal genomes. *Biochim Biophys Acta* 1577: 355-376.

Purdy, K.J., Cresswell-Maynard, T.D., Nedwell, D.B., McGenity, T.J., Grant, W.D., Timmis, K.N., Embley, T.M. (2004) Isolation of haloarchaea that grow at low salinities. *Environ Microbiol* 6: 591-595.

Reddy, D., Lancaster, J.R., Cornforth, D.P. (1983) Nitrite inhibition of *Clostridium botulinum*: electron spin resonance detection of iron-nitric oxide complexes. *Science* 221: 769-770.

Roco, C.A., Bergaust, L., Bakken, L.R., Yavitt, J.B., Shapleigh, J.P. (2017) Modularity of nitrogen-oxide reducing soil bacteria: linking phenotype to genotype. *Environ Microbiol* 19: 2507-2519.

Rodríguez-Valera, F., Ventosa, A., Juez, G., Imhoff, J.F. (1985) Variation of environmental features and microbial populations with salt concentration in a multi-pond saltern. *Microb Ecol* 11: 107-115.

Salomonsson, L., Reimann, J., Tosha, T., Krause, N., Gonska, N., Shiro, Y., Adelroth, P. (2012) Proton transfer in the quinol-dependent nitric oxide reductase from *Geobacillus stearothermophilus* during the reduction of oxygen. *Biochim Biophys Acta* 1817: 1914-1920.

Sherwood, J.E., Stagnitti, F., Kokkinn, M.J., Williams, W.D. (1991) Dissolved oxygen concentrations in hypersaline waters. *Limnol Oceanogr* 36: 235-250.

Sherwood, J.E., Stagnitti, F., Kokkinn, M.J., Williams, W.D. (1992) A standard table for predicting equilibrium dissolved oxygen concentrations in salt lakes dominated by sodium chloride. *Int J Salt Lake Res* 1: 1-6.

Tindall, B.J., Tomlinson, G.A., Hochstein, L.I. (1989) Transfer to *Halobacterium denitrificans* (Tomlinson, Jahnke and Hocstein) to the genus *Haloferax* as *Haloferax denitrificans* comb nov. *Int J Syst Bacteriol* 39: 359-360.

Yoshimatsu, K., Iwasaki, T., Fujiwara, T. (2002) Sequence and electron paramagnetic resonance analyses of nitrate reductase NarGH from a denitrifying halophilic euryarchaeote *Haloarcula marismortui*. *FEBS Lett* 516: 145-150.

Zumft, W.G, Kroneck, P.M. (2006) Respiratory transformation of nitrous oxide (N_2O) to dinitrogen by Bacteria and Archaea. *Adv Microb Physiol* 52: 107-227.

TRABAJOS PUBLICADOS

PUBLISHED WORKS

-CHAPTER ONE-

Torregrosa-Crespo J, Martínez-Espinosa RM, Esclapez J, Bautista V, Pire C, Camacho M, Richardson DJ, Bonete MJ. (2016). Anaerobic metabolism in *Haloferax* genus: denitrification as case of study. Advances in Microbial Physiology, 68: 41-85.

A number of species of *Haloferax* genus (halophilic archaea) are able to grow microaerobically or even anaerobically using different alternative electron acceptors such as fumarate, nitrate, chlorate, dimethyl sulphoxide, sulphide and/or trimethylamine. This metabolic capability is also shown by other species of the Halobacteriaceae and Haloferacaceae families (Archaea domain) and it has been mainly tested by physiological studies where cell growth is observed under anaerobic conditions in the presence of the mentioned compounds. This work summarises the main reported features on anaerobic metabolism in the *Haloferax,* one of the better described haloarchaeal genus with significant potential uses in biotechnology and bioremediation. Special attention has been paid to denitrification, also called nitrate respiration. This pathway has been studied so far from *Haloferax mediterranei* and *Haloferax denitrificans* mainly from biochemical point of view (purification and characterisation of the enzymes catalysing the two first reactions). However, gene expression and gene regulation is far from known at the time of writing this chapter.

doi: 10.1016/bs.ampbs.2016.02.001

-CHAPTER TWO-

Torregrosa-Crespo J, González-Torres P, Bautista V, Esclapez J, Pire C, Camacho M, Bonete MJ, Richardson DJ, Watmough NJ, Martínez-Espinosa RM. (2017). Analysis of multiple haloarchaeal genomes suggests that the quinone-dependent respiratory nitric oxide reductase is an important source of nitrous oxide in hypersaline environments. Environmental Microbiology Reports, 9(6): 788-796.

Microorganisms, including Bacteria and Archaea, play a key role in denitrification, which is the major mechanism by which fixed nitrogen returns to the atmosphere from soil and water. While the enzymology of denitrification is well understood in Bacteria, the details of the last two reactions in this pathway, which catalyse the reduction of nitric oxide (NO) via nitrous oxide (N_2O) to nitrogen (N_2), are little studied in Archaea, and hardly at all in haloarchaea. This work describes an extensive interspecies analysis of both complete and draft haloarchaeal genomes aimed at identifying the genes that encode respiratory nitric oxide reductases (Nors). The study revealed that the only nor gene found in haloarchaea is one that encodes a single subunit quinone dependent Nor homologous to the qNor found in bacteria. This surprising discovery is considered in terms of our emerging understanding of haloarchaeal bioenergetics and NO management.

doi: 10.1111/1758-2229.12596

-CHAPTER THREE-

Torregrosa-Crespo J, Pire C, Martínez-Espinosa RM, Bergaust L. (2019). Denitrifying haloarchaea within the genus *Haloferax* display divergent respiratory phenotypes, with implications for their release of nitrogenous gases. Environmental Microbiology, 21(1): 427-436.

Haloarchaea are extremophiles, generally thriving at high temperatures and salt concentrations, thus, with limited access to oxygen. As a strategy to maintain a respiratory metabolism, many halophilic archaea are capable of denitrification. Among them are members of the genus *Haloferax*, which are abundant in saline/hypersaline environments. Three reported haloarchaeal denitrifiers, *Haloferax mediterranei*, *Haloferax denitrificans* and *Haloferax volcanii*, were characterized with respect to their denitrification phenotype. A semi-automatic incubation system was used to monitor the depletion of electron acceptors and accumulation of gaseous intermediates in batch cultures under a range of conditions. Out of the species tested, only *H. mediterranei* was able to consistently reduce all available N-oxyanions to N_2, while the other two released significant amounts of NO and N_2O, which affect tropospheric and stratospheric chemistries respectively. The prevalence and magnitude of hypersaline ecosystems are on the rise due to climate change and anthropogenic activity. Thus, the biology of halophilic denitrifiers is inherently interesting, due to their contribution to the global nitrogen cycle, and potential application in bioremediation. This work is the first detailed physiological study of denitrification in haloarchaea, and as such a seed for our understanding of the drivers of nitrogen turnover in hypersaline systems.

doi: 10.1111/1462-2920.14474

-CHAPTER FOUR-

Torregrosa-Crespo J, Bergaust L, Pire C, Martínez-Espinosa RM. (2018). Denitrifying haloarchaea: sources and sinks of nitrogenous gases. FEMS Microbiology Letters, 365(3): 1-6.

Haloarchaea thrive under saline and hypersaline conditions and often dominate microbial communities in saltmarshes, salted lakes/soils and some oceanic areas. Some of the predominant species show denitrifying capabilities, although it remains unclear whether they are complete or partial denitrifiers. As complete denitrifiers, they could play important roles buffering ecosystems in which nitrate and nitrite appear as contaminants. However, partial denitrifying haloarchaea could contribute to the emission of nitrogenous gasses, thus acting as drivers of climate change and ozone depletion. In this review, we summarise some recent results on denitrification in haloarchaea, discuss the environmental implications and outline possible applications in mitigation. Finally, we list questions to be addressed in the near future, facilitating increased understanding of the role of these organisms in N turnover in arid and hypersaline environments.

doi: 10.1093/femsle/fnx270

TRABAJOS NO PUBLICADOS

UNPUBLISHED WORKS

APPENDIX 1

Haloferax mediterranei, an archaeal model for denitrification in saline systems, characterised through integrated phenotypic and transcriptional analyses

Javier Torregrosa-Crespo[a], Carmen Pire[a], Linda Bergaust[b] and Rosa María Martínez-Espinosa[a*]

[a]Departamento de Agroquímica y Bioquímica. División de Bioquímica y Biología Molecular. Facultad de Ciencias. Universidad de Alicante. Carretera San Vicente del Raspeig s/n - 03690 San Vicente del Raspeig, Alicante. E-mail: javitorregrosa@ua.es

[b]Faculty of Chemistry, Biotechnology and Food Science. Norwegian University of Life Sciences. Chr M Falsens vei 1 - 1430, Ås, Norway.

*Corresponding author: Rosa María Martínez-Espinosa

e-mail: rosa.martinez@ua.es

Telephone : +34 96 590 3400 ext. 1258; 8841

Fax: +34 96 590 3464

Abstract

*Haloferax mediterra*nei (R4) belongs to the group of halophilic archaea, one of the predominant microbial populations in hypersaline environments. In these ecosystems, the low availability of oxygen pushes the microbial inhabitants towards anaerobic pathways and the increasing concentrations of N-oxyanions favour denitrification. In a recent study comparing three *Haloferax* species carrying dissimilatory N-oxide reductases, *H. mediterranei* showed promise as a future model for archaeal denitrification. This work further explores the respiratory physiology of this haloarchaeon when challenged with ranges of nitrite and nitrate concentrations and at neutral or sub-neutral pH during the transition to anoxia. Moreover, to begin to unpick the transcriptional regulation of N-oxide reductases, detailed gas kinetics was combined with gene expression analyses at high resolution. The results show that *H. mediterranei* has an expression pattern similar to that observed in the bacterial Domain, well-coordinated at low concentrations of N-oxyanions. However, it could only sustain a few generations of exponential anaerobic growth, apparently requiring micro-oxic conditions for *de novo* synthesis of denitrification enzymes. This is the first integrated study within this field of knowledge in haloarchaea and Archaea in general, and it sheds lights on denitrification in salty environments.

Importance

Using *Haloferax mediterranei* as model organism, the present study means a very important advance in the knowledge of denitrification in hypersaline environments, which is scarce to date: on the one hand, it reveals the ability of this haloarchaeon to tolerate and reduce different concentrations of nitrates/nitrites (with potential biotechnological applications that it would have), the emission of NO_x gases (with important environmental consequences) and the need of minimum concentration of oxygen to denitrify in these ecosystems; on the other hand, the study presents the first analysis on gene expression at high resolution combined with detailed

gas kinetics during denitrification in extremophiles in general, and in Archaea domain in particular. Finally, proposing a theoretical model, the study lays the basis for the future studies on regulation of denitrification in these environments, that are increasingly predominant on Earth due to the effects of climate change and desertification.

Introduction

The ability to maintain a respiratory metabolism in lieu of oxygen is widespread. Among the many types of anaerobic dissimilatory pathways, denitrification is the most energetically profitable. Complete denitrification is the stepwise reduction of nitrate (NO_3^-) to dinitrogen (N_2) via nitrite (NO_2^-), nitric oxide (NO) and nitrous oxide (N_2O) (Zumft and Kroneck, 2006; Philippot *et al.,* 2007; Bakken *et al.*, 2012). Despite its ubiquity, our knowledge about the "nuts and bolts" of the process is based on detailed studies of a few model organisms, mainly proteobacteria with mesophilic lifestyles. The role of denitrification in nitrogen turnover and N-oxide emission have been studied at length in environments such as agricultural or forestry soils (Bru *et al.,* 2007; Samad *et al.,* 2016; Roco *et al.,* 2017). Less is known about saline and hypersaline ecosystems, where anaerobic respiration is prominent because the high salt concentrations result in low oxygen availability (Rodríguez-Valera *et al.,* 1985; Sherwood *et al.,* 1991; Sherwood *et al.,* 1992; Oren, 2013). Such systems are becoming increasingly interesting in terms of denitrification and N-oxide emissions because anthropogenic activities currently lead to contamination by nitrogenous compounds like nitrates and nitrites (Martínez-Espinosa *et al.,* 2007; Ochoa-Hueso *et al.,* 2014; Torregrosa-Crespo *et al.,* 2018). Moreover, their extent on a global scale is on the rise due to desertification, resulting from climate change (Torregrosa-Crespo *et al*., 2018).

Hypersaline environments accommodate representatives of all the three domains of Life, but when the salt concentration exceeds 16%, haloarchaea dominate (Andrei *et al.,* 2012; Edbeid *et al.,* 2016; Torregrosa-Crespo *et al.,* 2019). Among them are several denitrifiers and the microorganism that has emerged as a representative model is *Haloferax mediterranei*. It has the full set of metalloenzymes to catalyse the reduction of NO_3^- to N_2: the membrane-bound nitrate reductase facing the pseudo periplasm (NAR) (Lledó *et al.,* 2004; Martínez-Espinosa *et al.,* 2007), the copper-containing nitrite reductase (NIR) (Martínez-Espinosa *et al.,* 2006), the nitric oxide

reductase (NOR) (Torregrosa-Crespo *et al.,* 2017) and the nitrous oxide reductase (N_2OR) (Torregrosa-Crespo *et al.,* 2016). Currently, it is one out of very few archaea for which detailed phenotypic data exist, and it is the only one which has been shown to: i) be a complete denitrifier, able to reduce NO_3^- to N_2, and ii) display low and transient accumulation of the gaseous intermediates NO and N_2O (Torregrosa-Crespo *et al.,* 2019). This opens the door to further exploration of its respiratory physiology and regulation of denitrification.

Similar to its bacterial counterparts, *H. mediterranei* carry *nar, nir, nor* and *nos* gene clusters encoding the four structural enzymes of denitrification (Lledó *et al.,* 2004; Martínez-Espinosa *et al.,* 2006; Torregrosa-Crespo *et al.,* 2016). However, unlike some of the well-studied proteobacteria (Bergaust *et al.,* 2008, Qu *et al.,* 2016), little is known about the expression of the functional denitrification genes during the transition from aerobic to anaerobic respiration, or the effect of pH and electron acceptor concentrations on N-oxide accumulation. Through a combination of gene expression analyses and detailed physiological studies, this work begins to remedy this, finding evidence to suggest that regulatory similarities exist across domains. Thus, it bears implications for our understanding of denitrification in archaea in general, and in a representative of the halophilic community in particular.

Results

1. Effect of nitrate concentration on denitrification in *H. mediterranei*

H. mediterranei was exposed to different initial concentrations of nitrate (ranging from 2 mM to 2 M KNO_3) with 1 vol% initial O_2 in the headspace, and aerobic respiration and denitrification was monitored by frequent gas measurements (Molstad *et al.,* 2007). Nitrate concentrations did not severely affect the accumulation of gaseous intermediates during the oxic-anoxic transition or subsequent denitrification (Fig 1A, Table S1A). However, the two most extreme treatments (0.2 and 2M initial nitrate) led to a subtle increase in the transient NO peak following oxygen depletion (NO_{max}) as well as in the average NO concentration during balanced anaerobic growth (NO_{steady}). There was an approximate doubling and ten-fold increase in the accumulation of N_2O in 0.2 and 2 M cultures, respectively compared to 2-20 mM cultures, with observed N_2O_{max} of 0.21 ± 0.03 and 1.06 ± 0.08 µmol N_2O-N $vial^{-1}$ in the high nitrate cultures (Table S1A). The accumulation of nitrite ($NO_2^-{}_{max}$) increased with initial nitrate concentration up to 10 mM, but was apparently not affected beyond that point. The apparent decrease in cultures with 2 M initial nitrate most likely do not reflect the actual $NO_2^-{}_{max}$, because nitrite was still increasing at the end of the experiment (Fig 1A).

The e- flow towards terminal electron acceptors (Ve^-, µmol $vial^{-1}$ h^{-1}) was derived from the gas data and used to estimate the apparent specific growth rates during aerobic respiration and denitrification, μ_{oxic} and μ_{anoxic} h^{-1}, respectively. μ_{oxic} was largely unaffected by nitrate concentrations up to 0.2 M (μ_{oxic} = 0.201 ± 0.020 h^{-1}; average generation times G(t) ~ 3.5 h). However, cultures with 2 M nitrate displayed a clear decrease in μ_{oxic} (0.115 ± 0.019 h^{-1}) to a near doubling in G(t) (~6.0 h) (Fig 1B, Table S1B). Likewise, μ_{anoxic} and thus G(t) during denitrification was not significantly affected by nitrate within the range of 2-200 mM (Fig 1B, Table S1B, Fig S1), although a weak negative trend was observed (Fig S1, insert). However, the cultures with 2 M

nitrate showed a dramatic decrease in apparent anoxic growth rate, with an approximate 300% increase in average generation time relative to 2-200 mM cultures (Fig 1B).

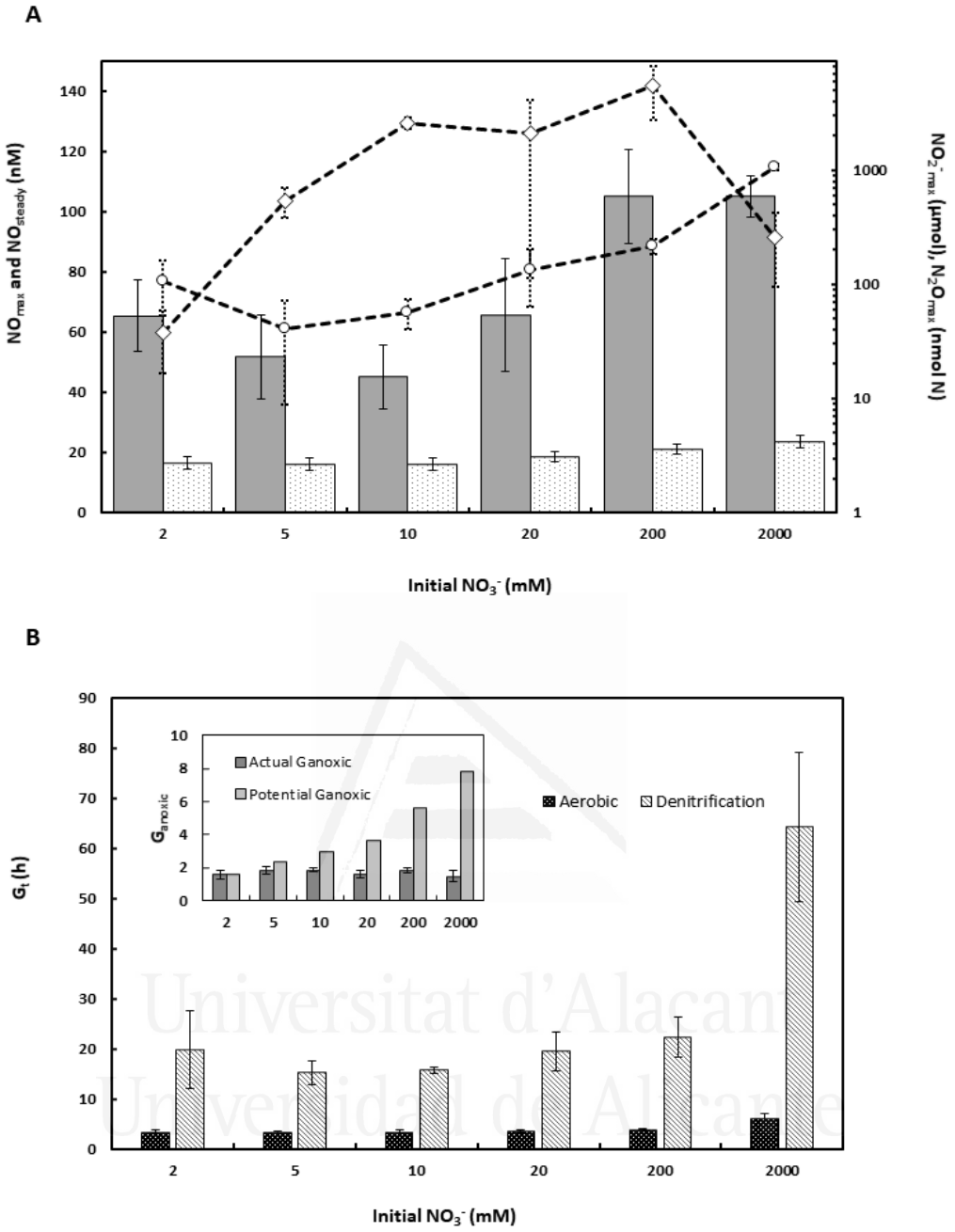

Figure 1. A) Accumulation of N-oxide intermediates during denitrification in *H. mediterranei* cultures supplemented with different initial KNO_3 concentrations (2-2000 mM). Bars, left y-axis: NO_{max} (grey bars) and NO_{steady} (dotted bars) (average NO concentration during exponential anaerobic growth), nM in liquid; plots, right y-axis (Log-scale): NO_2^- (diamonds) and N_2O_{max} (circles), µmol and nmol N $vial^{-1}$, respectively. **B)** Generation time (G_t, h) and duration of apparent exponential growth by denitrification in *H. mediterranei* supplemented with 2-2000 mM KNO_3. Main panel: generation time (h) during aerobic respiration (black bars) and denitrification (grey patterned bars), derived from apparent specific growth rates (µ h^{-1}). Oxic and anoxic µ h^{-1} were estimated based on the ln transformed e-flow rate to terminal electron acceptors during the exponential phase of oxygen respiration and denitrification, respectively. Insert: estimated actual (dark grey bars) and potential (light grey bars) generations of exponential growth by denitrification (G_{anoxic}) across nitrate treatments. For the cultures with 2 M nitrate, denitrification rate was still exponential at the end of the experiment, leading to a likely underestimation of actual G_{anoxic}.

The addition of high amounts of nitrate should support multiple generations of exponential anaerobic growth (G_{anoxic}), in proportion to initial nitrate concentration. However, regardless of the amount of nitrate available, *H. mediterranei* did not maintain exponential growth by denitrification beyond 1.5 to 2 generations (Fig 1B, insert). The electron flow (µmol e^- $vial^{-1}$ h^{-1}) towards NAR and NIR were derived from the gas data for cultures supplemented with 2, 5 and 10 mM KNO_3 respectively (Fig 2). In cultures with 2 mM nitrate (Fig 2A), both NAR and NIR rates increased exponentially until they stopped due to depletion of nitrate, whereas in cultures with 5 and 10 mM initial nitrate (Fig 2B and C), NIR reached a plateau stage first, while the relative NAR activity was still increasing. Towards the end of the incubations in cultures with 5 mM nitrate, NAR activity stopped before NIR due to nitrate depletion. The inserted panels show the ratio between the electron flow to NAR versus NIR, which should be 2 if the two enzymes operate at equal rates (2 electrons to reduce NO_3^- to NO_2^- and 1 electron to reduce NO_2^- to NO). In cultures supplemented with 2 mM KNO_3, the ratio was 2 during the incubation (Fig 2A, insert), whereas in the rest of the cultures it increased when the electron flow towards NIR reached the plateau (Fig 2B and C, inserts), reflecting higher NAR activity relative to NIR. Injection of O_2 and NO after decline in denitrification rates had no significant effect, although there was a slight increase in e- flow to N-oxides after addition of O_2 (Fig S2).

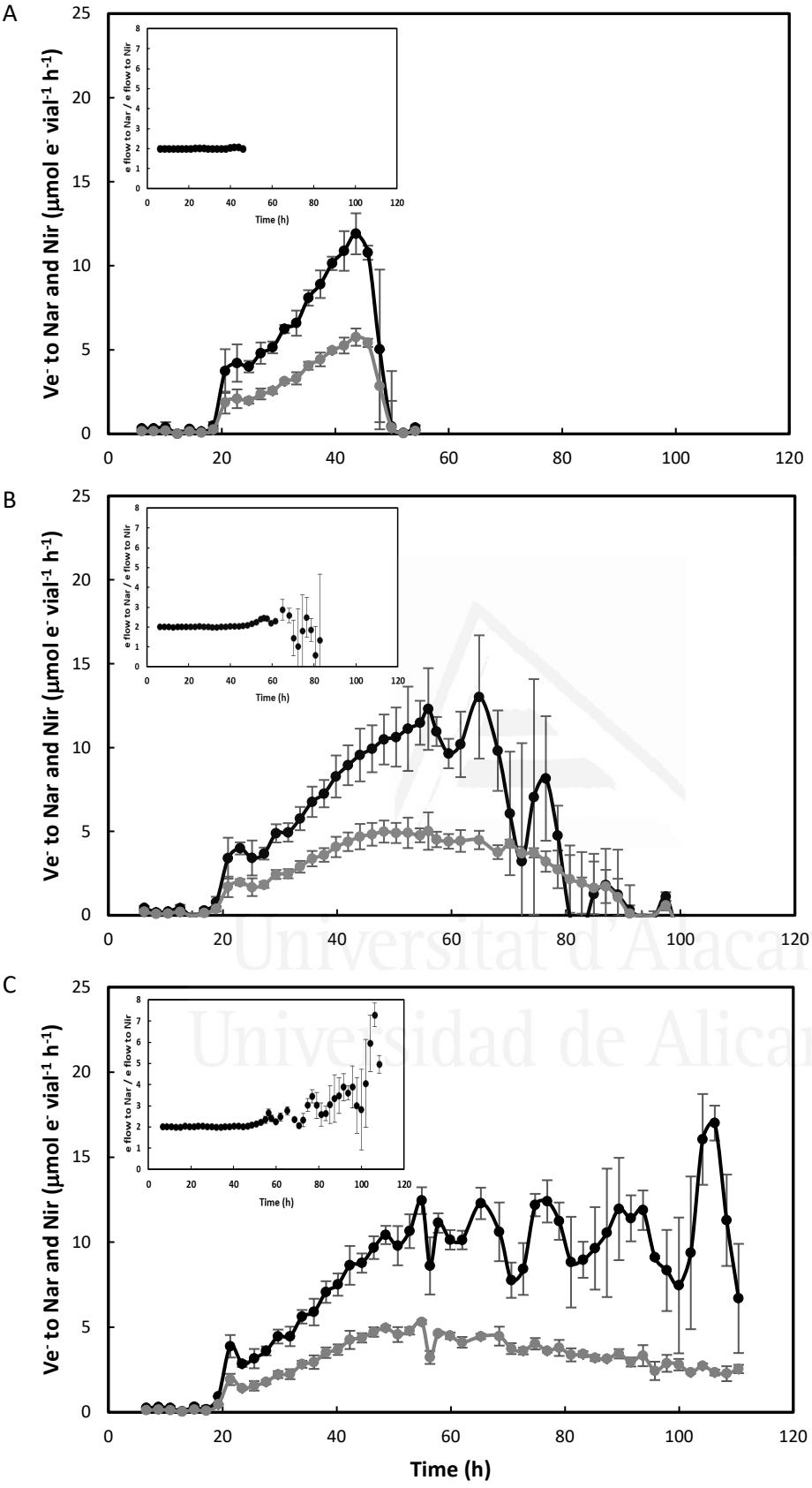

Figure 2. Electron flow (µmol e^- $vial^{-1}$ h^{-1}) to respiratory nitrate reductase (NAR – black lines) and nitrite reductase (NIR – grey lines) during the oxic-anoxic transition in batch cultures with 1% initial O_2 and different initial KNO_3 concentrations: 2 mM (top panel), 5 mM (mid panel), 10 mM (bottom panel). The inserts show the ratio between the electron flow to NAR and NIR using 2, 5, and 10 mM KNO_3, respectively

The 5 mM nitrate treatment was selected for further exploration of denitrification in *H. mediterranei*: effect of pH on denitrification and transcription of functional denitrification genes during transition to anoxia and subsequent anaerobic growth.

In order to test the effect of pH on denitrification, *H. mediterranei* was exposed to a range of pH levels (7.3, 7.0, 6.5, 6.0 and 5.7) using 100 mM Bis-Tris as buffer. *H. mediterranei* managed the transition to denitrification without any dramatic pH effects at pH ≥ 6.5, but at pH < 6.5, there was a general collapse of respiration upon oxygen depletion and the organism appeared unable to initiate denitrification (Table S2A).

2. Effect of nitrite concentration on denitrification in *H. mediterranei*

A set of experiments was carried out using nitrite (ranging between 1 and 40 mM) as an alternative electron acceptor in the presence of 1 vol% O_2 in headspace. The presence of nitrite had a negative effect on the O_2 consumption rate with an apparent log linear decline in μ_{oxic} with increasing nitrite concentration (slope: -0.032ln(x), R^2 = 0.961). Thus, while estimated μ_{oxic} in cultures with 1 mM initial nitrite was 0.119 ± 0.000 h^{-1} (approximately 50% of the observed rate in nitrite-free cultures), with 10 mM initial nitrite, the specific growth rate declined by approximately 76%, to 0.028 ± 0.004 h^{-1}. In cultures with 40 mM initial nitrite the inhibition was severe with a 98% decrease in apparent aerobic growth rate (0.002 ± 0.001 h^{-1}) (Fig 3A).

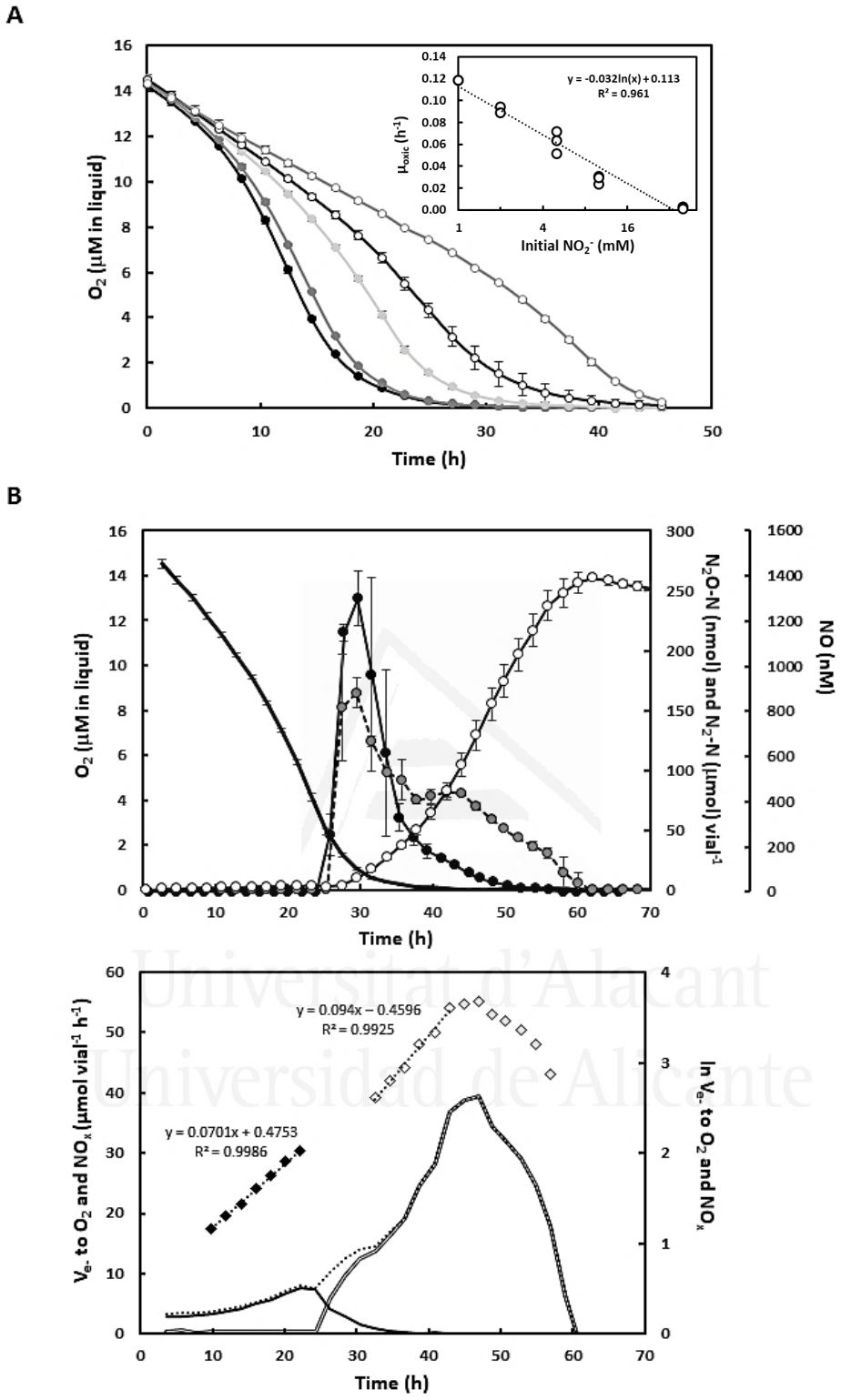

Figure 3. A) O_2 consumption during the incubation in the presence of 1 mM (black circles), 2 mM (dark grey circles), 5 mM (light grey circles), 10 mM (open black circles) and 40 mM KNO_2 (open grey circles). Insert: apparent specific anaerobic growth rates (μ_{anox} - h^{-1}) during log linear growth in the cultures with different initial KNO_2 concentrations. **B)** Gas kinetics and e-flow to terminal e-acceptors during transition to anoxia. Top panel: O_2 consumption (black line, no symbols) and accumulation of N-oxides (NO - closed black circles; N_2O – closed grey circles; N_2 – open circles) with 1% initial O_2 in headspace and 5 mM KNO_2 in the medium (n=3). Bottom panel: e-flow (µmol $vial^{-1}$ h^{-1}) to O_2 (black line) and N-oxides (double black line) for the respective KNO_2 concentrations.

During the anoxic phase at initial nitrite concentrations between 1 and 5 mM, *H. mediterranei* reduced all the available NO_2^- to N_2. However, in the presence of 5 mM KNO_2, the maximum concentration of nitric oxide increased significantly (to approximately 1.4 μM) (Fig 3B). The apparent anoxic growth rate was equal when comparing cultures with 2 and 5 mM of KNO_2 (μ_{anoxic} between 0.09 and 0.10 h^{-1} respectively). However, in the latter, exponential growth ceased prematurely, while more than half of the added nitrite remained. Denitrification continued, as seen in nitrate treated cultures, with declining e^- flow rates to N-oxides until nitrite depletion (Fig 3B). Finally, for the highest concentrations of nitrite tested (10 and 40 mM KNO_2), *H. mediterranei* accumulated high concentrations of NO (up to 18 μM in the liquid), with subsequent arrest in respiration (Fig S3).

Using nitrite as final electron acceptor (2 mM), the effect of pH in the slightly acidic to near- neutral range (5.7-7.3) was tested. In this case, low pH resulted in increased maximum concentrations of NO, reaching 490 nM and 960 nM at pH 7.3 and 6.5, respectively (Table S2B). At pH 6.5, some cultures were unable to respire nitrite after O_2 depletion, whereas at pH < 6.5 both aerobic and anaerobic respiration failed.

3. Transcription of *narG, nirK, norZ* and *nosZ* genes during O_2 depletion and subsequent denitrification.

The transcription of *narG, nirK, norZ* and *nosZ* was monitored alongside gas kinetics and NO_2^- accumulation during the transition from aerobic to anaerobic respiration, and the conspicuous decline in growth rate during late anoxia. The cultures were supplemented with 5 mM initial KNO_3 and 1 vol% initial O_2.

The observed gas kinetics were as expected for *H. mediterranei* under the relevant conditions (Torregrosa-Crespo *et al.,* 2019). It reduced all available nitrate to N_2 with minimal and transient accumulation of intermediates. Denitrification was initiated at low O_2 (2.49 ± 0.28 µM in liquid), as seen by transient peaks of NO and N_2O (NO_{max}: 51.02 ± 0.63 nM; N_2O_{max}: 95.13 ± 5.97 nM), which dropped to background semi-steady state levels that were maintained until depletion of N-oxides. As seen previously, N_2 increased exponentially during early anoxia, then at linear or declining rate until depletion of added nitrate (Fig 4, top panel). The activity of NirK (seen as e- flow to nitrite, µmol $vial^{-1}$ h^{-1}), slowed prior to, and more dramatically than Nar (Fig 4, bottom panel), which led to transient nitrite accumulation ($NO_2^-{}_{max}$: 67.56 µM $vial^{-1}$) during late anoxia (Fig 4, top panel).

The structural denitrification genes showed contrasting expression profiles. Unlike *nirK* and *norZ* whose expression showed a slight decline during the first 10 hours of the incubation, *narG* and *nosZ* transcription both increased by an order of magnitude within the first 3 h after inoculation and remained elevated throughout the semi-aerobic phase (Fig 4, middle panel). Immediately before the transient NO and N_2O peaks, *narG* and *nosZ* transcription increased by another order of magnitude, peaking at 7.5E4 ± 7.3E2 and 9.2E4 ± 4.0E4 copies ng^{-1} RNA, respectively. Transcription of *narG* subsequently decreased and was kept at a reasonably

constant number (4.9E3 ± 1.7E3 copies ng^{-1} RNA) during the anoxic phase. As NO peaked, *nosZ* reached a maximum of 1.8E5 ± 4.1E4 copies ng^{-1} RNA. This coincided with high expression of *nirK* and *norZ*, which both increased from background levels (fluctuating around 1E2 copies ng^{-1} RNA) to 2.9E5 ± 8.9E4 and 1.4E5 ± 2.0E4 copies ng^{-1} RNA, respectively. The *nirK, norZ* and *nosZ* transcription maxima were followed by a period of exponential N_2 accumulation, during which the expression of all three genes gradually dropped by an order of magnitude. As the apparent growth rate by denitrification declined, resulting in linear N_2 accumulation after approximately 40 hours, the transcription of denitrification genes showed a subtle, albeit variable increase, particularly visible in *nirK*. Gene expression dropped to low levels (1E0-1E3 copies ng^{-1} RNA) after nitrate depletion (78 hours).

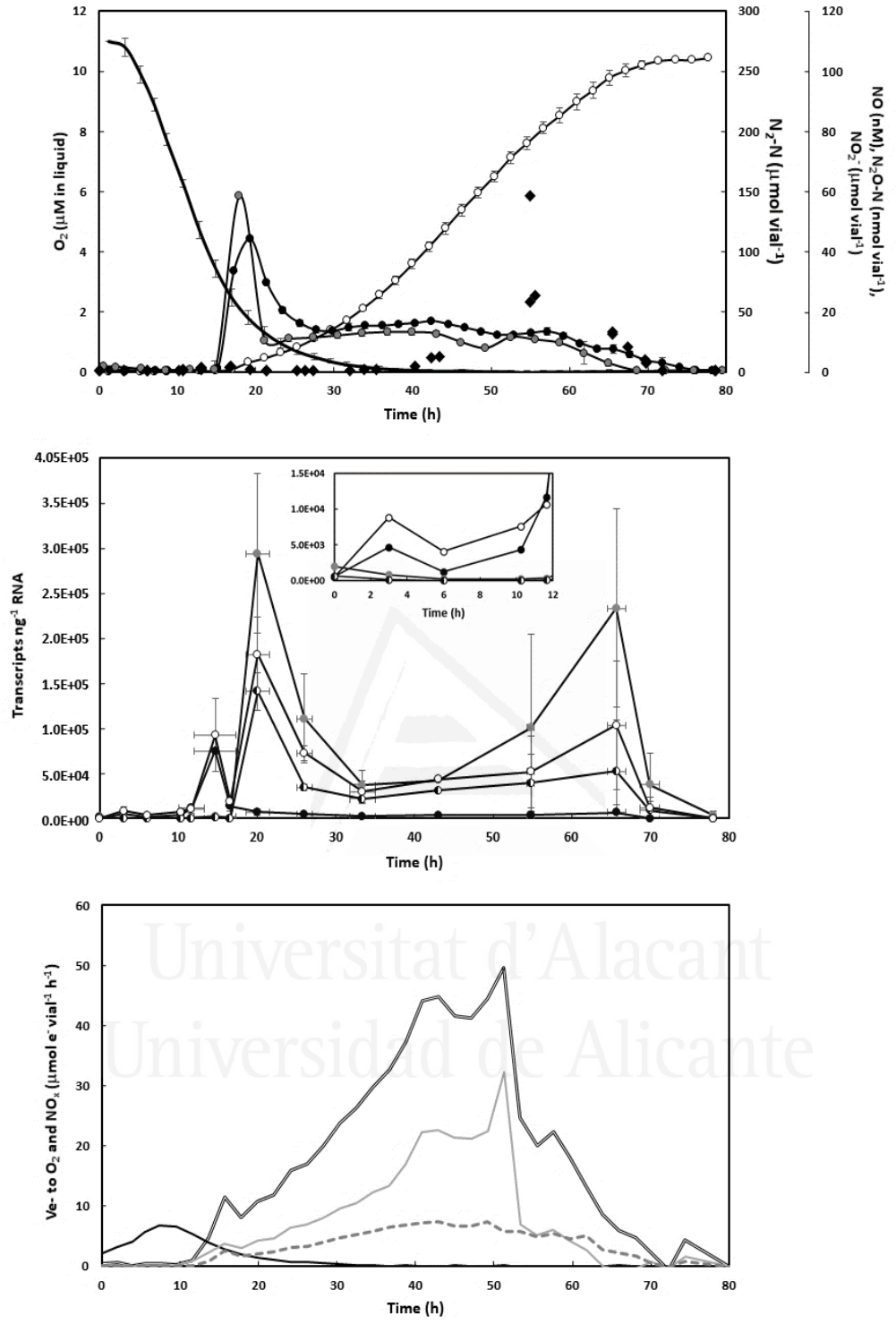

Fig. 4. Gas kinetics, gene transcription and electron flow through the transition from aerobic to anaerobic respiration. Top panel: consumption of O_2 (black line, no symbols) and subsequent accumulation of N-oxides (NO – closed black circles; N_2O – closed grey circles; N_2 – open circles) in nitrate-supplemented medium (5mM KNO_3) with 1% initial O_2 in headspace (*n=3*). Middle panel: number of gene transcripts per nanogram RNA which is shown with standard deviation as vertical lines (*n=3*) (*narG* – closed black circles; *nirK* – closed grey circles; *norZ* – half white and half black circles; and *nosZ* – open white circles). The large deviations were due to an overall higher signal during active denitrification from one of the three replicate series. The sample at time 0 is the result for the inoculum (prior to inoculation). Bottom panel: electron flow (µmol $vial^{-1}$ h^{-1}) to O_2 (black line), nitrate reductase (grey line), nitrite reductase (discontinuous grey line) and total N-oxides (double black line).

4. N_2OR activity during the semi-aerobic phase

The early expression of *nosZ* begs the question whether N_2OR is active in the presence of µM concentrations of O_2, preceding the "upstream" enzymes NIR and NOR. To test this, aerobically raised cells were transferred to vials injected with approximately 1 vol% each of O_2 and N_2O in headspace, and containing 5 mM KNO_3 in the medium. Due to differences in solubility, the initial concentrations of O_2 and N_2O in the liquid were approximately 9 and 20 µM, respectively. During the first 8 h after inoculation, the decrease in N_2O was chiefly attributable to dilution by sampling. However, as O_2 concentration reached approximately 50 % of the initial concentration (4.13 µM in liquid), N_2O was rapidly reduced and its exhaustion coincided with the appearance of NO (Fig 5). The O_2 and N_2O reduction rates were used to estimate the respective electron flow rates (Ve^-, µmol e^{-1} $vial^{-1}$ h^{-1}) to O_2 and N_2O (Fig 5, insert). Initially, the electron flow was directed towards O_2 as the only terminal acceptor. However, following the peak in Ve- to O_2 (at approximately 9 hours) Ve- to N_2O increased and peaked while Ve- to O_2 was still at approximately 50% of the observed maximum. Thus, there was parallel respiration of O_2 and N_2O for several hours, apparently preceding induction of NIR (NO increase), reflecting the observed early transcription of *nosZ*.

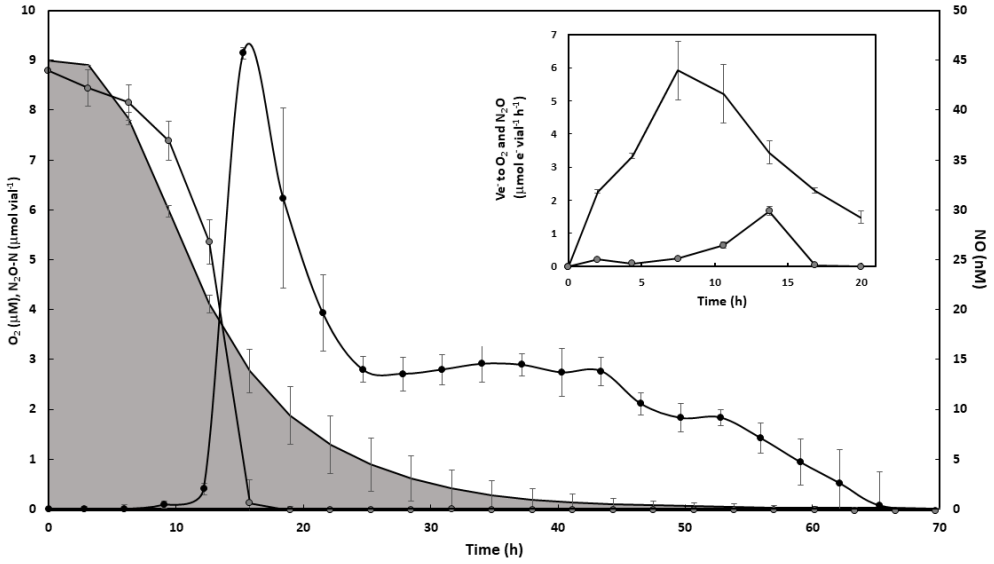

Fig. 5. Aerobic N_2O reduction in aerobically pre-cultured cells with 1% N_2O and O_2 injected in the headspace. Main panel: O_2 concentration in liquid (μM, shaded area), N_2O-N μmol $vial^{-1}$ (grey circles) and NO nM in liquid (black circles). Standard deviation (*n=4*) is shown as vertical lines. Insert: estimated rates of electron flow (Ve^-, μmol e^- $vial^{-1}$ h^{-1}) to O_2 (black line, no symbol) and N_2O (grey circles) during the first 20 hours of incubation.

Discussion

Denitrifying organisms are widespread and highly diverse. Even so, detailed studies of their physiology and biochemistry have chiefly been limited to a relatively small number of bacteria with mesophilic lifestyles. Thus, the knowledge of this pathway in extremophilic microorganisms, especially archaea, is scarce. Recently, *H. mediterranei* was identified as a promising candidate model organism for haloarchaeal denitrification (Torregrosa-Crespo *et al.,* 2019) and the present study elaborates on its respiratory physiology.

H. mediterranei maintained aerobic growth in the presence of high nitrate (mM to M) and mM nitrite concentrations, although negatively affected by the latter (Figs 3A and S1). During the transition to denitrification and subsequent nitrate/nitrite respiration, it displayed a robust phenotype in terms of accumulation of N-oxide intermediates at near-neutral pH and with mM concentrations of N-oxyanions in the medium. Initial nitrate concentration had little effect on transient NO accumulation and no discernible effect on the NO concentration during the anoxic phase (Fig 1A), reflecting a well-orchestrated denitrification apparatus tuned to control the accumulation of the most toxic intermediate. In contrast, and not unexpectedly, high initial nitrite concentrations did have a clear positive effect on NO accumulation. Even so, NO toxicity apparently only came into play for the highest concentrations tested, in which case it lead to complete arrest (10 and 40 mM – Fig S3). Thus, *H. mediterranei* is an organism showing a tolerance to nitrite like most heterotrophic denitrifers (Chen *et al.,* 2008; Chen *et al.,* 2009; Nájera-Fernández *et al.* 2012).

H. mediterranei was robust when facing high N-oxyanion concentrations in near-neutral medium (pH = 7.3) but was sensitive to acidification. When pH decreased from 7.3 to 6.5 in cultures supplemented with nitrate, there was an apparent generalized inhibition of all the N-

oxide reductases (Table S2A). This contrasts with other denitrifiers, such as *P. denitrificans*, where sub-neutral pH affects the function of N_2OR more than the rest of the denitrification enzymes (Bergaust *et al.,* 2010). When nitrite was added to the medium, *H. mediterranei* could not grow at the lowest pH values (6.0 and 5.7). In these cultures, cells could not even consume O_2 as final electron acceptor. This may have been due to the formation of toxic substances, a candidate being nitrous acid (HNO_2) derived from the protonation of nitrite at low pH (Almeida *et al.,* 1995; Reddy *et al.,* 1983).

A striking phenotypic trait was the conspicuous and reproducible decline in apparent specific growth rate after 1.5 to 2 generations of anoxic growth, irrespective of remaining nitrate/nitrite in the medium. This likely reflected lack of *de novo* synthesis of denitrification enzymes and thus dilution of per cell concentrations of the N-oxide reductases during subsequent cell division. From the observed accumulation of nitrogenous gases, and a steady increase in nitrite during late anoxia (Fig 2 and 4, upper panel), restraint of NIR synthesis appeared to marginally precede, and be more dramatic than, the decline in NAR synthesis. Moreover, the subsequent declining rate of e- flow towards NIR indicate net degradation of the existing enzyme pool. This effect was less dramatic in NAR, suggesting that the enzyme is less prone to degradation under these conditions. Lack of *de novo* synthesis would not necessarily result in any immediate decline in cell growth. This would depend on the margin by which the actual number of proteins per cell exceeds the critical number required to operate the metabolic machinery at normal rate. Cell/biomass yield per mole nitrate reduced to N_2 was not significantly affected by denitrification rate (Fig S4). However, in complex systems, failure to maintain *de novo* synthesis of denitrification enzymes would likely be a competitive disadvantage.

The observation that NAR outperforms NIR is reconcilable with previous work showing that the haloarchaeal NAR is a robust enzyme operating at high rates (Lledó *et al.,* 2004; Martínez-Espinosa *et al.,* 2007). However, the mechanisms underlying the apparent failure to maintain exponential growth (as seen by the activity of the enzyme pool) during denitrification (Fig 1B) are elusive. The transcription data (Fig 4) rule out any direct downregulation of N-oxide reductase genes, and the decline was clearly not caused by nitrate limitation because it occurred irrespective of residual nitrate (up to high mM range) in the medium. Moreover, it was unlikely to be due to lack of nutrients because i) the experiments were conducted in complex medium, and ii) previous results show that in cultures with higher initial oxygen (7 vol%) and thus higher cell density, 5 mM nitrate was reduced to N_2 without any premature decline in growth rate (Fig S5). However, in contrast to cultures with 1% initial O_2, cultures with 7% O_2 depleted the available nitrate while conditions remained micro-oxic. Inspection of gas data from cultures with 1% initial O_2 show that the decline in anaerobic growth rate typically co-occurs with O_2 exhaustion ($[O_2] < 0.1$ µM in liquid). However, if micro-oxic conditions are required for *de novo* synthesis of N-oxide reductases, the critical threshold is likely considerably higher than 0.1 µM O_2 because any observable effect would be delayed. The apparent O_2 threshold for induction of denitrification increases with initial concentration and has been observed to be > 20 µM in cultures with 7% initial O_2. In such cultures, O_2 still remained at concentrations of approximately 5 µM in the liquid at depletion of N-oxides (Fig S5). Put together, the data suggest that *H. mediterranei* requires the presence of low µM concentrations of O_2 for *de novo* synthesis of denitrification enzymes (NAR and NIR), and that this regulation/effect is post-transcriptional. In fact, we did observe a slight increase in e- flow to N-oxides after O_2 injection to anaerobic cultures (Fig S2).

To begin unpicking the transcriptional regulation of denitrification in *H. mediterranei,* we quantified the expression of *narG, nirK, norZ* and *nosZ* during the oxic-anoxic transition and subsequent anaerobic growth. Sampling was guided by observed gas kinetics, yielding a high-resolution profile of gene expression vs denitrification activity. Both *narG* and *nosZ* appeared to be induced directly by hypoxia and did not require the presence of NO or nitrite for expression (Fig 4). Thus, *narG* and *nosZ* are likely activated via an oxygen (and possibly nitrate) sensor. The negative regulation of NAR by O_2 via O_2-sensing transcription factors is common in denitrifying bacteria (Spiro, 2012) and has also been observed for N_2OR (Bergaust *et al.,* 2010 and 2012). In *H. mediterranei*, the AcrR-like transcriptional regulator occupies the same position as the NarO regulator in *H. volcanii*, recently identified as a putative O_2 sensor in this strain (Hattori *et al.,* 2016). The "core" reductases, NIR and NOR, were not induced by hypoxia alone, but apparently required the presence of NO (and possibly nitrite). The appearance of NO also coincided with a second peak in *nosZ* transcription. Thus, *nirK, norZ* and *nosZ* all appear to be under the control of unknown NO/nitrite sensor(s), again resembling bacterial denitrifiers in their regulatory circuits (van Spanning *et al.,* 1999; Zumft, 2002). Positive *nirK* regulation by nitrite may underlie the second peak in *nirK* expression during late anoxia when nitrite accumulates (Fig 4). Due to the sequential nature of denitrification, it seems intuitive that the synthesis of N-oxide reductases follows the same order. This has been shown to not always be the case in bacteria, where N_2OR activity may precede NIR and NOR during the transition to anoxia (Qu Z, *et al.,* 2016). *H. mediterranei* displayed a similar phenotype where active N_2OR was produced during the semi-aerobic phase, independent of NO/nitrite induction (Fig 5). The transcriptional regulation of denitrification in *H. mediterranei* is tentatively summarized in Figure 6.

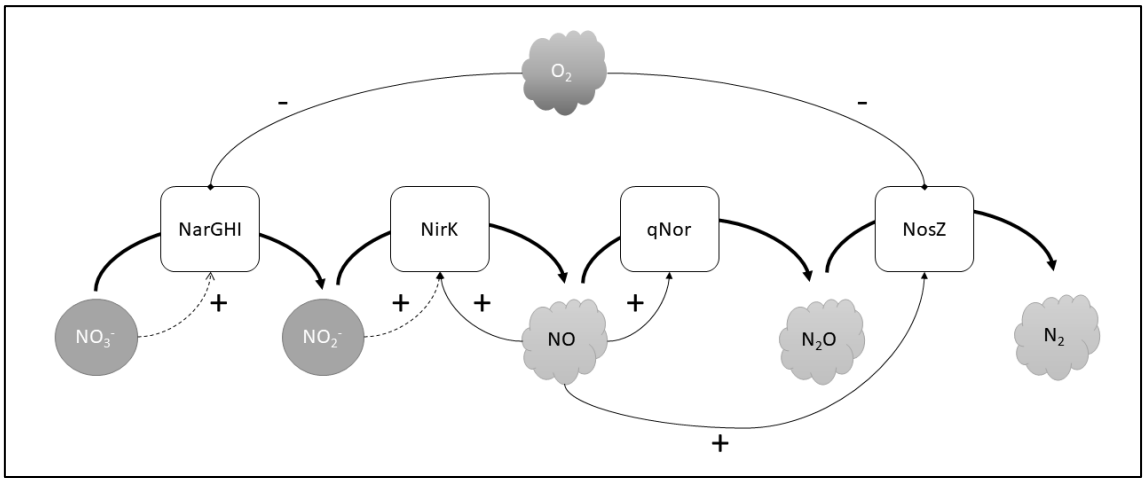

Figure 6. Tentative regulatory model of denitrification in *H. mediterranei*. (+) means a positive regulation; (-) means negative regulation.

H. mediterranei emerges as a suitable model organism for the study of denitrification in saline and hypersaline environments. It tolerates the presence of high concentrations of nitrates and nitrites at optimum pH but appears to require micro-oxic conditions to sustain anaerobic growth by denitrification. It shows, as previous studies point out (Chen & Strous, 2013), that denitrification is not an entirely anaerobic process in all organisms. However, more studies will be needed to confirm the hypothesized requirement for oxygen for *de novo* synthesis of N-reductases. *H. mediterranei* appears to have many regulatory traits in common with its bacterial counterparts, but in-depth molecular, physiological and biochemical studies are still needed to understand the respiratory metabolism of this extremophile.

Experimental procedures

(i) Physiological experiments testing different NO_3^- and NO_2^- concentrations and pH values.

Culturing conditions.

H. mediterranei (R4) was raised in complex medium (20% (w/v) mixture of salts and 0.5% (w/v) yeast extract) (Rodríguez-Valera *et al.,* 1980; DasSarma *et al.,* 1995), pH 7.3 at 35°C under aerobic conditions, with vigorous stirring (700 rpm) using a triangular magnetic stirring bar (Cowie 25 x 8 mm, VWR International) to ensure full dispersal of cells and oxic conditions. Moreover, the aerobic pre-cultures were never allowed to grow beyond densities of 1.94×10^8 cells ml^{-1}.

Aerobic pre-cultures were transferred to 120 ml serum vials containing a triangular magnetic stirring bar and 50 ml of complex medium at 35°C. All cultures were continuously stirred at 700 rpm, avoiding aggregation. The media contained different KNO_3 or KNO_2 concentrations depending on the assay: 2, 5, 10, 20, 200 and 2000 mM KNO_3; 1, 2, 5, 10 and 40 mM KNO_2. The pH was 7.3 (optimum for *H. mediterranei*) for all the experiments and the media were always buffered with Bis-Tris 100 mM. The different pH values for the experiments to test the effect of this factor on denitrification were: 7.3, 7.0, 6.5, 6.0, and 5.7.

Vials were crimp sealed with rubber septa (Matriks AS, Norway) and aluminium caps to ensure an airtight system. The vials were made anoxic by repeated cycles of evacuation and helium (He) filling with constant stirring to ensure optimal gas exchange between liquid and headspace. The initial availability of gaseous electron acceptors was then adjusted by injection of pure O_2. All experiments were performed at atmospheric pressure and 35°C.

Gas measurements.

The gas measurements were done in a robotized incubation system similar to that described by Molstad and colleagues (2007), with some improvements. The system monitored the headspace concentrations of relevant gases (O_2, CO_2, NO, N_2O and N_2) by repeated gas sampling through the butyl rubber septa of the incubation vials (30 stirred vials). The gas samples were drawn by a peristaltic pump coupled to an autosampler (Agilent GC Sampler 80), and with each sampling an equal volume of He was pumped back into the vials. This secured that the gas pressure was sustained near 1 atm despite repeated sampling but diluted the headspace atmosphere (with He). This dilution was considered when calculating the rates of production/consumption for each time increment (see Molstad *et al.,* 2007 for details). The sampling system was coupled to a gas chromatograph (GC) (Agilent GC – 7890A) with 30 m 0.53 mm id columns: a porous layer open tubular (PLOT) column for separation of CH_4. NO was measured by a chemiluminescence NO_x analyser (M200A or M200E, Teledyne).

Nitrite was measured by injecting 10 µl liquid sample into a purge vessel containing 3 ml reducing agent, (NaI, 1% w/v in acetic acid) connected to a chemiluminescence detector (Nitric Oxide Analyzer NOA 280i, General Electric). N_2 was continuously bubbled through the reducing agent to maintain an anoxic environment in the system and to transport the NO through the NO analyser (Walters *et al.,* 1987).

(ii) Gas kinetics and transcription of *narG, nirK, norZ* and *nosZ* genes during O_2 depletion and subsequent denitrification.

A total of 15 anoxic vials containing media supplemented with 5 mM KNO_3 were injected with pure O_2 to approximately 1 vol% in headspace and then inoculated with $2 \cdot 10^8$ cells from aerobic pre-cultures. Cultures were placed in the robotized incubation system at 35°C, with continuous stirring at 700 rpm, and the gas kinetics in each vial was monitored by headspace

measurements (1- to 3-h intervals). Samples for gene expression analysis (50, 10, 5 or 2 ml depending on cell density) were harvested at frequencies guided by the observed gas kinetics; at each time, cells were taken from three separated vials and considered biological replicates. Entire vials were sacrificed for 50 and 10 ml samples, whereas a maximum of two 5 ml samples were taken before vials were excluded from further gas measurements. Nitrite concentration and cell densities (OD_{600}) were measured for each sample. Three replicates were left undisturbed by liquid sampling and only headspace gases were monitored.

Gene expression analysis.

Guided by the observed gas kinetics, samples (50, 10, 5 or 2 ml, depending on cell density) were taken from the liquid phase of the vials throughout the experiment, as well as from the inoculum (time: 0 h). Samples were transferred to chilled, sterile 50 or 2 ml centrifugation tubes. One millilitre of the sample was taken to measure OD_{600} and NO_2^- concentration. The remaining sample volume was pelleted by centrifugation (10000 x g, 10 min) at 4°C. The supernatant was decanted, and 1 ml of a mixture of RNA protect Bacteria Reagent (Qiagen) with salty water 30% w/v in a 1:1 ratio was added to the cell pellet. After treatment with RNAprotect, the cells were pelleted once more by centrifugation (10000 x g, 10 min) at room temperature and then stored at -20°C awaiting RNA extraction. Due to the considerable number of samples, the biological replicates were divided into three times series; RNA extraction and DNAse treatment were done in three rounds, whereas for reverse transcription, all samples were collected and processed in one round. Total RNA was extracted from all samples using the RNeasy Mini Kit (Qiagen) and residual DNA removed by DNase treatment (TURBO DNA-free, Ambion) according to the suppliers' instructions. The concentration of total RNA was measured using the Qubit RNA BR assay and a Qubit fluorometer (Invitrogen). Absence of gDNA was confirmed in each sample by real-time PCR targeting the *norZ* gene, using RNA that had not been reverse transcribed. Reverse

transcription was performed using a SuperScript VILO cDNA Synthesis Kit (Invitrogen). Droplet Digital PCR (ddPCR) was performed on a QX200 Droplet Digital PCR (ddPCR^{TM}) System (Bio-Rad) using Bio-Rad's QX200 ddPCR EvaGreen supermix and primers to target *narG, nirk, norB* and *nosZ* (Table S3). The expression of each gene was calculated by absolute quantification. ddPCRs were set up in technical triplicate for each of the three biological replicates and normalized by (RNAtotal) ng sample^{-1}.

(iii) Aerobic N_2O reduction in early denitrification

Pre-culturing and gas measurements of batch cultures were carried out as described in the physiological experiments section. The aerobically raised cells were transferred to He-rinsed vials containing 50 ml complex medium with 5 mM KNO_3, and with 1 vol% O_2 100 ppmv N_2O (in triplicate). Cell-free vials were also included in triplicate for each treatment to provide accurate estimates of sampling dilution. Gas kinetics was monitored every 3.6 h in the robotized incubation system described under *Gas measurements*.

Acknowledgements

This work was funded by research grant from the MINECO Spain (CTM2013-43147R), VIGROB-309 (University of Alicante) and Generalitat Valenciana (ACIF 2016/077). J. Torregrosa-Crespo was financed by the European Molecular Biology Organization (EMBO – Short Term Fellowship ASTF No: 331-2016) to carry out the experiments at the Norwegian University of Life Sciences (NMBU). L Bergaust was funded by The Research Council of Norway (project no 275389).

Author contributions

The design of the experiments was conducted by LB and JTC. The experiments were done by JTC. Results were analyzed by LB and JTC. All the authors contributed to the discussion of the results and manuscript writing.

References

Almeida, J.S., Júlio, S.M., Reis, M.A.M., and Carrondo, M.J.T. (1995) Nitrite inhibition of denitrification by *Pseudomonas fluorescens*. *Biotech Bioeng* 46: 194-201.

Andrei, A.S., Banciu, H.L., and Oren, A. (2012) Living with salt: metabolic and phylogenetic diversity of archaea inhabiting saline ecosystems. *FEMS Microbiol Lett* 330: 1-9.

Bakken, L.R., Bergaust, L., Liu, B., and Frostegård, Å. (2012) Regulation of denitrification at the cellular level: a clue to understanding N_2O emissions from soils. *Philos Trans R Soc Lond B Biol Sci* 367: 1226-1234.

Bergaust, L., Shapleigh, J., Frostegård, Å., and Bakken, L.R. (2008) Transcription and activities of NOx reductases in *Agrobacterium tumefaciens*: the influence of nitrate, nitrite and oxygen availability. *Environ Microbiol* 10: 3070-3081.

Bergaust, L., Mao, Y., Bakken, L.R., and Frostegård, Å. (2010) Denitrification response patterns during the transition to anoxic respiration and posttranscriptional effects of suboptimal pH on nitrogen oxide reductase in *Paracoccus denitrificans*. *App Environ Microbiol* 76: 6387-6396.

Bergaust, L., van Spanning, R.J., Frostegård, Å., and Bakken, L.R. (2012) Expression of nitrous oxide reductase in *Paracoccus denitrificans* is regulated by oxygen and nitric oxide through FnrP and NNR. *Microbiology* 158: 826-834.

Bru, D., Sarr, A., and Philippot, L. (2007) Relative abundances of proteobacterial membrane-bound and periplasmic nitrate reductases in selected environments. *App Environ Microbiol* 73: 5971-5974.

Chen, J., and Strous, M. (2013) Denitrification and aerobic respiration, hybrid electron transport chain and co-evolution. *Biochim Biophys Acta* 1827: 136-144.

Chen, C., Wang, A., Ren, N.Q., Kan, H., and Lee, D.J. (2008) Biological breakdown of denitrifying sulfide removal process in high-rate expanded granular bed reactor. *Appl Microbiol Biotechnol* 81: 765-770.

Chen, C., Wang, A.J., Ren, N.Q., Lee, D.J., and Lai, J.Y. (2009) High-rate denitrifying sulfide removal process in expanded granular sludge bed reactor. *Bioresour Technol* 100: 2316-2319.

DasSarma, S., Fleischman, E.M., and Rodríguez-Valera, F. (1995) Media for halophiles. In Archaea, a laboratory manual. DasSarma, S., and Fleishman, E.M. (eds). ColdSpring Harbor, New York, USA, pp. 225-230.

Edbeib, M.F., Wahab, R.A., and Huyop, F. (2016). Halophiles: biology, adaptation, and their role in decontamination of hypersaline environments. *World J Microbiol Biotechnol* 32: 1-23.

Hattori, T., Shiba, H., Ashiki, K., Araki, T., Nagashima, Y., Yoshimatsu, K., and Fujiwara, T. (2016) Anaerobic growth of haloarchaeon *Haloferax volcanii* by denitrification is controlled by the transcription regulator NarO. *J Bacteriol* 198: 1077-1086.

Martínez-Espinosa, R.M., Richardson, D.J., Butt, J.N., and Bonete, M.J. (2006) Respiratory nitrate and nitrite pathway in the denitrifier haloarchaeon *Haloferax mediterranei*. *Biochem Soc Trans* 34(Pt 1): 115-117.

Martínez-Espinosa, R.M., Dridge, E.J., Bonete, M.J., Butt, J.N., Butler, C.S., Sargent, F., and Richardson, D.J. (2007) Look on the positive side! The orientation, identification and bioenergetics of "Archaeal" membrane-bound nitrate reductases. *FEMS Microbiol Lett* 276: 129-139.

Molstad, L., Dörsch, P., and Bakken, L.R. (2007) Robotized incubation system for monitoring gases (O_2, NO, N_2O, N_2) in denitrifying cultures. *J Microbiol Meth* 71: 202-211.

Nájera-Fernández, C., Zafrilla, B., Bonete, M.J., and Martínez-Espinosa, R.M. (2012) Role of the denitrifying Haloarchaea in the treatment of nitrite-brines. *Int Microbiol* 15: 111-119.

Lledó, B., Martínez-Espinosa, R.M., Marhuenda-Egea, F.C., and Bonete, M.J. (2004) Respiratory nitrate reductase from haloarchaeon *Haloferax mediterranei*: biochemical and genetic analysis. *Biochim Biophys Acta* 1674: 50-59.

Ochoa-Hueso, R., Arrónez-Crespo, M., Bowker, M.A., Maestre, F.T., Pérez-Corona, M.E., Theobald, M.R., *et al.* (2014) Biogeochemical indicators of elevated nitrogen depositions in semiarid Mediterranean ecosystems. *Environ Monit Assess* 186: 5831-5842.

Oren, A. (2013) Life at high salt concentrations, intracellular KCl concentrations and acidic proteomes. *Front Microbiol* 4: 1-6.

Philippot, L., Hallin, S., and Schloter, M. (2007) Ecology of denitrifying prokaryotes in agricultural soil. *Adv Agron* 96: 249-305.

Qu, Z., Bakken, L.R., Molstad, L., Frostegård, Å., and Bergaust, L.L. (2016) Transcriptional and metabolic regulation of denitrification in *Paracoccus denitrificans* allows low but significant activity of nitrous oxide reductase under oxic conditions. *Environ Microbiol* 18: 2951-2963.

Reddy, D., Lancaster, J.R., and Cornforth, D.P. (1983) Nitrite inhibition of *Clostridium botulinum:* electron spin resonance detection of iron-nitric oxide complexes. *Science* 221:769-770.

Roco, C.A., Bergaust, L.L., Bakken, L.R., Yavitt, J.B., and Shapleigh, J.P. (2017) Modularity of nitrogen-oxide reducing soil bacteria: linking phenotype to genotype. *Environ Microbiol* 19: 2507-2519.

Rodríguez-Valera, F., Ruiz-Berraquero, F., and Ramos-Cormenzana, A. (1980) Behaviour of mixed populations of halophilic bacteria in continuous cultures. *Can J Microbiol* 26: 1259-1263.

Rodríguez-Valera, F., Ventosa, A., Juez, G., and Imhoff, J.F. (1985) Variation of environmental features and microbial populations with salt concentration in a multi-pond saltern. *Microb Ecol* 11: 107-115.

Samad, M.S., Bakken, L.R., Nadeem, S., Clough, T.J., de Klein, C.A., Richards, K.G., Lanigan, G.J., and Morales, S.E. (2016) High-resolution denitrification kinetics in pasture soils link N_2O emissions to pH, and denitrification to C mineralization. *PLoS One* 11(3):e0151713.

Sherwood, J.E., Stagnitti, F., Kokkinn, M.J., and Williams, W.D. (1991) Dissolved oxygen concentrations in hypersaline waters. *Limnol Oceanogr* 36: 235-250.

Sherwood, J.E., Stagnitti, F., Kokkinn, M.J., and Williams, W.D. (1992) A standard table for predicting equilibrium dissolved oxygen concentrations in salt lakes dominated by sodium chloride. *Int J Salt Lake Res* 1: 1-6.

Spiro, S. (2012) Nitrous oxide production and consumption: regulation of gene expression by gas-sensitive transcription factors. *Philos Trans R Soc Lond B Biol Sci* 367: 1213-1225.

Torregrosa-Crespo, J., Martínez-Espinosa, R.M., Esclapez, J., Bautista, V., Pire, C., Camacho, M., *et al.* (2016) Anaerobic metabolism in *Haloferax* genus: denitrification as case of study. *Adv Microb Physiol* 68: 41-85.

Torregrosa-Crespo, J., González-Torres, P., Bautista, V., Esclapez, J., Pire, C., Camacho, M., *et al.* (2017) Analysis of multiple haloarchaeal genomes suggests that the quinone-dependent respiratory nitric oxide reductase is an important source of nitrous oxide in hypersaline environments. *Environ Microbiol Rep* 9: 788-796.

Torregrosa-Crespo, J., Bergaust, L., Pire, C., and Martínez-Espinosa, R.M. (2018) Denitrifying haloarchaea: sources and sinks of nitrogenous gases. *FEMS Microbiol Lett* 365: 1-6.

Torregrosa Crespo, J., Pire, C., Martínez-Espinosa, R.M., and Bergaust, L. (2019) Denitrifying haloarchaea within the genus *Haloferax* display divergent respiratory phenotypes, with implications for their release of nitrogenous gases. *Environ Microbiol* 21: 427-436.

van Spanning, R.J., Houben, E., Reijnders, W.N., Spiro, S., Westerhoff, H.V., and Saunders, N. (1999) Nitric oxide is a signal for NNR-mediated transcription activation in *Paracoccus denitrificans*. *J Bacteriol* 181: 4129-4132.

Walters, C.L., Gillatt, P.N., Palmer, R.C., and Smith, P.L. (1987) A rapid method for the determination of nitrate and nitrite by chemiluminescence. *Food Addit Contam* 4: 133-40.

Zumft, W.G. (2002) Nitric oxide signaling and NO dependent transcriptional control in bacterial denitrification by members of the FNR-CRP regulatory family. *J Mol Microbiol Biotechnol* 4: 277-286.

Zumft, W.G., and Kroneck, P.M. (2006) Respiratory transformation of nitrous oxide (N_2O) to dinitrogen by Bacteria and Archaea. *Adv Microb Physiol* 52: 107-227.

SUPPLEMENTARY INFORMATION

Haloferax mediterranei, an archaeal model for denitrification in saline systems, characterised through integrated phenotypic and transcriptional analyses

Javier Torregrosa-Crespo[a], Carmen Pire[a], Linda Bergaust[b] and Rosa María Martínez-Espinosa[a*]

[a]Departamento de Agroquímica y Bioquímica. División de Bioquímica y Biología Molecular. Facultad de Ciencias. Universidad de Alicante. Carretera San Vicente del Raspeig s/n - 03690 San Vicente del Raspeig, Alicante. E-mail: javitorregrosa@ua.es

[b]Faculty of Chemistry, Biotechnology and Food Science. Norwegian University of Life Sciences. Chr M Falsens vei 1 - 1430, Ås, Norway.

Table S1. A) Phenotypic parameters in *Haloferax mediterranei* cultures monitored during the transition from aerobic growth (initial O_2: 1% in headspace) to denitrification in nitrate-supplemented media (from 2 to 2000 mM KNO_3). B) Apparent specific aerobic and anaerobic growth rates (μ_{ox}, μ_{anox} – h^{-1}), generation times (G_{ox}, G_{anox} – h^{-1}) and number of generations of anoxic growth during log linear growth.

A

Initial NO_3^- (mM)	NO_2^- max (μM)		N_2O max (nmol $vial^{-1}$)		NO max (nM)		NO steady (nM)	
	Average	St. Dev.	Average	St. Dev.	Average	St. Dev.	Average	St. Dev.
2	38	21	107	54	65	12	17	2
5	535	154	41	32	52	14	16	2
10	2585	275	57	17	45	11	16	2
20	2081	1967	133	70	66	19	19	2
200	5399	2652	214	31	105	16	21	2
2000	257	161	1062	76	105	7	24	2

B

Initial NO_3^- (mM)	μ_{ox} (h^{-1})		μ_{anox} (h^{-1})		$G(t)_{ox}$ (h)		$G(t)_{anox}$ (h)		Generations of anoxic growth	
	Average	St. Dev.	Average	St. Dev.	Average	St. Dev.	Average	St. Dev.	Average	St. Dev.
2	0.207	0.024	0.039	0.013	3.383	0.411	19.835	7.756	1.571	0.270
5	0.209	0.011	0.046	0.007	3.317	0.173	15.262	2.352	1.817	0.229
10	0.207	0.022	0.044	0.002	3.373	0.360	15.687	0.681	1.847	0.127
20	0.198	0.019	0.037	0.017	3.532	0.268	19.438	3.857	1.602	0.215
200	0.178	0.009	0.032	0.006	3.892	0.183	22.316	3.994	1.802	0.150
2000	0.115	0.019	0.011	0.003	6.125	1.003	64.236	14.903	1.480	0.348

Table S2. A) Phenotypic parameters in *H. mediterranei* cultures monitored during the transition from aerobic growth (initial O_2: 1% in headspace) to denitrification in nitrate supplemented media (2mM KNO_3) with different pH values (7.3; 7.0; 6.5; 6.0; 5.7). The buffer used was Bis-Tris 100 mM. Values are presented as average of cultures by triplicate (*n=3*) with standard deviation. B) Phenotypic parameters in *H. mediterranei* cultures monitored during the transition from aerobic growth (initial O_2: 1% in headspace) to denitrification in nitrite supplemented media (2mM KNO_2) with different pH values (7.3; 7.0; 6.5; 6.0; 5.7). The buffer used was Bis-Tris 100 mM. Values are presented as average of cultures by triplicate (*n=3*) with standard deviation. *n.a. not applicable.*

A

	pH									
	7.3		**7.0**		**6.5**		**6.0**		**5.7**	
	Average	St. Dev.	Average	St. Dev.	Average	St. Dev.	Average	St. Dev.	Average	St. Dev.
O_{2init} (μM liquid)	1.58	0.14	2.18	0.29	2.16	0.73	3.29	1.00	2.63	0.89
$NO_2^-{}_{max}$ (μmol $vial^{-1}$)	77.05	5.09	31.91	2.26	5.67	3.23	15.07	1.58	9.03	1.86
NO_{max} (nM in liquid)	32.87	4.83	24.22	2.94	15.37	4.14	105.60	4.70	105.21	14.86
N_2O_{max} (nM in liquid)	307.43	33.77	148.49	54.06	142.15	42.54	0.22	0.17	0.61	0.25
% initial NO_3^- reduced to N_2	100.00	0.00	100.00	0.00	37.60	24.08	92.65	3.59	51.24	16.56

B

	pH									
	7.3		**7.0**		**6.5**		**6.0**		**5.7**	
	Average	St. Dev.	Average	St. Dev.	Average	St. Dev.	Average	St. Dev.	Average	St. Dev.
O_{2init} (μM liquid)	1.40	0.34	2.58	0.51	2.76	0.05	n.a.			
NO_{max} (nM in liquid)	489.76	37.76	769.71	198.56	960.38	141.96	254.72	53.36	367.43	5.05
N_2O_{max} (nM in liquid)	220.57	17.45	149.36	23.95	228.27	80.34	200.53	63.09	281.52	2.47
% initial NO_2^- reduced to N_2	100.00	00.00	100.00	00.00	80.47	33.82	2.73	3.77	2.10	2.59

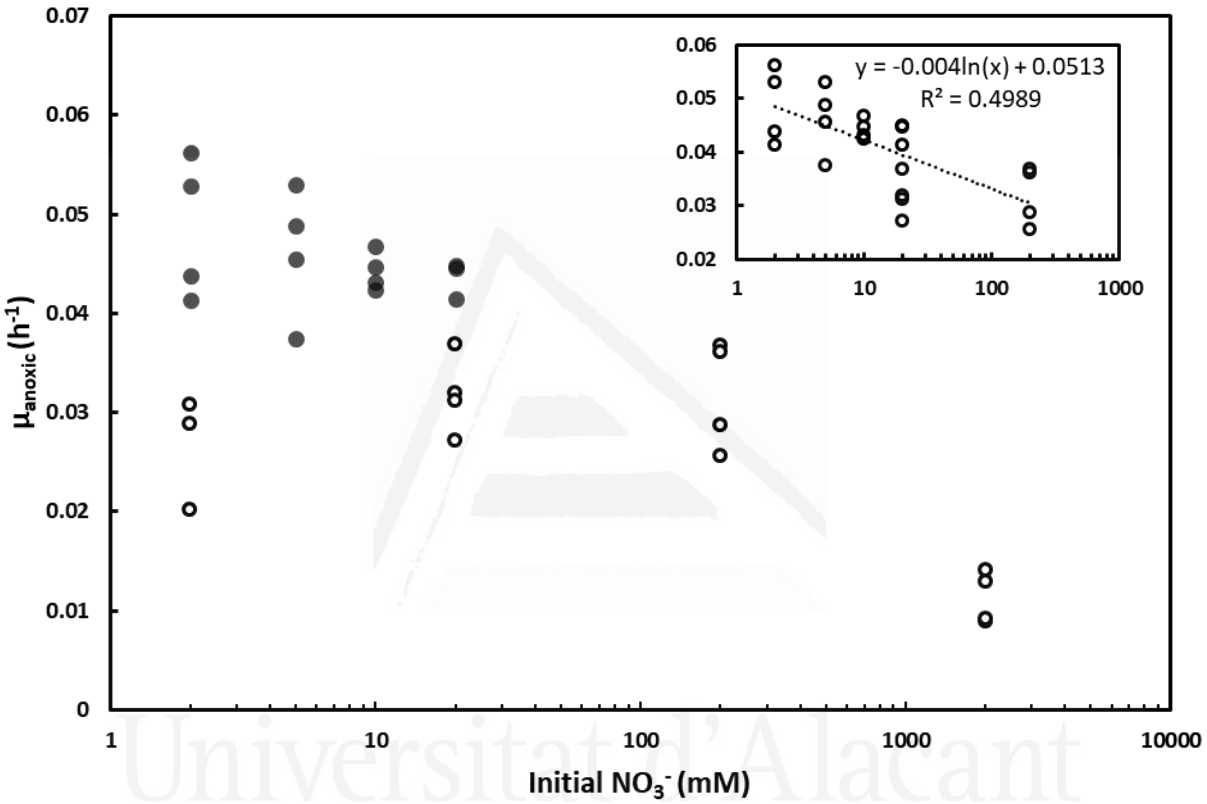

Figure S1. Apparent anaerobic growth rate by denitrification (μ_{anoxic}) in *H. mediterranei* exposed to KNO_3 concentrations ranging from 2 to 2000 mM. Each circle represents one culture. The main panel summarized data from two separate experiments, open and closed symbols, respectively. The insert shows the weak negative trend seen when disregarding the three deviant 2 mM cultures (open circles, main panel). μ_{anoxic} was estimated based on the exponential slope of the total e- flow to terminal electron acceptors during denitrification.

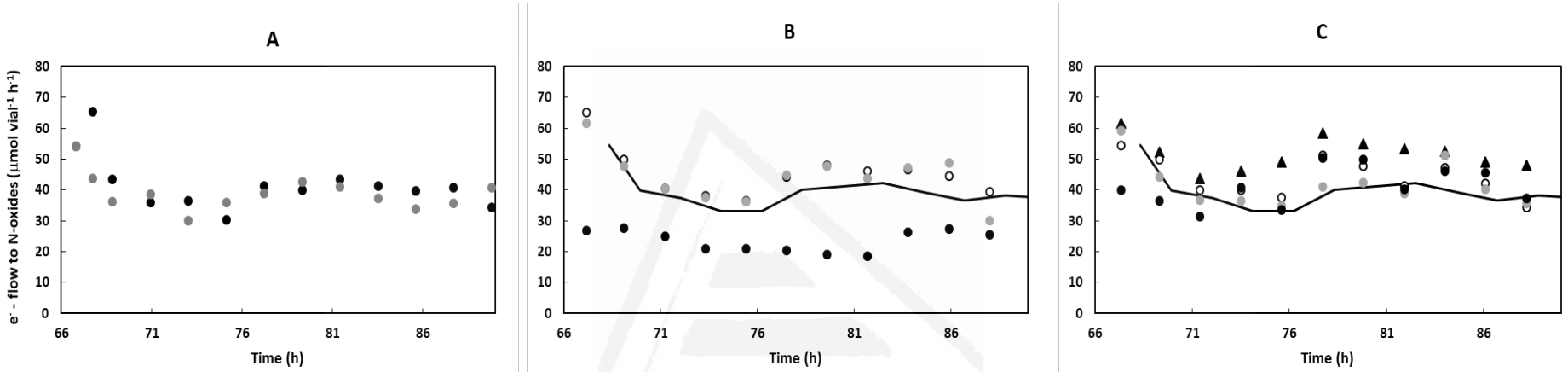

Figure S2. e^- - flow to terminal N-oxides (μmol $vial^{-1}$ h^{-1}) during denitrification in nitrate-supplemented media (5 mM KNO_3) and 1 vol% initial O_2. Panel A: e^- - flow to terminal N-oxides of two different vials (black and grey circles); Panel B: e^- - flow to terminal N-oxides of three different vials (black, grey and open black circles) in which NO (concentration) was injected in the headspace at 68 h of incubation (line represents the average of e^- - flow of the two vials of panel A, of which headspace remained untouched); Panel C: e^- - flow to terminal N-oxides of four different vials (black, grey, open black circles and black triangles) in which O_2 (concentration) was injected in the headspace at 68 h of incubation (line represents the average of e^- - flow of the two vials of panel A, of which headspace remained untouched).

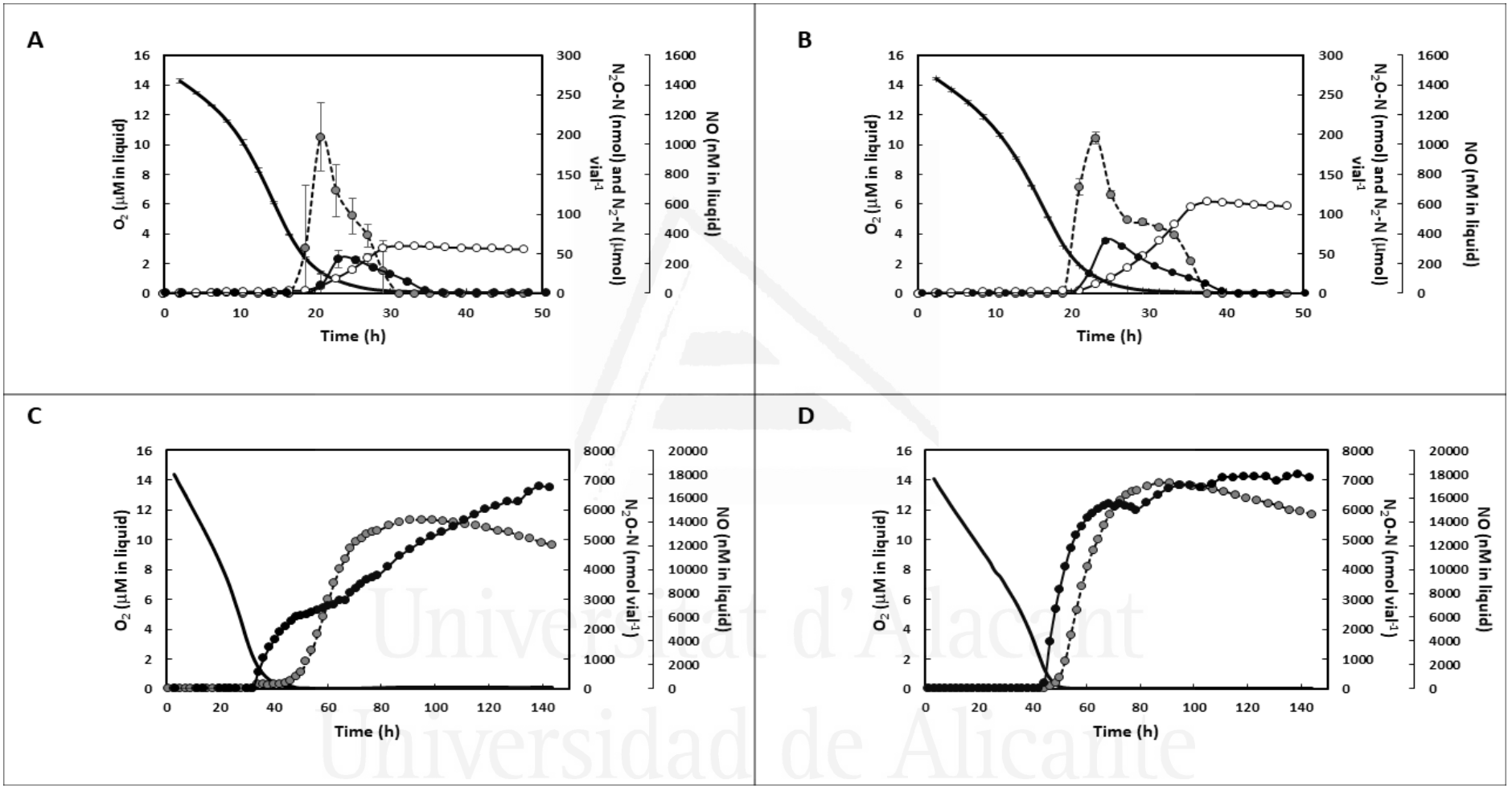

Figure S3. Gas kinetics to terminal e-acceptors during the transition to anoxia in media with 1 vol% initial O_2 and different initial nitrite concentrations: A (1 mM KNO_2), B (2 mM KNO_2), C (10 mM KNO_2), D (40 mM KNO_2). Consumption of O_2 (black line, no symbols) and subsequent accumulation of N-oxides (NO -closed black circles; N_2O –closed grey circles; N_2 – open circles). The experiment was conducted at 35ºC and in triplicate batch cultures. In panels C and D, N_2 accumulation is not shown because it was near zero: one representative replicate is displayed.

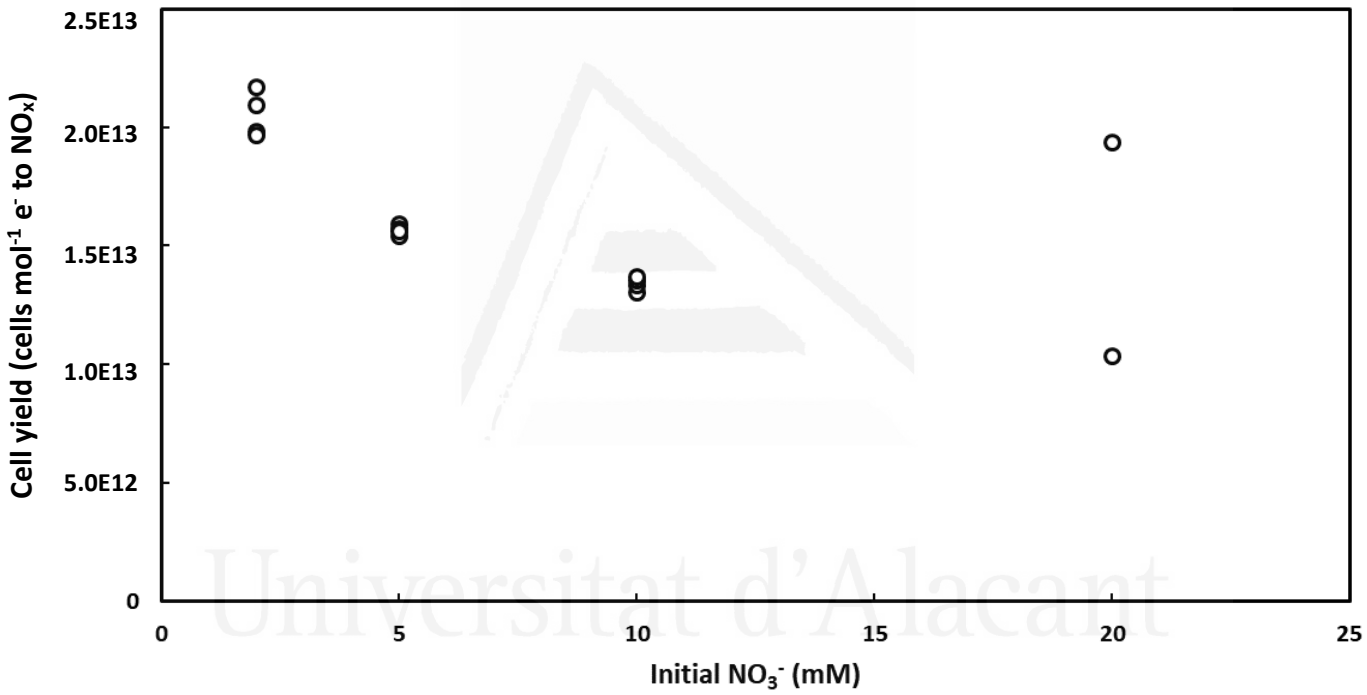

Figure S4. Cell yield (cells mol^{-1} e^{-1} to NO_x) of *H. mediterranei* exposed to KNO_3 initial concentrations ranging from 2 to 2000 mM. Each circle represents one culture.

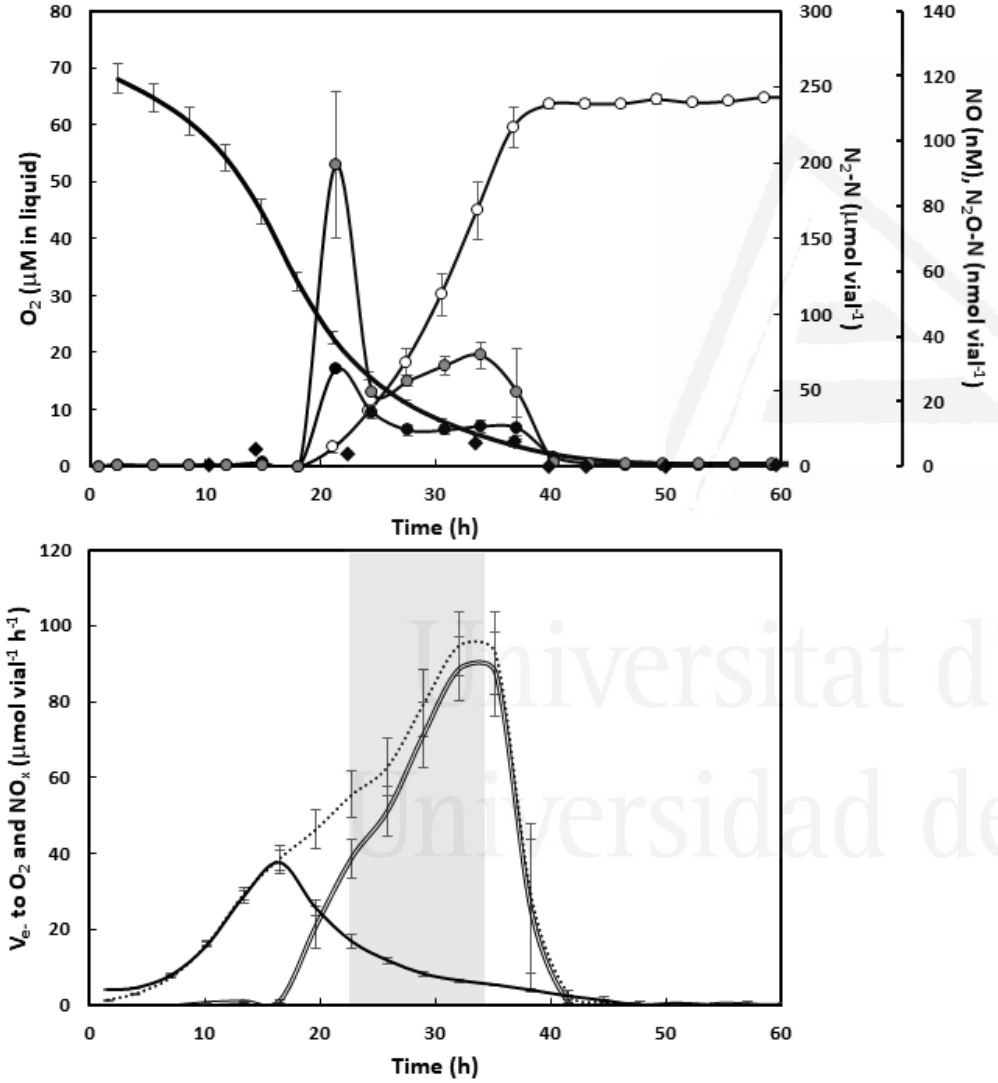

Figure S5. Gas kinetics and e-flow to terminal e-acceptors during the transition to anoxia in nitrate-supplemented medium. Top panel: consumption of O_2 (black line, no symbols) and accumulation of N-oxides (NO- closed black circles; N_2O- closed grey circles; N_2- open circles) with 7% initial O_2 in headspace and 5mM KNO_3 in the medium. The experiment was conducted at 35ºC and in triplicate batch cultures. Bottom panel shows e-flow (μmol $vial^{-1}$ h^{-1}) to O_2 (black line), N-oxides (double black line) and the total e-flow (discontinuous black line). The apparent exponential growth by denitrification is shown as a grey area (22-33 h).

Table S3. List of primers used for gene expression analysis.

Gene	Primer sequences (5'→3')	
narG	Forward:	ACTACTTCAACCAAGCCAAAGG
	Reverse:	ATTTGCCAGTCGGTCTTCG
nirK	Forward:	TCGCTGAGTACGGACCCA
	Reverse:	TACAACCCTTGCGTGTGACA
norZ	Forward:	TTGCGAAGACCTGGCATATC
	Reverse:	CGAGGGTGACGACGACGAT
nosZ	Forward:	CGAAGTGGACGGCAACCTC
	Reverse:	TTGTCGCCCTTGTTGAGTGA

APPENDIX 2

Exploring the molecular machinery of denitrification in *Haloferax mediterranei* through proteomics

Javier Torregrosa-Crespo[1], Carmen Pire[1], David J. Richardson[2], Rosa María Martínez-Espinosa[1]*

[1]Departamento de Agroquímica y Bioquímica, División de Bioquímica y Biología Molecular, Facultad de Ciencias, Universidad de Alicante, Carretera San Vicente del Raspeig s/n - 03690 San Vicente del Raspeig, Alicante, Spain

[2] School of Biological Sciences, University of East Anglia, Norwich Research Park, Norwich NR4 7TJ, UK

*Corresponding author: Rosa María Martínez-Espinosa

e-mail: rosa.martinez@ua.es

Telephone: +34 96 590 3400 ext. 1258; 8841

Fax: +34 96 590 3464

ABSTRACT:

Proteins and enzymes involved in denitrification in haloarchaea seem to be located between the membrane and the S-layer, based on the Tat system exportation and the orientation of the active site that some of these enzymes show. The membrane fraction of the haloarchaeon *Haloferax mediterranei* (R-4), grown under anaerobic conditions in the presence of nitrate, was solubilised to identify the respiratory proteins associated or anchored to it, paying special attention on proteins related to denitrification. Using some detergents (Triton X-100, CHAPS and n-Octyl-β-d-glucopyranoside) at different concentrations, we found the best conditions for isolating membrane proteins in micelles, in which the native structure and enzymatic activity were maintained. Then, they were subjected to enrichment based-purification process constituted on 2 chromatographic steps followed by the analysis of the eluents by LC-MS/MS. The results showed that the four main enzymes of denitrification (nitrate, nitrite, nitric oxide and nitrous oxide reductases) from *H. mediterranei* where co-purified thanks to the micelles made with Triton X-100 (20% w/v for membrane solubilization and 0.2% w/v in the buffers used during purification). Besides, several proteins involved in electron transfer processes during anaerobic respiration as well as proteins supporting ATP synthesis, redox balancing and oxygen sensing were detected. This is the first characterisation of the denitrifying machinery in haloarchaea using proteomics. It provides new information for a better understanding of the anaerobic respiration in haloarchaea.

Keywords: haloarchaea, denitrification, anaerobiosis, proteomics, electron transfer, *Haloferax*, liquid chromatography-mass spectrometry, detergents.

INTRODUCTION

In the absence of oxygen, the most energetically favourable pathway is denitrification: the reduction of nitrate (NO_3^-) via nitrite (NO_2^-), nitric oxide (NO) and nitrous oxide (N_2O) to dinitrogen (N_2) (Richardson, 2000; Zumft and Kroneck, 2006; Philippot *et al.,* 2007; Bakken *et al.,* 2012). Although there is extensive and detailed knowledge about this route, traditional studies have been restricted to a few model organisms, mostly bacteria that inhabit agricultural and forestry soils (Bergaust *et al.,* 2008; Samad *et al.,* 2016; Roco *et al.,* 2017). However, the role of denitrification is less known in saline and hypersaline ecosystems where the reduction of N-oxyanions is favoured by two main factors: on one hand, due to the high salt concentrations resulting in low oxygen solubility (Rodríguez-Valera *et al.,* 1985; Oren, 2013); on the other hand, because of the increasing nitrate/nitrite concentrations due to anthropogenic activities (Martínez-Espinosa *et al.,* 2007; Ochoa-Hueso *et al.,* 2014; Torregrosa-Crespo *et al.,* 2018). Moreover, saline and hypersaline areas are currently increasing in size and prevalence as a result of desertification (Torregrosa-Crespo *et al.,* 2018).

Hypersaline environments are dominated by haloarchaea when the salt concentration exceeds 16% (Andrei *et al.,* 2012; Edbeib *et al.,* 2016). In the last years, one of their members has been used as model organism for the study of denitrification: *Haloferax mediterranei.* It is an haloarchaeon able to carry out the complete reduction of nitrate to dinitrogen through the four key enzymes of denitrification: nitrate, nitrite, nitric oxide and nitrous oxide reductases (Torregrosa-Crespo et al., 2018).

The enzyme catalysing the first reaction, the respiratory nitrate reductase, is composed of three subunits: a catalytic α subunit containing a molybdopterin cofactor (NarG), a soluble β subunit containing four [4Fe-4S] (NarH) and the γ subunit containing *b*-type haems (NarI) (Lledó *et al.,* 2004). NarG and NarH subunits constitute the main core of the enzymes, which are facing the "pseudo periplasm" in haloarcahea and NarI is the membrane domain required for their

attachment to lipid bilayer (Martínez-Espinosa *et al.,* 2007). Nitrate reductase catalyses the reduction of nitrate to dinitrogen ($NO_3^- + 2e^- + 2H^+ \rightarrow NO_2^- + H_2O$) receiving electrons from the quinol pool via the *b*-haems groups of NarI subunit. They are then transferred to the active site of molybdenum cofactor (MoCo) containing subunit NarG via the [4Fe-4S] clusters of NarH (Martínez-Espinosa *et al.,* 2007; Borrero-de Acuña *et al.,* 2016).

During the second step of denitrification, the periplasmic nitrite reductase catalyses the reduction of nitrite to nitric oxide as follows: $NO_2^- + 2H^+ + e^- \rightarrow NO + H_2O$. In *H. mediterranei*, this enzyme is the copper containing Nir-type (CuNiR), encoded by the gene *nirK*. Although the native form has never been purified, it was expressed homologously using *H. volcanii* as host (Esclapez *et al.,* 2013). Its characterisation indicated that it is a green copper-dependent nitrite reductase like NirK isolated from *H. denitrificans*. In terms of structure, it is a homotrimer, in which a monomer contains one type I Cu and one type II Cu sites (Esclapez *et al.,* 2013). In CuNiR, the electron for nitrite reduction is supplied from a physiological redox partner, usually small electron-transfer proteins such as a cupredoxin (blue copper protein) or a cytochrome c (Nojiri, 2017). However, in case of *H. mediterranei*, it remains unknown which protein fulfils this function.

The third enzyme of denitrification is the nitric oxide reductase, producing nitrous oxide from nitric oxide: $2NO + 2H^+ + 2e^- \rightarrow N_2O + H_2O$. Bacterial respiratory Nors can be classified mainly as short-chain respiratory Nors (scNors) or long-chain respiratory Nors (lcNors) (Torregrosa-Crespo *et al.,* 2017): on one hand, scNors are characterised by a transmembrane catalytic subunit forming a complex with a *c*-type cytochrome, that is the electron receiving domain. These NorBC complexes are also known as cNors; on the other hand, lcNors contain a single subunit, NorZ, also named as qNors because they accept electrons directly from the reduced quinol pool (Hendriks *et al.,* 2000). Since the *H. mediterranei* genome had a chromosomal gene encoding for a putative nitric oxide reductase annotated as *norB* (Han *et al.,*

2012; Becker *et al.,* 2014), it was supposed that it had a nitric oxide reductase type scNor. However, subsequent bioinformatics studies revealed that *H. mediterranei* respiratory NO-reductase is a nonelectrogenic single subunit qNor closely related to the bacterial NorZs that derive their electrons directly from the quinone pool (Torregrosa-Crespo *et al.,* 2017).

For the final step, the periplasmic enzyme nitrous oxide reductase NosZ catalyses the reduction of nitrous oxide to dinitrogen: $N_2O + 2e^- + 2H^+ \rightarrow N_2 + H_2O$. Probably, it is the most unknown denitrification enzyme in haloarchaea. So far, only *in vivo* experiments have been performed to test its functionality in the presence of oxygen or low pH (Torregrosa-Crespo *et al.,* 2019b), but its structure remains unknown. *A priori*, based on the gene sequence, it must be a typical nitrous oxide reductase containing two multicopper sites: a binuclear CuA electron-transferring centre and a tetranuclear copper sulphide catalytic centre, named the "CuZ centre" (Pauleta *et al.,* 2017). As well as for NirK, its electron donor remains unknown in haloarchaea.

All these enzymes seem to be located between the cell membrane and the outer S-layer, in the so-called pseudo periplasm of the Archaea due to the following evidences: i) the purification of nitrate reductase in *H. mediterranei*, which showed that its active site is located on the positive side of the cell membrane, facing the pseudo periplasm (Martínez-Espinosa *et al.,* 2007); ii) the genes coding nitrate, nitrite and nitrous oxide reductases contain TAT sequences to be exported outside the membrane (Martínez-Espinosa *et al.,* 2007; Torregrosa-Crespo *et al.,* 2016); iii) nitric oxide reductase has been identified as integral protein of the membrane (Torregrosa-Crespo *et al.,* 2017).

To date, much of the experimental work about denitrification in haloarchaea has been focused on physiological studies or, more recently, transcriptional analysis (Torregrosa-Crespo *et al.,* 2019a; Torregrosa-Crespo *et al.,* 2019b). These approaches cannot get a global perspective on protein synthesis related to denitrification. Moreover, apart from nitrate reductase (Lledó *et al.,* 2004), none of denitrification enzymes have been purified or

characterized in native form, as well as any of the accessory elements of the electron transport chain. Therefore, in order to have a complete view, a proteomic approach was carried out to identify the components of denitrification machinery in *H. mediterranei* at the protein level. It is based on an integrated approach consisting on the production of lipid micelles encapsulating the proteins of interest for their subsequent enrichment and identification. This avoids any artificial interactions between them (which is quite common in other approaches like cross-linking) and allows the monitoring of enzymatic activities in environments that mimetic the lipid bilayer.

RESULTS AND DISCUSSION

Membranes solubilisation

Membrane solubilisation is a critical step in any *in vitro* analysis of proteins related to membrane as the aim is to maximally disrupt the lipid components while loading the proteins in an un-natural environment without perturbing them (Duquesne and Sturgis, 2010). Detergents interact with proteins and membranes as micelles, consequently, the solubilisation of these kind of proteins is dependent upon their formation, usually spherical shaped in solution. Several parameters must be considered when choosing them: critical micelle concentration (CMC), effects of hydrophilic or hydrophobic groups on CMC, effects of electrolytes on CMC (NaCl for instance), cloud point and aggregation numbers (the number of detergent monomers present within a micelle) (Rosen, 2004).

Thus, three detergents were chosen to solubilise the membrane extracts based on their physicochemical properties (non-ionic detergents) and their relatively low cost: Triton X-100, n-octyl-β-D-glucopyranoside and CHAPS. They were assayed at different concentrations between 0.5 and 20 % (w/v) in order to determine the optimal one to get the highest protein concentration, while showing the highest nitrate reductase activity. This was selected as target enzymatic activity to monitor the stability of the biological function of the enzymes within the micelles: it is a highly sensitive method, low cost and low time consuming compared to those usually used to measure nitrite, nitric oxide or nitrous oxide reductases activities. Table 1 displays the best results from each detergent.

Table 1. Parameters of the different detergents tested for the formation of micelles from crude extract: CMC (critical micelle concentration); % detergent (w/v); protein concentration (mg/mL); nitrate reductase specific activity (U/mg).

	DETERGENT		
	Triton X-100	**CHAPS**	**n-octyl-β-D-glucopyranoside**
CMC	0.2-0.9 mM	6-10 mM	18-20 mM
% Detergent (w/v)	1 (16 mM)	1.2 (20 mM)	1 (34 mM)
Protein concentration (mg/mL)	16.5	9.3	10.5
Nar activity (U/mg protein)	0.18	0.12	0.2

Detergents historically used for protein solubilisation are Triton X-100 (nonionic) and CHAPS (zwitterionic), used alone or in combination with urea or urea-thiourea (Luche *et al.,* 2003). Among them, CHAPS is highly chaotropic thus disrupting protein interactions that stablish protein complexes. Apart from them, in the last years, the most efficient non-ionic detergents reported belongs to the glycoside family (e.g. octyl glucoside, dodecylmaltoside) (Witzmann *et al.,* 1991; Taylor *et al.,* 2003). In this study, the membrane solubilised sample showed the highest Nar activity when using n-octyl-β-D-glucopyranoside, followed by Triton X-100 and CHAPS; protein concentration was higher in Triton X-100 followed by n-octyl-β-D-glucopyranoside and CHAPS. From these results, it can be concluded that both Triton X-100 and n-octyl-β-D-glucopyranoside were good enough to reach high ratio of solubilisation avoiding the loss of enzymatic activity. Considering that Nar activities were similar in both samples, but protein concentration was slightly higher in Triton X-100 samples, it was chosen as detergent to carried out protein enrichment and proteomic analysis. Another advantage of using this detergent is its low price compared to the other ones.

The enrichment of the molecular machinery of denitrification in *H. mediterranei*: from crude extract to micelles.

Denitrification enzymes

The different sets of micelles obtained in each chromatographic step were analysed by liquid chromatography coupled to mass spectrometry (LC/MS-MS). Regarding the enzymes of denitrification, the protocol managed to enrich the micelles in terms of score, protein sequence coverage, spectral intensity as well as Nar and Nir specific activities.

First, the catalytic subunit of nitrate reductase (NarG) was the most enriched protein in the micelles with respect to the crude extract: the score and protein sequence coverage improved by 218.91% and 194.02% respectively, and the spectral intensity increased from 2.58E6 ± 2.5E5 to 3.88E7 ± 2.9E5 (Fig 1-top panel, Table S1A). It was in line with Nar specific activity increment, from 0.028 ± 0.002 to 0.176 ± 0.009 U/mg (Fig 1-bottom panel, Table 2A). Considering that our goal was not the purification of nitrate reductase, the values obtained for NarG in terms of specific activity, purification (fold) and yield were very similar to those obtained in the penultimate step of the purification of Nar in *Haloferax mediterranei* (Lledó *et al.,* 2004).

The subunit NarH, involved in the electron transfer to NarG, improved the score and protein sequence coverage although not as much as the first (21.35% and 12.70%, respectively). The spectral intensity also increased by an order of magnitude (from 3.27E6 ± 2.7E4 to 2.12E7 ± 3.1E5) (Fig 1, Table S1A). Regarding the third subunit (NarI), the score and protein sequence coverage values remained practically constant after the first enrichment step (47.03 ± 2.4 and 13.40 ± 0.8, respectively), increasing the spectral intensity from 1.03E6 ± 7.5E4 to 1.43E6 ± 2.7E4 (Fig 1, Table S1A). However, at the end, it could not be detected.

Although NarG, NarH and NarI form a heterotrimer, their enrichment in the micelles was totally different, especially for the last one. It could be due to the type of interactions established between the three subunits of the enzyme: NarI and NarH could be weaker linked than NarG and NarH, which could explain their identification and the lack of NarI. Thus, during the purification of respiratory nitrate reductase from *H. mediterranei* membranes in 2004 (Lledó *et al.*, 2004), the enzyme was usually obtained, and consequently firstly described, as a heterodimer (NarGH). Considering that nitrate reductase activity has been used for monitoring the micelles and that the catalytic subunit is NarG, the enrichment procedure has promoted the selection of those containing NarG or NarGH and, to a lesser extent, NarGHI. The nitrate reductase activity can be measured even in the absence of NarH and NarI whose functions could be replaced during *in vitro* assays by dithionite and methylviologen present in the reaction mixture.

Results from proteomics of nitrite reductase were also very promising. Both, the score and the protein sequence coverage improved by 48.85 and 57.69%, respectively (Fig 1, Table S1B). The spectral intensity was the highest of all the enzymes for the last enrichment step, reaching 2.40E8 ± 4.0E6 (Fig 1, Table S1B). Despite this, the specific activity registered in the micelles was low compared to Nar activity (0.028 ± 0.004 U/mg), although 5.5 times higher than the obtained in the crude extract (0.005 U/mg) (Table 2). Testing different strategies of enrichment, nitrite reductase activity was always difficult to measure. In fact, when trying to apply a third chromatography, based on size exclusion (Superose^{TM} 6 Increase 10/300 GL – GE Healthcare), nitrite reductase activity could not be measured, although the enzyme was detected. This effect was probably due to the dilution effect of the samples when this chromatography is used.

Table 2. Purification parameters of Nar (panel A) and Nir (panel B) during the enrichment of micelles. Values are shown as the average of triplicates with standard deviation.

A

	Nar						
Fraction	**Volume (mL)**	**Protein concentration (mg/mL)**	**Total protein (mg)**	**Total activity (U)**	**Specific activity (U/mg)**	**Purification (Fold)**	**Yield (%)**
Crude extract	132 ± 2.0	5.64 ± 0.3	747.06 ± 49	20.86 ± 0.3	0.028 ± 0.002	1	100
DEAE-Sepharose	75 ± 1.7	1.70 ± 0.11	127.38 ± 5.0	8.29 ± 0.3	0.065 ± 0.005	2.33 ± 0.2	39.77 ± 1.8
Q-Sepharose	11.70 ± 0.8	1.41 ± 0.10	16.47 ± 0.6	2.90 ± 0.2	0.176 ± 0.009	6.32 ± 0.7	13.92 ± 0.8

B

	Nir						
Fraction	**Volume (mL)**	**Protein concentration (mg/mL)**	**Total protein (mg)**	**Total activity (U)**	**Specific activity (U/mg)**	**Purification (Fold)**	**Yield (%)**
Crude extract	132 ± 2.0	5.64 ± 0.3	747.06 ± 49	3.46 ± 0.2	0.005 ± 0.000	1.00	100
DEAE-Sepharose	75 ± 1.7	1.70 ± 0.1	127.38 ± 5.0	0.83 ± 0.10	0.007 ± 0.001	1.41 ± 0.1	24.09 ± 2.5
Q-Sepharose	11.70 ± 0.8	1.41 ± 0.10	16.47 ± 0.6	0.45 ± 0.10	0.028 ± 0.004	5.97 ± 1.0	13.10 ± 1.5

Third, nitric oxide reductase was the only one of the four enzymes of denitrification that did not improve its representativeness in the micelles using this protocol: the score and protein sequence remained fairly constant, from 126.21 ± 9.3 to 106.03 ± 7.0 and from 14.53 ± 0.8 to 15.6 ± 1.7, respectively, while the spectral intensity decreased until 4.20E6 ± 7.0E4 (Table S1B). In *Haloferax mediterranei*, qNor is a protein with 14 transmembrane segments, which could imply low detection by LC-MS/MS due mainly to two reasons: first, the lipids of the membrane or the micelle, that could prevent the access of trypsin to the transmembrane regions, which would adversely affect their digestion and subsequent detection. However, the protocol here applied involved the use of acetone previous resuspension of proteins in urea for the cleavage with trypsin. Because of this treatment, lipids and salts should precipitate thus realising proteins (Moore *et al.,* 2016). Consequently, this method allowed the access of trypsin to the hydrophobic regions; second, the membrane-bound proteins usually have not enough lysine and arginine residues for proteolytic cleavage with trypsin, yielding peptide fragments that are out of range for MS analysis (Wessels *et al.,* 2016). Despite this, 6 different peptides were detected in the mass analysis, two of which were transmembrane, so it seems that the trypsin was enough for its digestion and detection (Figure S1). Even with the controversy over the use of this protease in transmembrane proteins, it has been shown recently that it is the best option in this context, and the results get worse when combined with chymotrypsin or pepsin (Moore *et al.,* 2016).

Finally, nitrous oxide reductase also showed improved score values (32.60%) and protein sequence percentage (45.80%) (Fig 1, Table S1B). After the last step of enrichment, the spectral intensity reached 1.90E8 ± 2.1E6, the second higher after nitrite reductase. In fact, these two enzymes had the best spectral intensity values from the beginning. The data are in line with those obtained when trying to isolate the crude extract using less percentage of Triton X-100 (10% w/v). In that case, none of the denitrification enzymes were identified, except for nitrite and nitrous oxide reductase (Table S2). The predominance of these two proteins in the micelles

could be due since they are more expressed than the rest: a recent study showed that the highest peaks of expression during denitrification were reached by the genes that encode them (*nirK* and *nosZ*) (Torregrosa-Crespo *et al.,* 2019b). Despite these observations, this hypothesis should be addressed using quantitative proteomics.

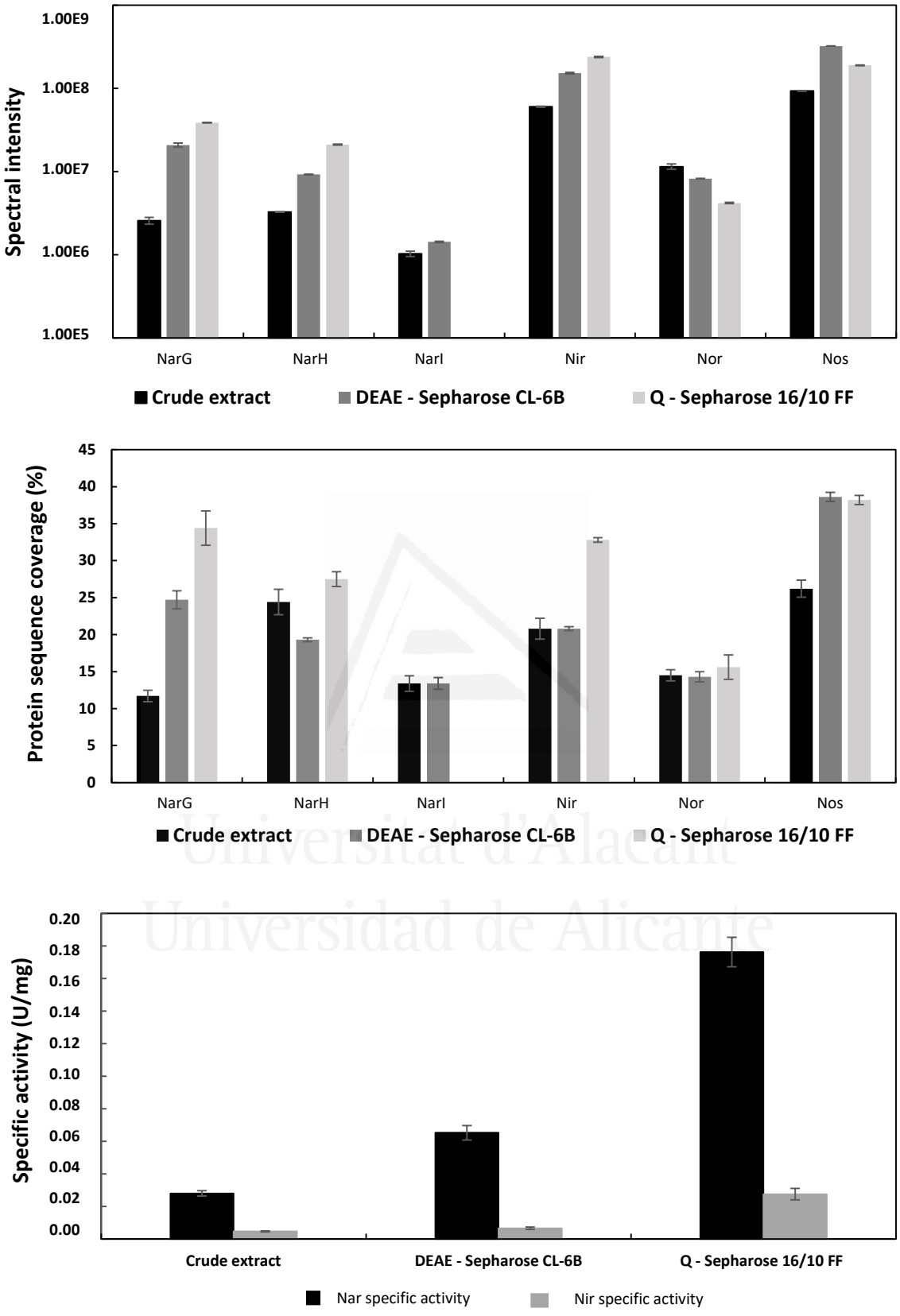

Fig 1. Spectral intensity (top panel), protein sequence coverage (middle panel) and specific Nar and Nir activities (bottom panel) data in the three steps of enrichment. The data are shown as the average of triplicates with standard deviation (bar error).

The enrichment process allowed to reduce the total number of proteins in the micelles by 43.20%: from 375 proteins in the crude extract to 162 obtained after HiPrep™ Q-Sepharose 16/10 FF. Likewise, the number of different peptides counted for the identification of denitrification enzymes increased considerably: NarG and Nos were the proteins with the highest number of different peptides identified from the whole protein set (22 and 23 peptides, respectively) (Fig 2). Nir peptides also increased, from 6 to 12, being this enzyme also one of the ten with the highest number of different peptides identified. In case of Nor, the values remained practically constant throughout the enrichment process (from 7 to 6), which was in line with the protein sequence coverage, score and spectral intensity data (Fig 2).

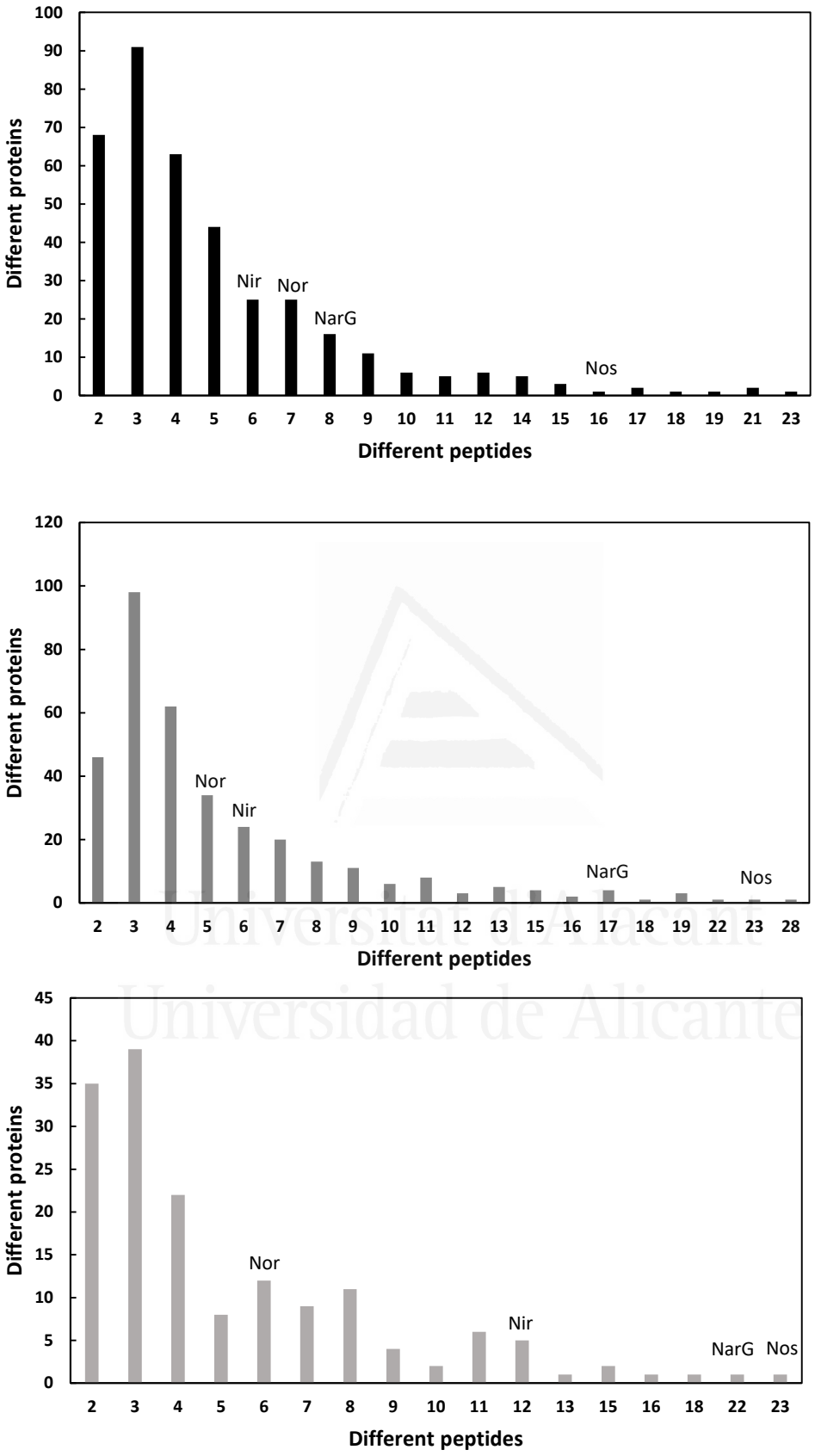

Figure 2. Total number of proteins identified vs different peptides obtained by LC-MS/MS in the micelles during the enrichment process: crude extract (top panel), DEAE-Sepharose (middle panel) and Q-Sepharose (bottom panel).

Accessory proteins for N-reductases

Denitrification enzymes are combined with a whole variety of electrons donors making possible the electron flux required to reduce the different N-substrates. With the proteomic approach here described, it was possible to identify the potential electron donors, some of them unknown or only annotated at gene level to date in *Haloferax* genomes.

As previously described, during respiratory electron transfer, Nar enzymes receive electrons from quinols located within the lipid phase of the cytoplasmic membrane (Martínez-Espinosa *et al.,* 2007). Nar from *H. mediterranei* was described as pNar, i.e. the active site is facing the positive site of the membrane. This orientation brings the question of whether being located at the positive face of the membrane, pNarG could be a poorly coupled enzyme, like NapA, or whether there is a mechanism by which pNarG can maintain bioenergetic equivalence with its nNarG bacterial counterpart. At present, it is not well known how electrons move from the Q-pool to pNarG in haloarchaea. However, this approach trough proteomics has allowed to identify several subunits closely related to proton-translocating enzymes like NADH dehydrogenase as well as several enzymes involved in ubiquinone/menaquinone biosynthesis (Table S5). Electrogenic enzymes like formate dehydrogenases or hydrogenases could also generate proton motive force (Jormakka *et al.,* 2002). However, this kind of enzymes have not been identified through proteomics in this approach. Consequently, it is possible to predict that electron transport to nitrate via the Nap system in *H. mediterranei* can only be energy conserving if the electron input into the Q-pool is protonmotive. This can be the case if electrons enter by a proton-translocating enzyme like NADH dehydrogenase (subunits constituting this enzyme have been identified in this study - Table S5). ATP synthases are also required in this system: most of the subunits of the rotary A-type ATP synthase have been identified in this study (Table S5). This was in line with the general postulate that the predominant ATP synthases in Archaea are those of type A (Grüber *et al.,* 2014).

Other interesting proteins detected, which are related to respiratory nitrate reductase, are NarC and NarB : NarC is a two *b*-haemes protein folded into nine transmembrane helices that transfer electrons to NarB, a Rieske iron-sulphur protein with the redox-active domain facing the periplasm in order to transfer electrons to NarI (Martínez-Espinosa *et al.,* 2007). The micelles were not enriched in NarC proteins during the purification steps, probably, as for the case of Nor, because it is a transmembrane protein which is harder to identify than the rest. (Table 3).

Next, different proteins that could act as electron donors located in the *nir-nor* cluster were identified. This is the case of an halocyanin whose gene was annotated as *hcy*. Halocyanins are small blue copper membrane associated proteins from halophilic archaea that are thought to act as mobile electron carriers similarly to plant plastocyanins with a molecular mass of about 15 kDa (Scharf *et al.,* 1993; Torregrosa-Crespo *et al.,* 2016). This finding suggests that it might be acting in the electron transfer during nitrite and/or nitric oxide reduction (Brischwein *et al.,* 1993; Mattar *et al.,* 1994). In fact, during the enrichment process, the score and protein sequence coverage showed an increment near 50 and 60%, very similar to Nir data (Table 3). The knowledge about halocyanins is scarce, being one belonging to *Natronomonas pharaonis* the only one purified to date (Mattar *et al.,* 1994).

Table 3. Score, protein sequence coverage and spectral intensity values of different accessory proteins of denitrification enzymes during the enrichment process. Data are shown as the average of triplicates with standard deviation. Panel A: proteins related to Nar; Panel B: proteins related to Nir and Nor; Panel C: proteins related to Nos.

n.a. not applicable

A

	NarB			NarC		
Fraction	**Score**	**%aa coverage**	**Spectral intensity**	**Score**	**%aa coverage**	**Spectral intensity**
Crude extract	46.02 ± 1.0	28.60 ± 0.8	9.83E5 ± 3.1E3	30.00 ± 1.3	3.90 ± 0.4	1.36E6 ± 1.7E3
DEAE-Sepharose	n.a.	n.a.	n.a.	40.50 ± 2.1	10.90 ± 0.6	9.75E6 ± 3.5E4
Q-Sepharose	n.a.	n.a.	n.a.	30.23 ± 1.2	8.60 ± 0.5	7.00E5 ± 1.5E3

B

	Nir-Copper containing			Halocyanin			HFX_2180		
Fraction	**Score**	**%aa coverage**	**Spectral intensity**	**Score**	**%aa coverage**	**Spectral intensity**	**Score**	**%aa coverage**	**Spectral intensity**
Crude extract	80.16 ± 3.8	17.30 ± 1.1	4.77E6 ± 2.1E4	88.97 ± 1.9	26.50 ± 1.3	1.52E7 ± 1.5E5	40.21 ± 1.9	8.70 ± 0.7	3.36E6 ± 2.1E4
DEAE-Sepharose	123.51 ± 6.2	25.10 ± 2.5	3.91E7 ± 6.7E5	107.3 ± 1.9	35.70 ± 1.3	3.41E7 ± 2.1E5	51.09 ± 1.8	8.70 ± 0.4	2.99E6 ± 4.9E5
Q-Sepharose	182.42 ± 8.7	46.30 ± 2.0	5.32E7 ± 2.1E5	136.09 ± 1.3	42.30 ± 1.1	1.16E7 ± 1.0E5	30.95 ± 3.4	3.50 ± 0.6	8.84E5 ± 4.2E3

C

	Copper-binding plastocyanin		
Fraction	**Score**	**%aa coverage**	**Spectral intensity**
Crude extract	34.00 ± 0.9	20.80 ± 1.0	1.90E6 ± 1.0E4
DEAE-Sepharose	61.54 ± 2.2	36.90 ± 1.0	1.08E7 ± 2.1E5
Q-Sepharose	59.55 ± 4.7	36.90 ± 2.8	1.25E7 ± 3.2E5

Another remarkable protein identified within the *nir-nor* cluster is the so-called "nitrite reductase-copper containing". Although its name in the database suggested that it could be a second copy of Nir, the alignment of its nucleotide sequences did not show any significant result, while their amino acid sequences had a very low similarity (23.30%) (Fig S2). It seems that it is a copper oxidoreductase, which could be involved in the electron transfer during nitrite/nitric oxide reduction (like halocyanin). For this protein, the results of the score and protein sequence coverage improved by 127.57 and 167.63%, respectively (Table 3). These values are higher than those for the nitrite reductase. In addition, the spectral intensity reached 5.32E7 ± 2.1E5, higher than for some structural denitrification enzymes such as Nar and Nor (Table 3).

Moreover, during the enrichment process, a hypothetical protein (named HFX_2180) of 440 amino acids whose gene is located very close to *nirK* was identified (Table 3). Although previously its gene had not been annotated as part of the *nir-nor* cluster, it could be a new candidate as an electron donor: it has a conserved COX-type domain, belonging to heme-Cu-oxidase I Superfamily.

Finally, in case of nitrous oxide reductase, the plastocyanin encoded by the gene located immediately upstream of *nosZ* (*pcy*) was identified. The results from score and protein sequence coverage for this protein improved around 75% and the spectral intensity reached 1.25E7 (Table 3). Being a small blue copper protein, it could act as potential electron donor to Nos. However, there are some facts that suggest that *pcy* is incorrectly annotated, and this protein was actually an azurin: i) plastocyanins are involved in electron transfer processes in the plant chloroplasts or in cyanobacteria, never found in non-photosynthetic organisms (Pérez-Henarejos *et al.,* 2015); ii) the number of amino acids contained in this protein (170) is very high to be a plastocyanin, which usually does not reach the hundred, while azurins from different species contain between 120 and 130 amino acids (Pérez-Henarejos *et al.,* 2015). Likewise, azurines have been identified in different denitrifying bacteria such as *Pseudomonas* or *Alcaligenes*

(Machczynski *et al.,* 2002; Dell'acqua *et al.,* 2011), being their function closely related to denitrification.

CONCLUSIONS

To our knowledge, proteomics has never been used as a tool for the study of denitrification in haloarchaea. In this group of microorganisms, this approach has been used to make comparative studies between mid-log and late-log phases in *Haloarcula marismortui* (Chu *et al.,* 2011), *Haloferax volcanii* or *Natrialba magadii* (Cerletti *et al.,* 2018), to compare differences in protein expression under different salt concentrations in *Halobacterium salinarum* (Leuko *et al.,* 2009) or to study the effect of proteases in *Haloferax volcanii* (Costa *et al.,* 2018).

Using proteomics and the generation of different populations of micelles, the proteins involved in denitrification can be identified. This is especially useful in organisms in which knowledge about this respiratory pathway is scarce, such as extremophiles, in which some agents involved in it remain unknown (such as some electron donors). Although there is a bias towards rich populations in nitrate reductases, it was demonstrated that the enrichment of the micelles based on Nar activity was a useful, fast and cheap tool that allows the co-purification of all the N-reductases together with their accessory proteins, essential to sustain the proton motive force and electron flow in native conditions.

With this work new questions marks have raised related to the molecular machinery for denitrification in haloarchaea including aspects directly connected to bioenergetics and redox status: in the next future, studies based on comparative and quantitative proteomics between different denitrifying conditions should be done in order to a better understand of this pathway in hypersaline environments.

EXPERIMENTAL PROCEDURES

Haloarchaeal strain, media and growth conditions

Haloferax mediterranei (R-4) was grown in optimal media: 20% (w/v) mixture of salts (20% SW) (Rodríguez-Valera *et al.,* 1980; Lledó *et al.,* 2004) and 0.5% (w/v) yeast extract. The pH was adjusted with NaOH to 7.3.

Pre-inocula were raised aerobically at 42 ºC and 200 rpm in 250 mL Erlenmeyers containing 50 mL medium. Upon reaching $OD_{600} \sim 0.3$, these cells served as inoculum (1% (w/v)) to the aerobic cultures: a total of 12 3L-Erlenmeyers containing 600 mL medium each, grown under the same conditions as the pre-inocula. When they reached the mid-stationary phase of growth ($OD_{600} \sim 1$), anaerobic conditions were applied by transferring the cultures to 10 L sterilised bottle, adding 1 L KNO_3 (0.5 M) to a final concentration of 50 mM and 2 L fresh medium, thus avoiding overhead space. Cultures were then incubated at 42 ºC without shaking for 6 days.

Insoluble fraction isolation, solubilisation and obtention of crude extract.

Cells were harvested by centrifugation at 16,300 x*g* for 45 min at 4ºC in a Beckman J-20 XP centrifuge, washed with 20% SW for three times and then centrifuged again at 16,300 x*g* for 60 min at 4ºC. The cell pellet obtained was resuspended in 10 mM Tris-HCl, 1 mM DTT buffer pH 8.0 (40 % w/v). After that, cells were disrupted by sonication and the suspension was centrifuged at 2,100 x*g* for 30 min at 4ºC in a Beckman J-20 XP to remove non-lysed cells. The supernatant (containing lysed cells) was centrifuged at 105,000 x*g* for 60 min at 4ºC in a Beckman Coulter Optima™ XL-100K Ultracentrifuge. The new supernatant was discarded and the pellet (containing the insoluble fraction) was then subjected to solubilisation using three different detergents in a range of concentrations (0.5-20 % (p/v)): Triton X-100, n-octyl-β-D-glucopyranoside and CHAPS (provided by Sigma or Anatrace companies). For each of the assays,

they were added to the buffer used for the isolation of the crude extract (10 mM Tris-HCl, 1 mM DTT, pH 8) at 40% (w/v), gently stirred at 4 ºC overnight. Then, the solubilised samples were centrifuged at 105,000 x*g* for 60 min at 4ºC in a Beckman Coulter Optima™ XL-100K Ultracentrifuge. Supernatants were collected to quantify protein by Bradford method and to measure nitrate reductase activity (see below for details). From these experiments the detergent showing the best results (Triton X-100) was selected to get the micelles at large scale for protein purification and proteomic analysis.

Enrichment of micelles involving proteins of denitrification.

The micelles obtained by solubilizing the membrane were then enriched in denitrification proteins following the next purification steps. All of them were carried out at 25ºC:

Step 1: DEAE-Sepharose CL-6B chromatography. The extract obtained (132 mL ± 2) was applied to a DEAE-Sepharose CL-6B column (2.5 x 10 cm) which had previously been equilibrated with 10 mM Tris-HCl, 1 mM DTT, Triton X-100 (0.2%) (pH 8.0). The column was washed with 250 mL of 10 mM Tris-HCl, 1 mM DTT, Triton X-100 (0.2%) (pH 8.0) containing 200 mM NaCl. Elution was carried out with an increasing linear gradient (500 mL) of 200 mM to 2 M NaCl in 10 mM Tris-HCl, 1 mM DTT, Triton X-100 (0.2%) buffer (pH 8.0), at a flow rate of 30 mL/h. Fractions containing Nar and Nir activity were pooled and dialyzed against 10 mM Tris-HCl, 1 mM DTT, Triton X-100 (0.2%) (pH 8.0). The resulting solution was applied to a HiPrep™ Q-Sepharose 16/10 FF column.

Step 2: HiPrep™ Q-Sepharose 16/10 FF. A HiPrep™ Q-Sepharose 16/10 FF column (1.6 x 10 cm) was equilibrated with 10 mM Tris-HCl, 1 mM DTT, Triton X-100 (0.2%) (pH 8.0). The column was washed using the same buffer, at a flow rate of 0.8 ml/h (100 mL). The final pool of micelles was

eluted using an increasing linear gradient (100 mL) of 0 to 2 M NaCl in 10 mM Tris-HCl, 1 mM DTT, Triton X-100 (0.2%) (pH 8.0).

Enzymatic activity assays and protein quantification

The protein content was determined by the Bradford method, with bovine serum albumin as a standard (Bradford, 1976). Nar and Nir activities were assayed in solubilised extracts as well as along the purification process as previously described (Martínez-Espinosa *et al.,* 2001a; Martínez-Espinosa *et al.,* 2001b; Lledó *et al.,* 2004). The assay mixture for Nar activity contained, in a final volume of 250 µL, 100 mM Tris-HCl pH 8, 3.6 M NaCl, 4 mM methyl viologen (MV), 35 mM KNO_3, 17 mM $Na_2S_2O_4$ (freshly prepared in 0.1 M $NaHCO_3$) and 50 µL of sample preparations; for Nir activity, the mixture contained, in a final volume of 250 µL, 50 mM phosphate buffer Ph 7.5, 3.2 M NaCl, 3 mM methyl viologen (MV), 5 mM KNO_2, 17 mM $Na_2S_2O_4$ (freshly prepared in 0.1 M $NaHCO_3$) and 50 µL of sample preparations The assay was developed at 40ºC for 15 min (Nar activity) or 20 min (Nir activity). Nar specific activity is expressed as micromoles of NO_2^- appearing per minute per milligram of protein, while Nir specific activity is expressed as micromoles of NO_2^- disappearing per minute per milligram of protein (U = µmol NO_2^-/min). All the assays were carried out in triplicate and against a control assay without enzyme.

Proteomic Analysis

Sample preparation

50 µg protein were precipitated with Tricloroacetic acid 10% (w/v) in a final volume of 500 µL overnight at -20ºC. Then, the proteins were pelleted by centrifugation at 16,000 x*g* in a centrifuge Eppendorf 5418 R for 5 minutes and washed three times using 1 mL of cold acetone for each sample. The clean precipitated was then resuspended in a solution containing urea 6 M (50 µL).

Tryptic in-solution digestion

For tryptic in-solution digestion, 50 µg of protein sample were reduced with 5 µL of 0.2 M dithiothreitol followed by incubation for 1 h at 37°C and S-alkylation with 20 µL of 0.2 M iodoacetamide followed by incubation for 1 h in the dark at room temperature. Then, 25 mM ammonium bicarbonate buffer was added to reduce the concentration of urea to 0.6 M. For in-solution digestion, trypsin was added to the protein mixture at an enzyme-to-substrate ratio of 1:30 (w/w). After incubation at 37°C for 16 h, additional trypsin (1:60, w/w) was added to the sample and incubation was continued for 5 h to ensure complete digestion. Tryptic peptides were dried down in a Speed-Vacbenchtop centrifuge and resuspended in 5% acetonitrile and 0.5% trifluoroacetic acid. The resulting peptides were desalted with PepClean C-18 Spin Columns (Agilent Technologies) in batches of 30 µg of protein according to manufacturer recommendations. Eventually, eluted peptides were dried down in a Speed-Vacbenchtop centrifuge and resuspended in 10 µL of first LC mobile phase (5% acetonitrile and 0.1% formic acid).

LC-MS/MS conditions

Peptide separation was performed using an Agilent 1290 Infinity LC system coupled to the 6550 Accurate-Mass QTOF (Agilent Technologies, Santa Clara, CA, USA) with electrospray interface (Jet Stream Technology) operating in positive-ion mode (3,500 V) and in high sensitivity mode. The best conditions for the electrospray interface were: gas temperature 250 °C, drying gas 14 L/min, nebulizer 35 psi, sheath gas temperature 250 °C, sheath gas flow 11 L/min. Samples were injected (10 µL) on an Agilent Advance Bio Peptide mapping column (2.1 × 250 mm, 2.7 µm) (Agilent Technologies) with a 3–40% gradient of solvent B (0.1% formic acid in 90% acetonitrile) for 140 min operating at 50 °C and a flow rate of 0.4 mL/min. The data were acquired with Agilent Mass Hunter Workstation Software, LC/MS Data Acquisition B.08.00 (Build 8.00.8058.0) operating in Auto MS/MS mode whereby the 20 most intense ions (charge states, 2–5) within

300–1,700 m/z mass range above a threshold of 1,000 counts were selected for MS/MS analysis. MS/MS spectra (50–1,700 m/z) were collected with the quadrupole set to "narrow" resolution and were acquired until 25,000 total counts were collected or for a maximum accumulation time of 333 ms. To assure the desired mass accuracy of recorded ions, continuous internal calibration was performed during analyses with the use of signals m/z 322.0481 (detected m/z $[C6H18N3O6P3 - H]^+$) and m/z 1221.9906 (detected m/z $[C24H18O6N3P3F36 -H]^+$).

Data analysis.

Each MS/MS spectra data set was processed to determine monoisotopic masses and charge states, to merge MS/MS spectra with the same precursor ($\Delta m/z < 1.4$ Da and chromatographic $\Delta t < 60$ s) and to select high quality spectra with the Extraction tool of SpectrumMill Proteomics Workbench (Agilent). The reduced data set was searched against the *Haloferax* NCBInr database in the identity mode with the MS/MS search tool of SpectrumMillProteomics Workbench and with the following settings: trypsin, up to 2 missed cleavages, carbamidomethylation of cysteines as fixed modifications, oxidation of methionine as variable, mass tolerance of ±20 ppm for precursor and ±50 ppm for product ions. The precursor mass shift was set between -18 Da to 177 Da to take into consideration variable modifications such as the presence of sodium and potassium adducts. Peptide hits were validated in the peptide mode to achieve a false discovery rate (FDR) of <1.2% and then in the protein mode according to the score settings recommended by the manufacturer. Positive identifications were considered only when two or more peptides were matched, and their summed score was >30.

ACKNOWLEDGMENTS

This work was funded by research grant from the MINECO Spain (CTM2013-43147-R; RTI2018-099860-B-I00), Generalitat Valenciana (ACIF 2016/077) and University of Alicante (VIGROB-309). The authors thank the technical support from the Research Technical Services at the University of Alicante.

AUTHOR CONTRIBUTIONS

The design of the experiments was conducted by CP and RMME. Membranes solubilization, protein purification and enzymatic activity measurements were performed by JTC and RMME. Proteomic analysis was performed by JTC. Conceptualization, administration, and funding of the project were supplied by DJR, CP and RMME. All the authors contributed to the manuscript writing.

CONFLICT OF INTEREST

The authors declare that the research was conducted in the absence of any commercial or financial relationships that could be construed as a potential conflict of interest.

REFERENCES

Andrei, A.S., Banciu, H.L., Oren, A. (2012) Living with salt: metabolic and phylogenetic diversity of archaea inhabiting saline ecosystems. *FEMS Microbiol. Lett.* 330, 1-9. doi: 10.1111/j.1574-6968.2012.02526.x

Bakken, L.R., Bergaust, L., Liu, B., Frostegård, Å. (2012). Regulation of denitrification at the cellular level: a clue to understanding N_2O emissions from soils. *Philos. Trans. R. Soc. Lond. B. Biol. Sci.* 367, 1226-1234. doi: 10.1098/rstb.2011.0321

Becker, E.A., Seitzer, P.M., Tritt, A., Larsen, D., Krusor, M., Yao, A.I., et al. (2014). Phylogenetically driven sequencing of extremely halophilic archaea reveals strategies for static and dynamic osmo-response. *PLoS. Genet.* 10, e1004784. doi: 10.1371/journal.pgen.1004784.

Bergaust, L., Shapleigh, J., Frostegård, Å., Bakken, L.R. (2008). Transcription and activities of NO_x reductases in *Agrobacterium tumefaciens*: the influence of nitrate, nitrite and oxygen availability. *Environ. Microbiol.* 10, 3070-3081.

Borrero-de Acuña, J.M., Rohde, M., Wissing, J., Jänsch, L., Schobert, M., Molinari, G., Timmis, K.N., Jahn, M., Jahn, D. (2006). Protein network of the *Pseudomonas aeruginosa* denitrification apparatus. *J. Bacteriol.* 198, 1401-1413. doi: 10.1128/JB.00055-16

Bradford, M.M. (1976). A rapid and sensitive method for the quantification of microgram quantities of protein utilizing the principle of protein dye binding. *Anal. Biochem.* 72, 248-256. doi: 10.1016/0003-2697(76)90527-3

Brischwein, M., Scharf, B., Engelhard, M., Mäntele, W. (1993). Analysis of the redox reaction of an archaebacterial copper protein, halocyanin, by electrochemistry and FTIR difference spectroscopy. *Biochemistry*. 32, 13710–13717. doi: 10.1021/bi00212a041

Cerletti, M., Giménez, M.I., Tröetschel, C., D'Alessandro, C., Poetsch, A., De Castro, R.E., Paggi, R.A. (2018). Proteomic study of the exponential-stationary growth phase transition in the haloarchaea *Natrialba magadii* and *Haloferax volcanii*. *Proteomics*. 18, e1800116. doi: 10.1002/pmic.201800116

Costa, M.I., Cerletti, M., Paggi, R.A., Trötschel, C., De Castro, R., Poetsch, A., et al. (2018). *Haloferax volcanii* proteome response to deletion of a rhomboid protease gene. *J. Proteome. Res.* 17, 961-977. doi: 10.1021/acs.jproteome.7b00530

Chu, L.J., Yang, H., Shih, P., Kao, Y., Tsai, Y.S., Chen, J., et al. (2011). Metabolic capabilities and systems fluctuations in *Haloarcula marismortui* revealed by integrative genomics and proteomics analyses. *J. Proteome. Res.* 10, 3261-3273. doi: 10.1021/pr200290x.

Dell'acqua, S., Moura, I., Moura, J.J., Pauleta, S.R. (2015). The electron transfer complex between nitrous oxide reductase and its electron donors. *J. Biol. Inorg. Chem.* 16, 1241-1254. doi: 10.1007/s00775-011-0812-9

Duquesne, K., Sturgis, J.N. (2010). Membrane protein solubilization. *Methods. Mol. Biol*. 601, 205-217. doi: 10.1007/978-1-60761-344-2_13.

Edbeib, M.F., Wahab, R.A., Huyop, F. (2016). Halophiles: biology, adaptation, and their role in decontamination of hypersaline environments. *World. J. Microbiol. Biotechnol.* 32, 1-23. doi: 10.1007/s11274-016-2081-9

Esclapez, J., Zafrilla B., Martínez-Espinosa, R.M., Bonete, M.J. (2013). Cu-NirK from *Haloferax mediterranei* as an example of metalloprotein maturation and exportation via Tat system. *Biochim. Biophys. Acta.* 1834, 1003-1009. doi: 10.1016/j.bbapap.2013.03.002

Fagan, R.P., Fairweather, N.F. (2014). Biogenesis and functions of bacterial S-layers. *Nat. Rev. Microbiol.* 12, 211-222. doi: 10.1038/nrmicro3213

Grüber, G., Manimekalai, M.S., Mayer, F., Müller, V. (2014). ATP synthases from archaea: the beauty of a molecular motor. *Biochim. Biophys. Acta.* 1837, 940-952. doi: 10.1016/j.bbabio.2014.03.004

Han, J., Zhang, F., Hou, J., Liu, X., Li, M., Liu, H., et al. (2012). Complete genome sequence of the metabolically versatile halophilic archaeon *Haloferax mediterranei*, a poly(3-hydroxybutyrate-co-3-hydroxyvalerate) producer. *J. Bacteriol.* 194, 4463-4464. doi: 10.1128/JB.00880-12

Hendriks, J., Oubrie, A., Castresana, J., Urbani, A., Gemeinhardt, S., Saraste, M. (2000). Nitric oxide reductases in Bacteria. *Biochim. Biophys. Acta.* 1459, 266-273. doi: 10.1016/s0005-2728(00)00161-4

Jormakka, M., Törnroth, S., Byrne, B., Iwata, S. (2002). Molecular basis of proton motive force generation: structure of formate dehydrogenase-N. *Science*. 295, 1863-1868. doi: 10.1126/sciencie.1068186

Machczynski, M.C., Gray, H.B., Richards, J.H. (2002). An outer-sphere hydrogen-bond network constrains copper coordination in blue proteins. *J. Inorg. Biochem.* 88, 375-380. doi: 10.1016/S0162-0134(02)00364-1

Martínez-Espinosa, R.M., Marhuenda-Egea, F.C., Bonete, M.J. (2001a). Purification and characterisation of a possible assimilatory nitrate reductase from the halophile archaeon *Haloferax mediterranei*. *FEMS Microbiol. Lett.* 196, 113-118. doi: 10.1111/j.1574-6968.2001.tb10550.x

Martínez-Espinosa, R.M., Marhuenda-Egea, F.C., Bonete, M.J. (2001b). Assimilatory nitrate reductase from the haloarchaeon *Haloferax mediterranei*: purification and characterisation. *FEMS Microbiol. Lett.* 204, 381-385. doi: 10.1016/s0378-1097(01)00431-1

Martínez-Espinosa, R.M., Richardson, D.J., Butt, J.N., Bonete, M.J. (2006). Respiratory nitrate and nitrite pathway in the denitrifier haloarchaeon *Haloferax mediterranei*. *Biochem. Soc. Trans.* 34(Pt 1), 115-117. doi: 10.1042/BST0340115

Martínez-Espinosa, R.M., Dridge, E.J., Bonete, M.J., Butt, J.N., Butler, C.S., Sargent, F., Richardson, D.J. (2007). Look on the positive side! The orientation, identification and bioenergetics of "Archaeal" membrane-bound nitrate reductases. *FEMS Microbiol. Lett.* 276, 129-139. doi: 10.1111/j.1574-6968.2007.00887.x

Mattar, S., Scharf, B., Kent, S. B., Rodewald, K., Oesterhelt, D., & Engelhard, M. (1994). The primary structure of halocyanin, an archaeal blue copper protein, predicts a lipid anchor for membrane fixation. *J. Biol. Chem*. 269, 14939–14945.

Moore, S.M., Hess, S.M., Jorgenson, W. (2016). Extraction, enrichment, solubilization, and digestion techniques for membrane proteomics. *J. Proteome. Res.* doi: 10.1021/acs.jproteome.5b01122

Nojiri, M. (2017). "Structure and function of copper nitrite reductase", in Metalloenzymes in denitrification: applications and environmental impacts, eds. I. Moura, J.J.G. Moura, S.R. Pauleta, L.B. Maia (Cambridge, UK: Royal Society of Chemistry), 91-113. doi: 10.1039/9781782623762-FP001

Lledó, B., Martínez-Espinosa, R.M., Marhuenda-Egea, F.C., Bonete, M.J. (2004). Respiratory nitrate reductase from haloarchaeon *Haloferax mediterranei*: biochemical and genetic analysis. *Biochim. Biophys. Acta.* 1674, 50-59. doi: 10.1016/j.bbagen.2004.05.007

Leuko, S., Raftery, M.J., Burns, B.P., Walter, M.R., Neilan, B.A. (2009). Global protein-level responses of *Halobacterium salinarum* NRC-1 to prolonged changes in external sodium chloride concentrations. *J. Proteome. Res.* 8, 2218-2225. doi: 10.1021/pr800663c.

Luche, S., Santoni, V., Rabilloud, T. (2003). Evaluation of nonionic and zwitterionic detergents as membrane protein solubilizers in two-dimensional electrophoresis. *Proteomics.* 3, 249-253. doi: 10.1002/pmic.200390037

Ochoa-Hueso, R., Arrónez-Crespo, M., Bowker, M.A., Maestre, F.T., Pérez-Corona, M.E., Theobald, M.R., *et al.* (2014). Biogeochemical indicators of elevated nitrogen depositions in semiarid Mediterranean ecosystems. *Environ. Monit. Assess.* 186, 5831-5842. doi: 10.1007/s10661-014-3822-6

Oren, A. (2013). Life at high salt concentrations, intracellular KCl concentrations and acidic proteomes. *Front*. *Microbiol.* 4, 1-6. doi: 10.3389/fmicb.2013.00315

Pauleta, S.R., Carreira, C., Moura, I. (2017). "Insights into nitrous oxide reductase", in Metalloenzymes in denitrification: applications and environmental impacts, eds. I. Moura, J.J.G. Moura, S.R. Pauleta, L.B. Maia (Cambridge, UK: Royal Society of Chemistry), 141-169. doi: 10.1039/9781782623762-FP001

Pérez-Henarejos, S.A., Alcaraz, L.A., Donaire, A. (2015). Blue copper proteins: a rigid machine for efficient electron transfer, a flexible device for metal uptake. *Arch. Biochem. Biophys.* 584, 134-148. doi: 10.1016/j.abb.2015.08.020

Philippot, L., Hallin, S., Schloter, M. (2007). "Ecology of denitrifying prokaryotes in agricultural soil", in Advances in Agronomy, eds. D.L. Sparks (London: Elsevier), 96, 249-305. doi: 10.1016/S0065-2113(07)96003-4

Richardson, D.J. (2000). Bacterial respiration: a flexible process for a changing environment. *Microbiology* 146, 551-571. doi: 10.1099/00221287-146-3-551

Roco, C.A., Bergaust, L., Bakken, L.R., Yavitt, J.B., Shapleigh, J.P. (2017). Modularity of nitrogen-oxide reducing soil bacteria: linking phenotype to genotype. *Environ. Microbiol.* 19, 2507-2519. doi: 10.1111/1462-2920.13250

Rodrigues-Oliveira, T., Belmok, A., Vasconcellos, D., Schuster, B., Kyaw, C.M. (2017). Archaeal S-layers: overview and current state of the art. *Front. Microbiol.* 8, 1-17. doi: 10.3389/fmicb.2017.02597

Rodríguez-Valera, F., Ruiz-Berraquero, F., Ramos-Cormenzana, A. (1980). Behaviour of mixed populations of halophilic bacteria in continuous cultures. *Can. J. Microbiol.* 26, 1259–1263.

Rodríguez-Valera, F., Ventosa, A., Juez, G., Imhoff, J.F. (1985). Variation of environmental features and microbial populations with salt concentration in a multi-pond saltern. *Microb. Ecol.* 11, 107-115. doi: 10.1007/BF02010483

Rosen, M.J. (2004). Surfactants and Interfacial Phenomena, ed. M.J. Rosen (New Jersey, USA: Wiley Hoboken, John Wiley & Sons, Inc.). doi: 10.1002/0471670561.

Samad, M.S., Bakken, L.R., Nadeem, S., Clough, T.J., de Klein, C.A., Richards, K.G., Lanigan, G.J., Morales, S.E. (2016). High-resolution denitrification kinetics in pasture soils link N_2O emissions to pH, and denitrification to C mineralisation. *PLoS One* 11(3):e0151713. doi: 10.1371/journal.pone.0151713

Scharf, B., Engelhard, M. (1993). Halocyanin, an archaebacterial blue copper protein (type I) from *Natronobacterium pharaonis*. *Biochemistry.* 32, 12894-12900. doi: 10.1021/bi00210a043

Taylor, C.M., Pfeiffer, S.E. (2003). Enhanced resolution of glycosylphosphatidylinositol-anchored and transmembrane proteins from the lipid-rich myelin membrane by two-dimensional gel electrophoresis. *Proteomics.* 3, 1303-1312. doi: 10.1002/pmic.200300451

Torregrosa-Crespo, J., Martínez-Espinosa, R.M., Esclapez, J., Bautista, V., Pire, C., Camacho, M., et al. (2016). Anaerobic metabolism in *Haloferax* genus: denitrification as case of study. *Adv. Microb. Physiol.* 68, 41-85. doi: 10.1016/bs.ampbs.2016.02.001

Torregrosa-Crespo, J., González-Torres, P., Bautista, V., Esclapez, J., Pire, C., Camacho, M., et al. (2017). Analysis of multiple haloarchaeal genomes suggests that the quinone-dependent respiratory nitric oxide reductase is an important source of nitrous oxide in hypersaline environments. *Environ. Microbiol. Rep.* 9, 788-796. doi: 10.1111/1758-2229.12596

Torregrosa-Crespo, J., Bergaust, L., Pire, C., Martínez-Espinosa, R.M. (2018). Denitrifying haloarchaea: sources and sinks of nitrogenous gases*. FEMS Microbiol. Lett.* 365, 1-6. doi: 10.1093/femsle/fnx270.

Torregrosa-Crespo, J., Pire, C., Martínez-Espinosa, R.M., Bergaust, L. (2019a). Dentrifying haloarchaea withing the genus *Haloferax* display divergent respiratory phenotypes, with implications for their release of nitrogenous gases. *Environ. Microbiol.* 21, 427-436. doi: 10.1111/1462-2920.14474

Torregrosa-Crespo, J., Bergaust, L., Pire, C., Martínez-Espinosa, R.M. (2019b). *Haloferax mediterranei,* an archaeal model for denitrification in saline systems, characterised through integrated phenotypic and transcriptional analyses. *App. Environ. Microbiol.* (Submitted).

Wessels, H.J.C.T., de Almeida, N.M., Kartal, B., Keltjens, J.T. (2016) Bacterial electron transfer chains primed by proteomics. *Adv. Microb. Physiol.* 68, 41-85. doi: 10.1016/bs.ampbs.2016.02.006.

Witzmann, F., Jarnot, B., Parker, D. (1991). Dodecyl maltoside detergent improves resolution of hepatic membrane proteins in two-dimensional gels. *Electrophoresis.* 12, 687-688. doi: 10.1002/elps.1150120919

Zumft, W.G., Kroneck, P.M. (2006). Respiratory transformation of nitrous oxide (N_2O) to dinitrogen by Bacteria and Archaea. *Adv. Microb. Physiol.* 52, 107-227. doi: 10.1016/S0065-2911(06)52003-X

SUPPLEMENTARY INFORMATION

Exploring the molecular machinery of denitrification in *Haloferax mediterranei* through proteomics

Javier Torregrosa-Crespo[1], Carmen Pire[1], David J. Richardson[2] and Rosa María Martínez-Espinosa[1]*

[1]Departamento de Agroquímica y Bioquímica. División de Bioquímica y Biología Molecular. Facultad de Ciencias. Universidad de Alicante. Carretera San Vicente del Raspeig s/n - 03690 San Vicente del Raspeig, Alicante. E-mail: javitorregrosa@ua.es

[2]School of Biological Sciences, University of East Anglia, Norwich Research Park, Norwich NR4 7TJ, UK

*Corresponding author: Rosa María Martínez-Espinosa

e-mail: rosa.martinez@ua.es

Telephone: +34 96 590 3400 ext. 1258; 8841

Fax: +34 96 590 3464

Table S1. Score, protein sequence coverage and spectral intensity values of the N-reductases during the enrichment process. Data are shown as the average of triplicates with standard deviation.

A

	NarG			NarH			NarI		
Fraction	**Score**	**%aa coverage**	**Spectral intensity**	**Score**	**%aa coverage**	**Spectral intensity**	**Score**	**%aa coverage**	**Spectral intensity**
Crude extract	119.17 ± 19.8	11.70 ± 0.8	2.58E6 ± 2.5E5	112.14 ± 4.7	24.40 ± 1.7	3.27E6 ± 2.7E4	49.88 ± 1.5	13.40 ± 1.1	1.03E6 ± 7.5E4
DEAE-Sepharose	269.39 ± 9.1	24.70 ± 1.2	2.09E7 ± 1.2E6	95.18 ± 1.7	19.30 ± 0.3	9.26E6 ± 2.3E4	47.03 ± 2.4	13.40 ± 0.8	1.43E6 ± 2.7E4
Q-Sepharose	380.05 ± 11.3	34.40 ± 2.3	3.88E7 ± 2.9E5	136.08 ± 2.7	27.50 ± 1.0	2.12E7 ± 3.1E5	n.a.	n.a.	n.a.

B

	Nir			Nor			Nos		
Fraction	**Score**	**%aa coverage**	**Spectral intensity**	**Score**	**%aa coverage**	**Spectral intensity**	**Score**	**%aa coverage**	**Spectral intensity**
Crude extract	108.21 ± 1.7	20.80 ± 1.4	6.04E7 ± 7.4E5	126.21 ± 9.3	14.53 ± 0.8	1.15E7 ± 8.5E5	263.67 ± 14.8	26.2 ± 1.2	9.36E7 ± 2.1E5
DEAE-Sepharose	112.23 ± 8.0	20.80 ± 0.3	1.53E8 ± 3.2E6	99.58 ± 2.5	14.3 ± 0.7	8.25E6 ± 2.7E4	381.40 ± 3.1	38.6 ± 0.6	3.24E8 ± 1.5E6
Q-Sepharose	161.07 ± 4.9	32.80 ± 0.3	2.40E8 ± 4.0E6	106.03 ± 7.0	15.6 ± 1.7	4.20E6 ± 7.0E4	349.62 ± 5.3	38.2 ± 0.6	1.90E8 ± 2.1E6

Table S2. Representative proteins identified in the crude extract using Triton X-100 (10% w/v) from 3 LC-MS/MS runs.

Protein Name	Database Accession	Spectra	Distinct Peptides	Distinct Summed MS/MS Search Score	% aa Coverage	Total Protein Spectral Intensity
SPFH domain, Band 7 family protein	AFK18490.1	32	23	400.03	59.1	2.70e+008
SPFH domain, Band 7 family protein	AFK17777.1	11	9	147.90	29.1	5.11e+007
AAA-type ATPase (transitional ATPase-like protein)	AFK20074.1	28	25	391.22	46	4.41e+007
A-type ATP synthase subunit A	AFK18041.1	27	17	306.52	35.6	1.19e+008
succinate dehydrogenase, subunit A (flavoprotein)	AFK20495.1	20	16	293.07	35.9	6.45e+007
dipeptide ABC transporter dipeptide-binding protein	AFK17806.1	20	17	281.44	27.9	1.21e+008
A-type ATP synthase subunit C	AFK18039.1	22	16	271.71	64.6	6.55e+007
dipeptide/oligopeptide/nickel ABC transporter periplasmic substrate-binding protein	AFK18790.1	19	16	262.89	34.6	5.37e+007
A-type ATP synthase subunit B	AFK18042.1	23	15	256.40	38.4	1.11e+008
poly(3-hydroxyalkanoate) synthase subunit PhaC (plasmid)	AFK21054.1	19	14	253.12	41.4	2.41e+007
sugar ABC transporter substrate binding protein	AFK20386.1	17	14	247.01	40.9	1.04e+008
NADH dehydrogenase, subunit CD (ubiquinone)	AFK18696.1	20	15	245.61	30.5	7.21e+007
NADH dehydrogenase, subunit D (ubiquinone)	AFK18684.1	6	4	71.91	7.9	2.88e+007
halocyanin hcpG	AFK18949.1	17	13	242.96	26.5	3.84e+007
A-type ATP synthase subunit I	AFK18036.1	15	13	238.25	22.4	5.86e+007
periplasmic solute binding protein	AFK20085.1	16	13	235.59	46	1.35e+008
dipeptide ABC transporter ATP-binding protein	AFK18330.2	18	13	231.75	32.8	9.04e+007
nucleoside-binding protein	AFK19185.1	15	12	209.36	33.4	7.45e+007
thermosome alpha subunit	AFK18461.1	14	12	196.35	31.4	3.04e+007
thermosome, beta subunit	AFK18158.2	14	11	190.56	29.4	2.80e+007
thermosome, alpha subunit	AFK17883.2	12	11	187.62	33	2.01e+007
PBS lyase HEAT-like repeat protein	AFK18736.1	14	10	176.14	34	4.15e+007
transmembrane oligosaccharyl transferase / dolichyl-diphosphooligosaccharide--protein glycosyltransf	AFK19298.1	12	11	168.62	11.6	1.21e+007
A-type ATP synthase subunit D	AFK18044.1	14	11	159.41	48.6	2.28e+007
stress response protein	AFK20336.2	12	10	158.80	46.6	2.67e+007
ABC-type dipeptide/oligopeptide/nickel transport system, substrate binding protein	AFK20131.1	11	10	157.17	29.7	1.79e+007
hypothetical protein HFX_2220	AFK19909.2	13	9	152.71	5.7	5.08e+007

glutamine synthetase	AFK17986.2	11	9	150.61	31.1	3.64e+007
NADH dehydrogenase	AFK19343.1	11	8	148.16	38	1.97e+007
flavin-dependent dehydrogenase	AFK20419.1	11	9	145.44	26.1	1.43e+007
nitrous-oxide reductase (plasmid)	AFK20926.1	9	9	140.39	11.7	2.96e+007
A-type ATP synthase subunit E	AFK18038.1	9	7	135.59	58.7	2.24e+007
membrane protease subunit, stomatin/prohibitin	AFK17891.1	11	8	134.69	34.3	2.95e+007
ABC-type dipeptide/oligopeptide/nickel transport system, substrate-binding protein	AFK19559.1	10	9	132.98	17.1	8.67e+006
poly(3-hydroxyalkanoate) synthase subunit PhaE (plasmid)	AFK21053.1	12	7	131.64	53.2	1.14e+008
potassium transport protein kefC	AFK19701.1	12	9	130.26	17.9	1.90e+007
glutamate dehydrogenase (NAD(P)+)	AFK19225.1	10	9	129.78	24.9	1.02e+007
glycosyl transferase	AFK19287.1	8	8	129.57	29.1	4.73e+006
putative phosphonate ABC transporter, periplasmic phosphonate-binding protein	AFK19847.1	8	7	129.42	23.4	2.49e+007
ABC-type iron(III) transport system,substrate-binding protein	AFK19499.1	9	7	128.61	33.5	5.05e+007
serine protease (plasmid)	AFK21203.1	10	9	128.28	20.8	1.74e+007
immunogenic protein	AFK20638.1	8	7	124.73	40.4	5.53e+007
isocitrate dehydrogenase (NADP+)	AFK20291.1	9	9	124.35	23.3	9.85e+006
CBS domain-containing protein	AFK20079.1	10	7	122.70	28.1	2.11e+007
putative signal transduction protein with CBS domains (plasmid)	AFK21146.1	8	8	122.31	20.2	7.92e+006
hypothetical protein HFX_5081 (plasmid)	AFK20916.2	9	8	121.68	32.1	2.95e+007
NADH dehydrogenase, subunit B (ubiquinone)	AFK18695.1	13	8	120.79	48.4	2.81e+007
hypothetical protein HFX_2459	AFK20144.2	13	6	116.86	8.4	2.04e+008
amino acid-binding protein (plasmid)	AFK21485.1	7	7	116.54	28.4	5.41e+006
hypothetical protein HFX_6053 (plasmid)	AFK21180.1	7	7	113.93	26.6	5.42e+006
phosphate ABC transporter periplasmic substrate-binding protein	AFK20069.1	8	7	111.81	20.6	1.19e+007
ABC-type dipeptide/oligopeptide/nickel transport system, substrate-binding protein (plasmid)	AFK21027.1	8	8	108.79	14.9	1.52e+007
phosphonates ABC transporter ATP-binding protein	AFK19846.1	9	6	108.71	36.7	7.96e+006
aldehyde dehydrogenase	AFK20313.1	7	7	107.77	18.6	6.00e+006
FAD dependent oxidoreductase	AFK19621.1	7	7	103.68	19.6	3.88e+006
dihydrolipoamide S-acyltransferase (pyruvate dehydrogenase E2 component)	AFK20618.1	7	7	103.54	15.6	6.61e+006
putative hydrolase or acyltransferase of alpha/beta superfamily	AFK18525.1	7	6	101.36	30.8	1.28e+007
hypothetical protein HFX_1950	AFK19646.1	6	6	99.96	45.2	6.92e+006
aldehyde dehydrogenase (NAD+)	AFK18912.1	7	7	99.83	15.3	3.36e+006

prepilin signal peptidase	AFK20651.1	7	7	98.16	22.8	5.51e+006
S-adenosylmethionine-dependent methyltransferase-like protein	AFK18456.1	7	7	97.99	29.7	4.86e+006
biotin carboxylase	AFK20173.1	6	6	97.76	10.9	3.72e+006
phosphoenolpyruvate synthase / pyruvate, water dikinase	AFK18505.1	7	7	94.93	9.1	3.59e+006
succinate dehydrogenase, subunit B (iron-sulfur protein)	AFK20496.1	7	7	94.87	23.8	9.42e+006
ABC-type dipeptide/oligopeptide/nickel transport system, substrate binding protein (plasmid)	AFK20740.1	6	6	94.51	14.5	5.81e+006
A-type ATP synthase subunit H	AFK18035.1	6	6	93.99	62.7	4.64e+006
NADH dehydrogenase/oxidoreductase-like protein	AFK19950.1	8	6	93.42	28.9	8.53e+006
gluconate dehydratase	AFK19260.1	6	6	93.39	17.9	1.37e+007
succinate--CoA ligase beta subunit (ADP-forming)	AFK20155.1	6	6	93.00	22.5	2.59e+006
oxidoreductase	AFK18898.2	6	6	92.12	30.4	6.93e+006
glutamate-1-semialdehyde aminotransferase	AFK17832.1	6	6	91.87	19.7	4.32e+006
proline dehydrogenase	AFK18055.1	7	6	90.53	24.7	5.87e+006
catalase (including: peroxidase)	AFK19564.1	6	6	90.52	10.3	6.53e+006
ABC-type branched-chain amino acid transport systems, substrate-binding protein	AFK20482.1	10	5	90.41	20.5	2.92e+007
hypothetical protein HFX_2976	AFK20640.1	6	6	87.60	6.4	1.07e+007
ATP-dependent protease Lon	AFK18465.1	5	5	85.62	9.4	3.61e+006
branched-chain-amino-acid aminotransferase	AFK18053.1	6	6	85.22	26.9	5.02e+006
dipeptide/oligopeptide/nickel ABC transporter ATP-binding protein	AFK17802.1	6	5	85.13	14.7	4.73e+006
hypothetical protein HFX_1766	AFK19471.1	7	6	84.98	30.5	2.09e+007
gas-vesicle operon protein gvpC	AFK19401.1	7	5	84.95	17.8	8.55e+006
ABC-type glutamine/glutamate/polar amino acids transport system, ATP-binding protein	AFK20124.1	5	5	84.49	22.3	5.17e+006
hypothetical protein HFX_2780	AFK20456.1	7	6	82.95	21.2	3.46e+006
pyruvate--ferredoxin oxidoreductase, alpha subunit	AFK19081.1	7	5	82.63	12.6	4.88e+006
oligopeptide ABC transporter ATPase component	AFK17803.1	5	5	79.94	18.8	2.50e+007
short chain dehydrogenase/ reductase	AFK18407.1	5	5	78.60	26.3	4.63e+006
dihydrolipoamide dehydrogenase	AFK20619.1	5	5	78.57	12.6	4.45e+006
gas-vesicle operon protein gvpA	AFK19402.1	5	4	78.17	70.5	3.01e+007
ABC transporter ATP-binding protein	AFK20685.1	5	5	78.12	19.3	2.14e+006
poly(3-hydroxyalkanoate) granule-associated 12 kDa protein (plasmid)	AFK21051.1	7	4	77.21	34.5	2.33e+007
poly(3-hydroxyalkanoate) synthase subunit PhaC	AFK20356.1	6	5	76.87	17.4	2.19e+006
iron-sulfur protein (4Fe-4S)	AFK17960.2	5	5	76.20	7.8	6.36e+006
putative mechanosensitive ion channel	AFK19964.1	5	5	75.61	24.6	3.80e+006

ArsR family regulatory protein	AFK19320.1	4	4	74.93	34.4	3.55e+006
menaquinol--cytochrome-c reductase (cytochrome bc complex) cytochrome b/c subunit	AFK18533.1	5	4	73.76	18.1	1.22e+007
cytochrome bc1 complex cytochrome b/c subunit	AFK18497.1	4	4	67.42	17.4	9.19e+006
hypothetical protein HFX_0293	AFK18032.2	5	5	73.04	14.9	1.11e+006
menaquinol--cytochrome-c reductase	AFK20314.1	5	4	72.52	19.5	2.14e+007
zinc-transporting ATPase (plasmid)	AFK21399.1	5	5	71.52	7.7	1.23e+006
oxidoreductase (geranylgeranyl hydrogenase-like protein)	AFK19602.1	5	4	71.13	13.1	1.99e+006
poly(3-hydroxyalkanoate) granule-associated protein(phasin) (plasmid)	AFK21052.1	12	5	70.72	27.2	1.44e+008
methanol dehydrogenase regulatory protein	AFK18978.1	5	5	70.71	15.1	3.06e+006
methanol dehydrogenase regulatory protein (plasmid)	AFK21086.1	1	1	21.38	4.6	6.91e+005
hypothetical protein HFX_0491	AFK18222.1	6	4	69.82	34.1	3.62e+006
3-oxoacyl-[acyl-carrier protein] reductase	AFK19230.1	5	4	69.76	19.4	8.13e+006
hypothetical protein HFX_0588	AFK18313.1	5	4	68.80	16.2	8.92e+006
pyridoxal biosynthesis lyase PdxS	AFK20032.1	5	5	68.42	17.5	2.53e+006
sugar ABC transporter ATP-binding protein	AFK20383.1	6	4	68.19	17.2	1.03e+007
hypothetical protein HFX_1575	AFK19282.2	5	4	68.10	22.3	1.46e+007
lysophospholipase	AFK20242.1	4	4	67.95	16.6	6.68e+006
hypothetical protein HFX_2555	AFK20236.1	4	4	67.69	17.2	5.96e+006
orotate phosphoribosyltransferase-like protein/conserved Entner-Douderoff pathway protein	AFK18805.1	6	5	67.52	25.2	4.56e+006
putative RNA-associated protein	AFK19132.1	4	4	67.21	23.9	3.98e+006
AAA-type ATPase (transitional ATPase-like protein)	AFK20391.1	5	5	67.09	6.4	1.75e+006
pyruvate--ferredoxin oxidoreductase, beta subunit	AFK19080.1	4	4	67.04	16.9	2.66e+006
aminopeptidase (plasmid)	AFK21163.2	5	5	66.23	11.1	1.40e+007
hypothetical protein HFX_1249	AFK18962.1	5	5	66.15	8.7	1.73e+006
hypothetical protein HFX_6278 (plasmid)	AFK21400.1	4	4	66.00	29.9	5.21e+006
hypothetical protein HFX_6273 (plasmid)	AFK21396.2	4	4	65.92	15.1	1.61e+006
ferredoxin (2Fe-2S)	AFK19572.1	4	4	65.80	29.3	4.85e+006
ABC-type dipeptide/oligopeptide/nickel transport systems, ATP-binding protein I & II	AFK18329.1	5	5	65.62	6.9	3.26e+006
preprotein translocase subunit SecY	AFK20246.1	6	4	65.47	8.5	9.77e+006
transport ATPase (substrate arsenite)	AFK18406.1	4	4	65.24	12.3	2.82e+006
hypothetical protein HFX_2088	AFK19779.1	4	4	65.09	13.7	2.81e+006
2-oxoglutarate ferredoxin oxidoreductase, subunit alpha	AFK18583.1	4	4	64.41	7.8	3.49e+006

aspartyl-tRNA synthetase	AFK18364.2	5	5	64.21	15.4	5.25e+006
electron transfer flavoprotein alpha subunit	AFK20418.1	5	5	63.30	9.5	4.79e+006
putative hydrolase or acyltransferase of alpha/beta superfamily	AFK19333.1	4	4	62.24	18.7	5.44e+006
hypothetical protein HFX_0292	AFK18031.1	4	4	61.00	12.1	2.74e+006
aldehyde dehydrogenase (NAD+) (plasmid)	AFK21494.1	4	4	60.56	13.4	1.27e+006
molybdate transport protein	AFK19675.1	4	4	60.19	14.5	2.77e+006
ABC-type glutamine/glutamate/polar amino acids transport system, substrate-binding protein	AFK20126.1	6	4	60.00	23	7.55e+006
hypothetical protein HFX_0195	AFK17936.1	4	3	59.03	52.7	1.86e+007
phosphopyruvate hydratase	AFK20460.1	4	4	59.02	13.5	2.58e+006
branched-chain/neutral amino acids amide ABC transporter periplasmic substrate-binding protein	AFK19529.1	4	4	58.85	12.6	1.06e+007
Pyruvate dehydrogenase E1 component subunit beta	AFK20617.1	4	4	58.52	14.6	3.84e+006
regulatory protein PrrC	AFK18961.1	4	3	57.51	21.5	1.07e+007
aconitate hydratase	AFK18238.1	4	4	57.48	6.2	4.26e+006
hypothetical protein HFX_1448	AFK19156.1	4	3	57.44	23.6	7.50e+006
preprotein translocase subunit SecD	AFK19761.1	4	4	57.28	8.2	2.26e+006
hypothetical protein HFX_1776	AFK19481.1	4	4	57.20	8.4	3.24e+006
uracil phosphoribosyltransferase	AFK20636.1	4	4	56.80	28.7	2.56e+006
putative hydrolase of the metallo-beta-lactamase superfamily	AFK20411.1	4	4	55.79	10.6	4.54e+006
CBS domain-containing protein	AFK18713.2	5	4	55.56	14.5	4.38e+006
hypothetical protein HFX_1243	AFK18956.1	4	3	55.36	10.6	8.30e+006
metalloprotease	AFK18012.1	4	4	55.33	14.1	3.56e+006
hypothetical protein HFX_2114	AFK19805.1	3	3	55.09	12.8	2.56e+006
glutaryl-CoA dehydrogenase	AFK17952.2	4	4	54.82	13.1	1.69e+006
phosphate ABC transporter ATP-binding protein	AFK20072.1	4	4	54.15	12.5	3.44e+006
ubiquinone/menaquinone biosynthesis methyltransferase	AFK18034.2	3	3	53.94	16.3	6.87e+006
ABC-type transport system ATP-binding protein	AFK20086.1	4	3	53.27	16.5	4.49e+006
3-hydroxyacyl-CoA dehydrogenase	AFK20502.1	4	4	53.07	6.8	1.45e+006
molecular chaperone DnaK	AFK19355.1	4	4	52.60	9.7	2.50e+006
phosphonates ABC transporter permease protein	AFK19844.1	5	4	52.31	14.9	3.19e+006
enoyl-CoA hydratase	AFK19171.2	4	4	52.25	14.3	3.85e+006
putative iron transport protein	AFK19393.1	4	4	51.71	10.3	3.65e+006
methylmalonyl-CoA decarboxylase alpha chain	AFK20161.1	4	4	51.71	8.9	3.14e+006

putative sugar ABC transporter permease protein	AFK20384.1	3	3	51.47	10.9	7.19e+006
3-ketoacyl-acyl carrier protein reductase (PhaB) (plasmid)	AFK21048.1	3	3	50.80	19.7	2.89e+006
hypothetical protein HFX_0697	AFK18420.1	5	3	50.68	45.1	1.87e+007
gas-vesicle operon protein gvpH	AFK19407.1	4	3	50.64	23.1	2.89e+006
hypothetical protein HFX_6434 (plasmid)	AFK21553.1	4	3	49.62	10.3	1.12e+007
cellulase, endo-1,3(4)-beta-glucanase, peptidase M42 family protein / endoglucanase	AFK20447.1	3	3	49.44	9.3	1.36e+006
proteasome beta subunit	AFK19329.1	4	3	49.08	17.1	5.73e+006
NADH dehydrogenase, subunit H (ubiquinone)	AFK18697.1	4	3	48.67	9.4	2.58e+007
anthranilate phosphoribosyltransferase	AFK19965.1	3	3	47.98	13.2	1.08e+006
S-adenosylmethionine synthetase	AFK19445.1	3	3	47.65	8.7	1.14e+006
hypothetical protein HFX_6075 (plasmid)	AFK21202.1	3	3	47.52	33.3	4.90e+006
hypothetical protein HFX_1178	AFK18891.1	4	3	47.15	58.5	1.52e+006
hypothetical protein HFX_5167 (plasmid)	AFK21001.1	3	3	46.53	16	1.04e+006
hypothetical protein HFX_2040	AFK19732.2	3	3	45.83	10.2	7.15e+005
hypothetical protein HFX_2772	AFK20448.1	5	3	45.61	26.4	1.98e+007
ABC-type cobalamin/Iron(III)-siderophore transport systems, substrate-binding protein	AFK18834.1	3	3	45.24	11.2	2.31e+006
Ca2+-transporting ATPase	AFK18654.1	3	3	45.14	3.8	1.71e+006
hypothetical protein HFX_0671	AFK18394.1	4	3	45.12	20.4	4.52e+006
nitrite reductase (NO-forming)	AFK19872.1	4	3	43.76	10.8	2.24e+006
sugar phosphotransferase system (PTS) IIB component	AFK19266.1	3	3	43.30	29.8	1.79e+006
hypothetical protein HFX_1804	AFK19508.1	3	3	43.23	20.7	2.64e+006
glycosyltransferase	AFK19379.1	3	3	43.08	15.7	5.86e+006
purK operon protein / membrane-bound mannosyltransferase	AFK18691.1	3	3	42.15	6.3	1.26e+006
NADH dehydrogenase-like complex, subunit I	AFK18698.1	3	3	42.06	16.3	3.25e+006
putative ABC transporter permease protein	AFK20385.1	2	2	41.96	7.3	5.20e+006
acyl-CoA synthetase	AFK19702.1	3	3	41.90	5.9	1.65e+006
hypothetical protein HFX_2509	AFK20191.2	3	3	41.51	7.8	3.43e+006
superoxide dismutase, Fe-Mn family	AFK20579.1	3	3	41.45	16	1.46e+006
superoxide dismutase, Fe-Mn family (plasmid)	AFK21528.1	2	2	24.76	10	1.04e+006
propionyl-CoA carboxylase carboxyltransferase component	AFK19220.2	3	3	40.79	5.1	1.02e+006
universal stress protein UspA-like protein	AFK19887.1	3	3	40.74	9.5	3.27e+006
sec-independent protein translocase component TatC2	AFK17925.1	3	3	40.72	5.2	1.18e+006

acyl-CoA synthetase (plasmid)	AFK20965.1	3	3	40.35	4.5	6.85e+005
N-methylhydantoinase B (ATP-hydrolyzing) (plasmid)	AFK21025.1	3	3	39.75	5.5	1.15e+006
NADH dehydrogenase, subunit M (ubiquinone)	AFK18703.1	3	3	39.66	5.5	8.30e+006
hypothetical protein HFX_0728	AFK18451.1	3	3	39.19	19.4	1.28e+006
putative membrane-associated Zn-dependent protease	AFK19648.2	3	3	39.10	5	9.71e+005
putative signal peptide peptidase SppA	AFK18576.1	2	2	39.05	15.6	1.70e+006
putative phosphate acetyltransferase	AFK18715.1	3	3	38.88	9	2.39e+006
protein-disulfide isomerase	AFK18965.1	4	2	38.69	13.8	1.89e+006
hypothetical protein HFX_2876	AFK20546.1	3	2	38.26	11.2	1.85e+007
RecJ-like exonuclease	AFK20553.1	3	3	38.24	4	7.59e+005
dihydroorotate dehydrogenase 2	AFK20600.1	2	2	38.24	12	1.54e+006
hypothetical protein HFX_1273	AFK18986.1	2	2	38.05	12.1	5.34e+006
phytoene dehydrogenase (phytoene desaturase)	AFK18509.1	3	3	37.90	7.7	1.16e+006
ferredoxin:NAD+ oxidoreductase	AFK20041.1	2	2	37.71	7.5	1.60e+006
acyl-CoA synthetase	AFK19349.1	3	3	37.48	4.2	9.61e+005
sialidase-1	AFK20474.1	2	2	37.25	6.2	1.58e+006
NADH dehydrogenase, subunit N (ubiquinone)	AFK18704.1	2	2	36.97	3.5	3.88e+006
universal stress protein UspA-like protein	AFK18989.1	3	2	36.81	26.2	4.11e+006
oxidoreductase	AFK18724.1	2	2	36.71	6.7	6.18e+005
aminopeptidase	AFK18528.1	2	2	36.69	5.2	8.99e+005
hypothetical protein HFX_1684	AFK19390.1	3	2	36.48	21.6	1.49e+007
CBS domain-containing protein	AFK17996.1	2	2	36.39	6.6	1.49e+006
hypothetical protein HFX_2260	AFK19948.1	2	2	36.34	19.4	1.09e+006
ornithine cyclodeaminase	AFK18155.1	2	2	36.15	8.7	1.03e+006
electron transfer flavoprotein beta subunit	AFK18030.1	4	2	36.06	12.1	2.89e+006
hypothetical protein HFX_1141	AFK18857.1	3	2	36.06	31.6	1.96e+006
serine hydroxymethyltransferase	AFK20524.1	2	2	35.37	5.7	1.34e+006
adenylosuccinate synthetase	AFK18856.1	2	2	35.02	6.5	1.18e+006
nitrite reductase copper containing protein	AFK19882.1	2	2	34.98	6.4	9.31e+005
serine protease inhibitor family protein	AFK20013.1	2	2	34.92	6.8	3.56e+006
glycosyl transferase (plasmid)	AFK21270.1	2	2	34.39	7.2	1.32e+006
geranylgeranyl hydrogenase-like protein / electron-transferring-flavoprotein dehydrogenase	AFK19181.1	2	2	34.34	4.8	1.76e+006

cytochrome c oxidase polypeptide I	AFK18663.1	2	2	34.33	2.5	1.20e+007
hypothetical protein HFX_1139	AFK18855.1	3	2	33.73	55.7	5.68e+006
hypothetical protein HFX_0940	AFK18659.1	2	2	33.36	7.5	3.30e+006
ABC-type transport system ATP-binding protein	AFK18720.1	2	2	32.98	12.1	9.41e+005
3-hydroxyacyl-CoA dehydrogenase	AFK19216.2	2	2	32.65	8	4.60e+006
glucose-1-phosphate thymidylyltransferase	AFK19833.1	2	2	32.61	6.6	1.27e+006
ferredoxin (2Fe-2S)	AFK20674.1	2	2	32.59	19.3	2.45e+006
hypothetical protein HFX_5285 (plasmid)	AFK21116.1	2	2	32.58	13.4	9.54e+005
hypothetical protein HFX_1650	AFK19356.1	2	2	32.48	9.6	1.35e+006
carbohydrate ABC transporter substrate-binding protein, CUT1 family	AFK20566.1	2	2	32.11	5.2	3.64e+006
enoyl-CoA hydratase (plasmid)	AFK21050.1	2	2	31.71	14.6	1.61e+006
DNA-binding ferritin-like protein (oxidative damage protectant)	AFK19391.2	2	2	31.48	20.4	2.14e+006
copper-transporting ATPase CopA (plasmid)	AFK21064.1	2	2	31.46	3.7	1.99e+005
hsp20-type chaperone (plasmid)	AFK20982.1	2	2	31.42	15.6	5.76e+005
ABC transporter ATP-binding protein	AFK18549.1	2	2	31.35	7.6	1.22e+006
cell division protein ftsZ	AFK19949.2	2	2	31.29	7.3	5.88e+005
electron transfer flavoprotein beta subunit	AFK20417.2	2	2	31.28	10.6	2.40e+006
halocyanin precursor-like protein	AFK18843.1	2	2	31.14	15.6	5.16e+006
putative extracellular solute binding protein (plasmid)	AFK21314.1	3	2	30.95	5	1.34e+006
NADH dehydrogenase, subunit L (ubiquinone)	AFK18702.1	2	2	30.88	4.8	6.16e+006
tryptophanase	AFK17753.2	2	2	30.81	5.8	8.10e+005
hypothetical protein HFX_0214	AFK17955.1	3	2	30.78	8.4	6.59e+006
stress response protein	AFK18921.1	2	2	30.74	15.1	1.26e+006
hypothetical protein HFX_1590	AFK19296.1	2	2	30.70	2.9	3.01e+006
hypothetical protein HFX_0016	AFK17760.1	2	2	30.57	11.9	9.86e+005
hypothetical protein HFX_1138	AFK18854.1	2	2	30.39	13.5	2.06e+006
sulfatase arylsulfatase A-like protein	AFK19826.1	2	2	30.18	4.4	2.38e+006
endoglucanase	AFK18519.1	2	2	30.11	7.1	1.36e+006
hypothetical protein HFX_0813	AFK18535.1	2	2	30.00	13.7	3.58e+006

Tabla S3. Representative proteins identified in the crude extract using Triton X-100 (20% w/v) from 3 LC-MS/MS runs.

Protein Name	Database Accession	Spectra	Distinct Peptides	Distinct Summed MS/MS Search Score	% AA Coverage	Total Protein Spectral Intensity
SPFH domain, Band 7 family protein	AFK18490.1	26	23	412.83	61.5	1.82e+008
SPFH domain, Band 7 family protein	AFK17777.1	14	12	194.21	36.5	4.33e+007
NADH dehydrogenase, subunit CD (ubiquinone)	AFK18696.1	26	21	345.12	50	7.64e+007
NADH dehydrogenase, subunit D (ubiquinone)	AFK18684.1	7	5	84.06	8.3	2.05e+007
Dimethylsulfoxide reductase	AFK19896.1	21	21	333.00	35.7	1.68e+007
Dimethylsulfoxide reductase	AFK19898.1	21	19	307.07	31.7	1.54e+007
Succinate dehydrogenase, subunit A (flavoprotein)	AFK20495.1	22	18	315.95	45.2	4.73e+007
A-type ATP synthase subunit A	AFK18041.1	27	17	299.09	38.3	7.98e+007
Thermosome, beta subunit	AFK18158.2	25	17	285.26	41.1	3.31e+007
Nitrous-oxide reductase (plasmid)	AFK20926.1	21	16	263.70	26.2	9.36e+007
Thermosome alpha subunit	AFK18461.1	20	15	263.30	43.1	1.68e+007
Poly(3-hydroxyalkanoate) synthase subunit PhaC (plasmid)	AFK21054.1	20	14	258.26	41	3.87e+007
Serine protease (plasmid)	AFK21203.1	21	15	252.64	38.8	1.47e+008
Dipeptide ABC transporter dipeptide-binding protein	AFK17806.1	15	14	245.78	25.3	4.34e+007
A-type ATP synthase subunit C	AFK18039.1	20	15	242.40	59.7	5.21e+007
A-type ATP synthase subunit B	AFK18042.1	21	14	239.76	44.8	8.40e+007
FAD dependent oxidoreductase	AFK19621.1	15	14	228.61	39.1	1.23e+007
Dipeptide/oligopeptide/nickel ABC transporter periplasmic substrate-binding protein	AFK18790.1	16	14	221.56	31.2	8.57e+006
Nucleoside-binding protein	AFK19185.1	16	12	214.50	41.7	2.02e+007
A-type ATP synthase subunit I	AFK18036.1	16	12	201.11	20.5	3.69e+007
Sugar ABC transporter substrate binding protein	AFK20386.1	13	11	194.32	32.2	3.04e+007
Potassium transport protein kefC	AFK19701.1	17	12	189.75	24.5	1.19e+007
Periplasmic solute binding protein	AFK20085.1	13	11	186.53	36	9.40e+006
Transmembrane oligosaccharyl transferase / dolichyl-diphosphooligosaccharide--protein glycosyltransferase	AFK19298.1	13	12	186.07	13.7	1.59e+007
AAA-type ATPase (transitional ATPase-like protein)	AFK20074.1	13	12	184.10	24.2	7.28e+006
Poly(3-hydroxyalkanoate) synthase subunit PhaE (plasmid)	AFK21053.1	25	9	181.07	71.4	1.59e+008
Dipeptide ABC transporter ATP-binding protein	AFK18330.2	14	10	180.90	26.3	2.76e+007

Thermosome, alpha subunit	AFK17883.2	14	11	180.87	28.3	1.36e+007
ABC-type dipeptide/oligopeptide/nickel transport system, substrate-binding protein	AFK19559.1	11	11	175.35	25.7	7.09e+006
Glutamate dehydrogenase (NAD(P)+)	AFK19225.1	11	10	166.21	38.6	7.64e+006
Hypothetical protein HFX_6053 (plasmid)	AFK21180.1	12	11	164.38	53.2	8.17e+006
PBS lyase HEAT-like repeat protein	AFK18736.1	12	9	164.04	31.4	3.01e+007
CBS domain-containing protein	AFK20079.1	14	10	159.04	32.8	3.02e+007
Aldehyde dehydrogenase (NAD+)	AFK18912.1	11	10	158.34	24.8	7.53e+006
Halocyanin hcpG	AFK18949.1	12	9	156.44	16.1	1.60e+007
Oxidoreductase	AFK18898.2	10	9	155.67	41.8	3.97e+006
Membrane protease subunit, stomatin/prohibitin	AFK17891.1	10	9	151.96	30.1	1.08e+007
AAA-type ATPase (transitional ATPase-like protein)	AFK20391.1	12	10	151.58	14.5	1.09e+007
AAA-type ATPase (transitional ATPase-like protein)	AFK19115.1	3	3	35.34	5.3	5.53e+005
NADH dehydrogenase	AFK19343.1	9	9	150.39	37.2	7.04e+006
Gluconate dehydratase	AFK19260.1	10	9	148.39	29.1	7.26e+006
Hypothetical protein HFX_1529	AFK19236.1	11	9	140.87	34.3	6.56e+006
Hypothetical protein HFX_1777	AFK19482.1	9	8	139.90	73	3.61e+007
Arylsulfatase	AFK18199.1	11	10	139.81	25.9	6.72e+006
Hypothetical protein HFX_2220	AFK19909.2	11	7	136.19	4.9	6.07e+007
A-type ATP synthase subunit D	AFK18044.1	11	8	135.61	47.8	1.11e+007
Putative hydrolase or acyltransferase of alpha/beta superfamily	AFK18525.1	9	8	133.91	49.3	1.54e+007
Isocitrate dehydrogenase (NADP+)	AFK20291.1	10	9	133.18	32.6	5.83e+006
Glycosyl transferase	AFK19287.1	9	8	133.00	28.9	4.86e+006
Putative phosphonate ABC transporter, periplasmic phosphonate-binding protein	AFK19847.1	9	7	131.51	25.3	8.29e+006
Gas-vesicle operon protein gvpC	AFK19401.1	10	7	129.44	28.8	1.31e+007
Hypothetical protein HFX_2459	AFK20144.2	14	7	126.81	13	1.07e+008
A-type ATP synthase subunit H	AFK18035.1	8	7	126.73	40.9	7.02e+006
Cytochrome b subunit of nitric oxide reductase	AFK19877.1	10	7	126.10	14.5	1.15e+007
Ca2+-transporting ATPase	AFK18654.1	8	8	125.96	15.8	2.43e+006
Dipeptide/oligopeptide/nickel ABC transporter ATP-binding protein	AFK17802.1	12	9	125.78	21.9	8.72e+006
Dipeptide/oligopeptide/nickel ABC transporter ATP-binding protein	AFK18794.1	2	2	25.80	5	9.44e+005
Pyruvate--ferredoxin oxidoreductase, alpha subunit	AFK19081.1	8	8	125.77	17.9	3.54e+006
Enoyl-CoA hydratase (plasmid)	AFK21050.1	13	8	125.47	58.9	2.29e+007
A-type ATP synthase subunit E	AFK18038.1	13	7	125.09	52.5	2.86e+007

Hypothetical protein HFX_1679	AFK19385.1	9	9	124.41	22.4	3.01e+006
ABC-type dipeptide/oligopeptide/nickel transport system, substrate-binding protein (plasmid)	AFK21027.1	9	8	122.71	16.9	1.32e+007
Short chain dehydrogenase/ reductase	AFK18407.1	8	8	122.28	42.3	3.81e+006
Flavin-dependent dehydrogenase	AFK20419.1	9	8	120.55	23.4	1.02e+007
Hypothetical protein HFX_2509	AFK20191.2	8	8	120.25	32.7	6.66e+006
3-ketoacyl-acyl carrier protein reductase (PhaB) (plasmid)	AFK21048.1	9	7	119.22	39.1	1.20e+007
Nitrate reductase alpha chain (plasmid)	AFK20939.1	8	8	119.17	11.7	2.58e+006
Glutamine synthetase	AFK17986.2	10	7	118.08	26.3	9.51e+006
Succinate dehydrogenase, subunit B (iron-sulfur protein)	AFK20496.1	8	7	114.61	22.1	8.77e+006
Nitrate reductase beta chain (plasmid)	AFK20938.1	10	8	112.14	24.4	3.27e+006
ABC-type dipeptide/oligopeptide/nickel transport system, substrate binding protein	AFK20131.1	9	8	110.90	20.1	4.31e+006
Sulfatase arylsulfatase A-like protein	AFK18425.2	8	8	110.68	15.1	4.71e+006
Sulfatase arylsulfatase A-like protein	AFK19826.1	4	4	50.72	9.5	3.38e+006
Putative cation-transporting ATPase	AFK18658.2	7	7	109.48	12.8	2.08e+006
Hypothetical protein HFX_1249	AFK18962.1	8	8	109.48	21.7	3.40e+006
Nitrite reductase (NO-forming)	AFK19872.1	7	6	108.21	20.8	6.04e+007
2-oxoglutarate ferredoxin oxidoreductase, subunit alpha	AFK18583.1	8	7	108.01	15	5.25e+006
Aldehyde dehydrogenase	AFK20313.1	8	7	108.01	19	3.72e+006
Hypothetical protein HFX_6273 (plasmid)	AFK21396.2	7	7	107.41	23.3	2.91e+006
CBS domain-containing protein	AFK17996.1	8	6	106.44	19.5	4.56e+006
Hypothetical protein HFX_6060 (plasmid)	AFK21187.1	7	7	104.79	25.3	1.73e+006
Acyl-CoA synthetase	AFK18591.1	7	7	104.55	14.9	8.83e+005
Acyl-CoA synthetase (plasmid)	AFK20965.1	3	3	36.12	4.8	4.17e+005
Aconitate hydratase	AFK18238.1	8	6	103.87	10.6	8.26e+006
NADH dehydrogenase, subunit B (ubiquinone)	AFK18695.1	9	6	103.65	33.4	1.72e+007
Urocanate hydratase (plasmid)	AFK21450.1	6	6	103.49	16.2	1.67e+006
Orotate phosphoribosyltransferase-like protein/conserved Entner-Douderoff pathway protein	AFK18805.1	8	7	102.33	39	3.43e+006
Hypothetical protein HFX_1776	AFK19481.1	7	7	102.01	15	9.43e+006
Prepilin signal peptidase	AFK20651.1	7	7	101.73	24	5.35e+006
Poly(3-hydroxyalkanoate) granule-associated 12 kDa protein (plasmid)	AFK21051.1	8	5	101.10	77.2	5.70e+007
Molecular chaperone DnaK	AFK19355.1	6	6	100.93	16.4	2.21e+006
Hypothetical protein HFX_0293	AFK18032.2	7	7	100.55	18.3	1.89e+006
Catalase (including: peroxidase)	AFK19564.1	6	6	99.39	11.6	4.86e+006

CBS domain-containing protein	AFK18713.2	7	7	97.53	25.2	2.45e+006
ABC transporter ATP-binding protein	AFK20685.1	7	7	96.76	33.3	2.85e+006
Dihydrolipoamide S-acyltransferase (pyruvate dehydrogenase E2 component) +	AFK20618.1	7	7	94.55	17	5.49e+006
ABC-type dipeptide/oligopeptide/nickel transport systems, ATP-binding protein I & II	AFK18329.1	7	7	94.45	10.9	1.41e+006
Phosphonates ABC transporter ATP-binding protein	AFK19846.1	7	6	94.10	34	5.68e+006
Hypothetical protein HFX_2088	AFK19779.1	7	6	92.94	20.2	2.21e+006
Branched-chain/neutral amino acids amide ABC transporter periplasmic substrate-binding protein	AFK19529.1	7	5	92.49	19.9	9.04e+006
Stress response protein	AFK20336.2	6	6	92.47	28.8	6.29e+006
Zinc-transporting ATPase (plasmid)	AFK21399.1	6	6	92.33	10.6	2.54e+006
Proline dehydrogenase	AFK18055.1	6	6	91.23	25	5.49e+006
ABC-type iron(III) transport system,substrate-binding protein	AFK19499.1	9	5	90.78	23.2	1.21e+007
purK operon protein / membrane-bound mannosyltransferase	AFK18691.1	7	6	90.72	13.1	2.24e+006
Pyruvate dehydrogenase E1 component subunit beta	AFK20617.1	7	5	90.40	21.7	6.80e+006
Molybdopterin oxidoreductase	AFK19899.1	6	5	90.39	22.7	8.23e+006
Phenylacetic acid degradation protein PaaC (plasmid)	AFK21497.1	6	6	89.78	27.5	2.26e+006
Carbohydrate ABC transporter substrate-binding protein, CUT1 family	AFK20566.1	6	5	89.25	21.5	6.84e+006
Halocyanin precursor-like protein	AFK19879.1	6	5	88.97	26.5	1.52e+007
Iron-sulfur protein (4Fe-4S)	AFK17960.2	7	7	88.70	10.6	6.10e+006
Hypothetical protein HFX_2555	AFK20236.1	6	6	88.38	23.5	7.21e+006
Sugar ABC transporter ATP-binding protein (UGPC)	AFK20563.1	7	6	88.32	25.8	3.05e+006
Phosphohexomutase (phosphoglucomutase, phosphomannomutase)	AFK17941.1	6	6	88.05	15.7	2.95e+006
Hypothetical protein HFX_1575	AFK19282.2	6	5	85.06	31.5	1.06e+007
Phosphoenolpyruvate synthase / pyruvate, water dikinase	AFK18505.1	6	6	84.92	7.9	2.29e+006
S-adenosylmethionine-dependent methyltransferase-like protein	AFK18456.1	6	6	84.78	26.9	2.57e+006
Phytoene dehydrogenase (phytoene desaturase)	AFK18509.1	6	6	83.82	20.1	1.97e+006
Molybdate transport protein	AFK19675.1	5	5	82.51	18.5	9.33e+005
Sugar ABC transporter ATP-binding protein	AFK20383.1	7	5	82.43	19.7	6.86e+006
Protein-disulfide isomerase	AFK18965.1	4	4	82.27	29.7	2.19e+006
Hypothetical protein HFX_2780	AFK20456.1	6	5	82.24	24.6	1.90e+006
Preprotein translocase subunit SecY	AFK20246.1	9	6	82.18	13	1.05e+007
Glutamate/aspartate transport protein	AFK19350.1	7	6	81.86	17.7	5.00e+006
Phosphopyruvate hydratase	AFK20460.1	5	5	81.59	21.3	3.03e+006
Preprotein translocase subunit SecD	AFK19761.1	5	5	80.89	18.5	5.38e+006

Nitrite reductase copper containing protein	AFK19882.1	6	5	80.16	17.3	4.77e+006
Gas-vesicle operon protein gvpH	AFK19407.1	5	4	79.99	30	3.84e+006
Pyridoxal biosynthesis lyase PdxS	AFK20032.1	6	6	79.90	22.1	3.34e+006
Hypothetical protein HFX_6074 (plasmid)	AFK21201.1	8	4	79.80	36.1	1.33e+007
Hypothetical protein HFX_6434 (plasmid)	AFK21553.1	6	5	79.23	16.9	2.59e+006
Phosphate ABC transporter ATP-binding protein	AFK20072.1	6	6	79.13	18.9	3.95e+006
Putative hydrolase or acyltransferase of alpha/beta superfamily	AFK19333.1	5	5	78.52	26.3	4.89e+006
Aspartate aminotransferase	AFK18689.1	5	5	78.36	22.3	1.34e+006
Glycerol kinase	AFK19308.1	5	5	77.77	17.1	1.14e+006
Dihydrolipoamide dehydrogenase	AFK20619.1	5	5	77.35	13.8	3.03e+006
Phosphate ABC transporter periplasmic substrate-binding protein	AFK20069.1	5	5	76.85	14.8	2.54e+006
4-aminobutyrate aminotransferase	AFK19853.1	6	5	76.63	18.3	4.04e+006
Putative signal transduction protein with CBS domains (plasmid)	AFK21146.1	5	5	76.55	11.8	3.11e+006
Hypothetical protein HFX_1950	AFK19646.1	5	5	76.03	36.8	2.83e+006
Proteasome subunit alpha	AFK18815.1	6	6	75.73	22.2	8.89e+006
Molybdopterin oxidoreductase	AFK19900.1	4	4	75.68	10.2	8.97e+006
Putative mechanosensitive ion channel	AFK19964.1	7	4	74.75	26.6	3.34e+006
Oxidoreductase	AFK18724.1	6	5	73.90	19.1	1.39e+006
Biotin carboxylase	AFK20173.1	5	5	73.51	9.9	2.16e+006
IMP dehydrogenase	AFK18995.1	5	5	73.44	12.4	1.50e+006
ABC transporter ATP-binding protein (plasmid)	AFK20923.1	5	5	73.34	21.1	3.06e+006
Hypothetical protein HFX_1590	AFK19296.1	5	5	73.19	12.8	2.26e+006
Putative hydrolase of the metallo-beta-lactamase superfamily	AFK20411.1	5	5	73.09	12.2	3.86e+006
Aconitate hydratase	AFK19741.1	5	5	72.92	10.5	1.81e+006
Geranylgeranyl hydrogenase-like protein / electron-transferring-flavoprotein dehydrogenase	AFK19181.1	5	5	71.74	12.2	2.79e+006
Enoyl-CoA hydratase	AFK19171.2	5	5	71.56	22.5	3.22e+006
Putative phosphate acetyltransferase	AFK18715.1	5	5	71.40	18.4	2.27e+006
Hypothetical protein HFX_1239	AFK18952.1	5	4	71.15	25.3	1.18e+006
Lysophospholipase	AFK20242.1	5	4	71.01	16.9	3.92e+006
Sec-independent protein translocase component TatC2	AFK17925.1	4	4	70.77	6.6	1.19e+006
Glutaryl-CoA dehydrogenase	AFK17952.2	4	4	70.40	16.7	1.02e+006
Putative membrane-associated Zn-dependent protease	AFK19648.2	5	5	70.06	9	1.79e+006
Hypothetical protein HFX_1766	AFK19471.1	5	5	69.34	31	5.86e+006

Hypothetical protein HFX_5285 (plasmid)	AFK21116.1	5	5	68.78	28.9	2.90e+006
Tryptophanase	AFK17753.2	4	4	68.67	16	1.19e+006
Electron transfer flavoprotein alpha subunit	AFK20418.1	5	5	68.64	10.2	2.69e+006
Branched-chain-amino-acid aminotransferase	AFK18053.1	6	5	68.61	23.7	1.46e+006
ABC-type branched-chain amino acid transport systems, substrate-binding protein	AFK20482.1	5	4	68.06	18.4	3.52e+006
Transport ATPase (substrate arsenite)	AFK18406.1	4	4	67.76	14.3	2.08e+006
Citrate (si)-synthase	AFK18167.1	5	5	67.65	14.7	1.53e+006
ABC-type transport system ATP-binding/permease protein	AFK18212.1	5	5	66.57	7.9	1.64e+006
Metalloprotease	AFK18012.1	5	4	66.45	14.1	2.53e+006
Hypothetical protein HFX_6278 (plasmid)	AFK21400.1	5	4	65.90	41.7	5.38e+006
Pyruvate--ferredoxin oxidoreductase, beta subunit	AFK19080.1	4	4	65.82	16.9	3.52e+006
Stress response protein	AFK18921.1	5	5	65.71	43.4	4.15e+006
Menaquinol--cytochrome-c reductase (cytochrome bc complex) cytochrome b/c subunit	AFK18533.1	5	4	65.61	17.7	7.01e+006
Cytochrome bc1 complex cytochrome b/c subunit	AFK18497.1	3	3	47.39	11.4	4.65e+006
Hypothetical protein HFX_1586	AFK19292.1	5	5	65.47	14.3	2.45e+006
Regulatory protein PrrC	AFK18961.1	4	3	65.26	29.1	3.40e+006
Poly(3-hydroxyalkanoate) granule-associated protein(phasin) (plasmid)	AFK21052.1	9	4	65.02	24.6	1.80e+008
ATP-dependent protease Lon	AFK18465.1	5	4	64.65	8	1.36e+006
Oligopeptide ABC transporter ATPase component	AFK17803.1	4	4	64.50	15.1	2.36e+006
Amino acid-binding protein (plasmid)	AFK21485.1	4	4	64.49	12.4	9.47e+005
Hypothetical protein HFX_1692	AFK19398.1	4	4	64.32	13.9	9.04e+005
3-oxoacyl-[acyl-carrier protein] reductase	AFK19230.1	5	4	64.27	21.4	5.48e+006
Hypothetical protein HFX_2807	AFK20480.1	5	4	64.16	32	4.34e+006
Ornithine cyclodeaminase	AFK18155.1	6	4	63.75	17.7	2.29e+006
Phosphoserine phosphatase	AFK20621.1	4	4	63.31	27.3	1.23e+006
Oxidoreductase	AFK18675.1	4	4	62.73	21.8	1.25e+006
Dihydroorotate dehydrogenase 2	AFK20600.1	4	4	62.14	24.6	1.31e+006
2-methylcitrate dehydratase (plasmid)	AFK21002.1	4	4	61.74	14	7.86e+005
Pyruvate kinase	AFK18496.2	5	5	61.41	10.7	1.32e+006
Cellulase, endo-1,3(4)-beta-glucanase, peptidase M42 family protein / endoglucanase	AFK20447.1	4	4	61.20	12.7	1.14e+006
Ribulose-bisphosphate carboxylase large chain	AFK18685.1	4	4	61.19	11.8	3.27e+006
Hypothetical protein HFX_0697	AFK18420.1	4	4	60.79	52.6	1.09e+007
Glucose-1-phosphate thymidylyltransferase	AFK19833.1	4	4	60.67	11.5	1.58e+006

Oxidoreductase (glycolate oxidase iron-sulfur subunit)	AFK19493.1	4	4	59.87	4	1.60e+006
Electron transfer flavoprotein alpha subunit	AFK19622.1	5	4	59.51	13.9	1.60e+006
Cytochrome c oxidase polypeptide I	AFK18663.1	5	4	59.40	7.6	1.94e+007
Succinate--CoA ligase beta subunit (ADP-forming)	AFK20155.1	4	4	59.37	14.1	1.67e+006
GMP synthase (glutamine-hydrolysing)	AFK20320.1	4	4	59.06	14.7	1.43e+006
Gas-vesicle operon protein gvpA	AFK19402.1	4	3	59.05	57.6	2.38e+007
Putative permease	AFK19808.1	4	4	58.65	21.2	9.09e+005
RecJ-like exonuclease	AFK20553.1	4	4	58.46	8.1	1.17e+006
Ferredoxin (2Fe-2S)	AFK19572.1	5	4	58.34	33.5	3.40e+006
3-hydroxyacyl-CoA dehydrogenase	AFK20502.1	4	4	58.29	9.2	1.76e+006
Hypothetical protein HFX_2772	AFK20448.1	6	4	58.24	53.9	8.97e+006
Putative acylaminoacyl-peptidase	AFK18673.1	4	4	58.13	6.4	8.54e+005
Oligopeptide ABC transporter permease protein	AFK17804.1	4	4	57.69	12.3	3.12e+006
Stress response protein (plasmid)	AFK21518.1	4	4	57.68	17.6	2.61e+006
Endoglucanase	AFK18519.1	4	4	57.53	16	1.33e+006
NADH dehydrogenase-like complex, subunit I	AFK18698.1	5	4	57.46	40.5	2.28e+006
Hypothetical protein HFX_0482	AFK18214.1	3	3	57.12	32.8	9.92e+005
NADH dehydrogenase, subunit M (ubiquinone)	AFK18703.1	5	4	56.88	7.6	8.35e+006
FKBP-type peptidylprolyl isomerase 2	AFK19430.2	3	3	56.73	12.2	6.92e+006
Phosphonates ABC transporter permease protein	AFK19844.1	5	4	56.69	17.5	2.11e+006
Acyl-CoA synthetase	AFK19702.1	4	4	56.61	5.9	1.89e+006
Hypothetical protein HFX_5081 (plasmid)	AFK20916.2	4	3	56.60	11	9.97e+006
Phosphoenolpyruvate carboxylase	AFK20315.2	4	4	56.38	5.2	6.23e+005
Superoxide dismutase, Fe-Mn family	AFK20579.1	3	3	56.28	16	3.95e+006
Superoxide dismutase, Fe-Mn family (plasmid)	AFK21528.1	3	3	53.69	16	2.63e+006
Hypothetical protein HFX_1243	AFK18956.1	6	3	56.23	10.6	1.85e+007
Hypothetical protein HFX_5167 (plasmid)	AFK21001.1	4	3	55.83	19.2	2.86e+006
FAD-dependent pyridine nucleotide-disulfide oxidoreductase	AFK17859.1	3	3	55.74	10.7	9.99e+005
Dipeptidyl aminopeptidase/acylaminoacyl peptidase	AFK18522.1	4	4	55.49	9	9.17e+005
Hypothetical protein HFX_1272	AFK18985.1	4	4	55.39	25.2	4.83e+006
Acyl-CoA synthetase, acetate--CoA ligase-like protein (ADP-forming)	AFK18716.1	5	4	55.14	7	1.25e+006
Sulfatase-like protein	AFK19290.1	5	4	54.82	10.5	2.30e+006
Citryl-CoA lyase (citrate lyase beta subunit / ATP citrate synthase beta subunit)	AFK19224.2	3	3	54.78	19.3	1.53e+005

Succinate--CoA ligase, alpha subunit (ADP-forming)	AFK20154.1	3	3	53.94	19	7.92e+005
NADH dehydrogenase, subunit H (ubiquinone)	AFK18697.1	4	3	53.53	9.4	2.65e+007
Cyclase/dehydrase	AFK17928.1	4	4	52.72	15.8	1.83e+006
N-methylhydantoinase B (ATP-hydrolyzing) (plasmid)	AFK21025.1	4	4	52.56	7.9	1.11e+006
Immunogenic protein	AFK20638.1	4	3	52.20	12.7	2.29e+007
Putative monovalent cation/H+ antiporter subunit E	AFK18782.1	4	4	52.14	17.6	9.07e+005
Putative iron transport protein	AFK19393.1	4	3	51.75	11.3	2.63e+006
Carboxypeptidase	AFK18120.1	4	4	51.71	10.7	1.06e+006
Ferredoxin (2Fe-2S)	AFK20674.1	3	3	51.64	34.8	6.23e+006
Putative patatin-like phospholipase (plasmid)	AFK21580.1	6	3	51.43	12.7	3.15e+006
Hypothetical protein HFX_0118	AFK17860.1	4	3	51.17	38.6	7.63e+005
Hypothetical protein HFX_2876	AFK20546.1	3	3	50.96	20.8	1.61e+007
Hypothetical protein HFX_5226 (plasmid)	AFK21058.1	4	3	50.73	50.4	5.76e+007
ABC-type glutamine/glutamate/polar amino acids transport system, ATP-binding protein	AFK20124.1	3	3	50.52	13.6	1.71e+006
Hypothetical protein HFX_0195	AFK17936.1	5	3	50.40	52.7	9.06e+006
Hemerythrin HHE cation binding region (plasmid)	AFK20978.1	3	3	50.08	17.4	7.51e+005
DMSO reductase family type II enzyme, heme b subunit (plasmid)	AFK20937.1	3	3	49.88	13.4	1.03e+006
Hypothetical protein HFX_5272 (plasmid)	AFK21103.1	4	4	49.79	21.4	1.86e+006
N-acyl-L-amino acid amidohydrolase	AFK19179.1	3	3	49.69	10.3	1.12e+006
Aldehyde reductase	AFK18579.1	3	3	49.41	13	1.29e+006
ABC-type dipeptide/oligopeptide/nickel transport system, substrate binding protein (plasmid)	AFK20740.1	3	3	49.36	7.4	1.20e+006
3-hydroxyacyl-CoA dehydrogenase	AFK19216.2	3	3	48.90	10.1	4.08e+006
NADH dehydrogenase 32K chain-like protein	AFK17846.1	4	4	48.50	14.5	7.77e+005
Hypothetical protein HFX_0292	AFK18031.1	4	3	48.14	10.2	2.75e+006
Menaquinol--cytochrome-c reductase (cytochrome bc complex) cytochrome b subunit	AFK18534.1	4	3	48.00	14.7	1.41e+007
Putative cationic amino acid transport protein (plasmid)	AFK21046.1	3	3	47.99	6	6.45e+005
Universal stress protein UspA-like protein	AFK19887.1	4	3	47.97	14.6	3.67e+006
Branched-chain amino acid ABC transporter ATP-binding protein	AFK19533.1	3	3	47.53	17.6	6.57e+005
ABC-type transport system ATP-binding protein	AFK18720.1	3	3	47.10	17.2	1.79e+006
Hsp20-type chaperone	AFK18151.1	3	3	47.08	22.9	4.90e+006
Ubiquinone/menaquinone biosynthesis methyltransferase	AFK18034.2	4	3	46.44	19.7	2.97e+006
Cystathionine synthase/lyase (cystathionine gamma-synthase, cystathionine gamma-lyase, cystathionine beta-lyase)	AFK20603.1	3	3	46.44	8.9	9.79e+005
Ribose ABC transporter ATP-binding protein	AFK19184.1	3	3	46.25	7.5	9.84e+005

Putative inosine monophosphate dehydrogenase	AFK17799.1	4	4	46.15	21.8	1.01e+006
Hypothetical protein HFX_0728	AFK18451.1	3	3	46.02	28.3	1.04e+006
Putative Rieske iron-sulfur protein (plasmid)	AFK20942.1	3	3	46.02	28.6	9.83e+005
Hypothetical protein HFX_0671	AFK18394.1	5	3	46.01	20.4	4.27e+006
Menaquinol--cytochrome-c reductase	AFK20314.1	5	3	45.96	13.5	1.51e+007
N-methylhydantoinase A (ATP-hydrolyzing) (plasmid)	AFK21026.1	3	3	45.48	6.7	4.55e+005
Signal sequence peptidase	AFK17747.2	3	3	45.42	12.3	1.12e+006
Nucleoside diphosphate kinase	AFK20428.1	3	3	45.38	26.6	2.53e+006
Thiosulfate sulfurtransferase	AFK17767.2	3	3	45.27	15	3.33e+006
Glycosyltransferase (dolichyl-phosphate beta-D-mannosyltransferase)	AFK19286.1	3	3	45.17	13.9	1.46e+006
Ubiquinone biosynthesis transmembrane protein	AFK19999.1	3	3	45.02	6.4	8.40e+005
Hypothetical protein HFX_0662	AFK18386.1	3	3	44.91	5.7	8.08e+005
ABC-type transport system involved in Fe-S cluster assembly, permease protein II	AFK18551.1	4	3	44.82	10.9	1.43e+006
Nonhistone chromosomal protein	AFK20598.1	3	3	44.68	25	8.03e+005
Hypothetical protein HFX_0680	AFK18403.2	3	3	44.54	13.3	4.58e+005
Fumarate hydratase, class II	AFK20567.2	3	3	44.50	7	8.24e+005
MaoC family protein (plasmid)	AFK21063.1	3	3	44.44	35.2	4.86e+006
Poly(3-hydroxyalkanoate) synthase subunit PhaC	AFK20356.1	3	3	44.39	10.4	8.06e+005
NADH dehydrogenase, subunit L (ubiquinone)	AFK18702.1	4	3	44.06	4.4	4.01e+006
Hypothetical protein HFX_2976	AFK20640.1	3	3	43.98	3	1.98e+006
Hypothetical protein HFX_1953	AFK19649.1	3	3	43.79	5.8	5.12e+005
Signal transduction histidine kinase / two-component system, OmpR family, sensor histidine kinase CreC (plasmid)	AFK21044.1	3	3	43.76	7.8	8.42e+005
Quinoprotein glucose dehydrogenase	AFK18721.1	3	3	43.20	7.6	9.47e+005
Hypothetical protein HFX_2039	AFK19731.2	3	3	43.01	11.7	7.84e+005
Sialidase-1	AFK20474.1	3	3	42.72	9	6.84e+005
Hypothetical protein HFX_2758	AFK20435.1	3	3	42.61	17.3	7.09e+006
Hypothetical protein HFX_0661	AFK18385.1	4	3	42.42	27.5	1.20e+007
4Fe-S protein	AFK19488.1	3	3	42.38	5.7	4.65e+005
Acyl-CoA synthetase	AFK19839.1	3	3	42.38	7.9	7.86e+005
Prefoldin beta subunit	AFK18347.1	2	2	41.96	25.8	2.17e+006
Putative sugar ABC transporter permease protein	AFK20384.1	3	3	41.62	10.6	3.30e+006
Hypothetical protein HFX_2182	AFK19871.1	3	3	41.51	12.1	8.81e+005
ABC-type copper transport system, permease protein	AFK20684.1	3	3	41.47	13.3	1.43e+006

Aldehyde dehydrogenase (NAD+) (plasmid)	AFK21494.1	3	3	41.19	9.1	5.80e+005
Acyl-CoA dehydrogenase	AFK18868.1	3	3	41.02	11.3	4.33e+005
Universal stress protein	AFK18810.1	3	2	40.97	19	7.73e+005
Carbonic anhydrase	AFK18667.1	3	3	40.96	16	7.23e+005
Hypothetical protein HFX_6067 (plasmid)	AFK21194.1	4	3	40.89	8.4	1.33e+006
NADH dehydrogenase/oxidoreductase-like protein	AFK19950.1	3	2	40.57	10.2	3.78e+006
Hypothetical protein HFX_1684	AFK19390.1	2	2	40.52	21.6	7.58e+006
Menaquinone biosynthesis methyltransferase UbiE	AFK20539.1	3	3	40.30	21.2	8.27e+005
Hypothetical protein HFX_2180	AFK19869.1	4	3	40.21	8.7	3.36e+006
A-type ATP synthase subunit F	AFK18040.1	3	2	39.37	36.7	4.30e+006
Hypothetical protein HFX_0016	AFK17760.1	3	3	39.00	15.1	1.23e+006
Hypothetical protein HFX_1141	AFK18857.1	2	2	38.52	31.6	1.92e+006
F420-dependent NADP reductase	AFK18135.1	2	2	38.47	12.1	9.22e+005
Phosphonates ABC transporter permease protein	AFK19845.1	3	3	38.36	17.4	1.78e+006
UpsA domain-containing protein	AFK19975.2	4	3	38.25	26.7	1.44e+006
Short-chain dehydrogenase / reductase SDR / glucose 1-dehydrogenase	AFK20158.1	3	3	37.90	16.1	2.77e+005
Hypothetical protein HFX_0214	AFK17955.1	4	2	37.89	8.4	5.22e+006
Oxidoreductase (geranylgeranyl hydrogenase-like protein)	AFK19602.1	3	3	37.67	8.7	4.62e+005
Na+/H+ antiporter	AFK19178.1	2	2	37.56	6.3	2.33e+005
Methylmalonyl-CoA decarboxylase alpha chain	AFK20161.1	3	3	37.55	7.5	6.99e+005
2-oxoglutarate ferredoxin oxidoreductase, subunit beta	AFK18582.1	3	3	37.45	9.7	8.79e+005
S-adenosylmethionine synthetase	AFK19445.1	2	2	37.11	6.2	2.25e+005
Hypothetical protein HFX_0940	AFK18659.1	2	2	37.03	9.4	2.83e+006
Glutamate-1-semialdehyde aminotransferase	AFK17832.1	2	2	36.77	6.2	7.08e+005
Halocyanin precursor-like protein	AFK18536.1	2	2	36.71	15.8	4.95e+006
Halocyanin precursor-like protein	AFK18518.1	2	2	36.71	16.5	4.95e+006
Peptidyl-prolyl cis-trans isomerase B (cyclophilin B)	AFK19961.1	2	2	36.67	23.8	1.07e+006
Acyl-CoA synthetase	AFK19349.1	3	3	36.61	5.4	4.48e+005
ABC-type glutamine/glutamate/polar amino acids transport system, substrate-binding protein	AFK20126.1	3	2	36.59	10.5	2.82e+006
Hypothetical protein HFX_1589	AFK19295.1	3	3	36.55	6.6	1.22e+006
NADPH-dependent FMN reductase	AFK20556.2	2	2	35.75	24.4	1.88e+005
Malate dehydrogenase	AFK20690.2	2	2	35.73	11.1	4.78e+005
Ferredoxin:NAD+ oxidoreductase	AFK20041.1	2	2	35.55	7.5	8.11e+005

Hypothetical protein HFX_0639	AFK18363.1	2	2	35.46	20.9	1.13e+006
Inorganic pyrophosphatase	AFK18410.1	3	3	35.22	20.3	1.74e+006
ABC transporter ATP-binding protein	AFK18549.1	2	2	35.10	7.6	7.31e+005
Gas-vesicle operon protein gvpF	AFK19405.1	2	2	34.77	15	3.80e+005
Hypothetical protein HFX_1000	AFK18718.1	2	2	34.61	22.3	2.43e+006
Hypothetical protein HFX_1656	AFK19362.1	2	2	34.58	20	6.82e+005
Hypothetical protein HFX_0491	AFK18222.1	3	2	34.15	14	4.21e+006
Dipeptide ABC transporter permease	AFK17805.1	3	2	34.12	10	1.36e+006
Hypothetical protein HFX_6075 (plasmid)	AFK21202.1	2	2	34.07	22.6	1.17e+007
Copper-binding plastocyanin like protein (plasmid)	AFK20927.1	3	2	34.00	20.8	1.90e+006
hypothetical protein HFX_0366	AFK18102.2	2	2	33.98	31.3	1.16e+006
Putative intracellular protease	AFK19063.1	2	2	33.91	8	5.92e+006
Hypothetical protein HFX_1448	AFK19156.1	4	2	33.89	12.7	3.62e+006
Hypothetical protein HFX_0620	AFK18344.1	3	3	33.68	5.4	6.55e+005
Phosphate ABC transporter permease	AFK20070.1	2	2	33.64	8.1	1.06e+006
Hypothetical protein HFX_0856	AFK18577.1	3	3	33.53	7.9	6.35e+005
Proteasome beta subunit	AFK19329.1	2	2	33.52	13	1.34e+006
Hypothetical protein HFX_2040	AFK19732.2	2	2	33.39	7.6	6.06e+005
Ferritin-like protein	AFK17959.1	2	2	33.32	30	9.40e+005
ABC-type transport system ATP-binding protein	AFK20086.1	2	2	33.30	14.2	1.01e+006
Protein of unknown function DUF1486	AFK20429.1	2	2	33.08	15.7	8.55e+005
Electron transfer flavoprotein alpha-subunit	AFK18029.1	2	2	32.99	13.5	9.38e+005
Putative membrane protein	AFK17823.1	2	2	32.84	15.7	6.01e+005
Cell division protein ftsZ	AFK19949.2	2	2	32.84	7.3	5.99e+005
Copper-transporting ATPase CopA (plasmid)	AFK21064.1	2	2	32.81	3.5	6.92e+005
Diphosphomevalonate decarboxylase	AFK19194.1	2	2	32.76	6.1	8.48e+005
Aminopeptidase	AFK18528.1	3	2	32.71	5.9	8.58e+005
Short chain dehydrogenase	AFK20232.1	2	2	32.68	11.7	7.26e+005
ArsR family regulatory protein	AFK19320.1	3	2	32.60	18.9	1.14e+006
Glutamate dehydrogenase (NAD(P)+)	AFK19867.1	2	2	32.45	8.6	8.21e+005
Histidine ammonia-lyase (plasmid)	AFK21453.1	2	2	32.44	4.5	5.54e+005
Mechanosensitive ion channel	AFK19459.1	2	2	32.39	7.7	1.15e+006
Anthranilate phosphoribosyltransferase	AFK19965.1	2	2	32.31	8.7	1.10e+006

Dodecin	AFK20375.1	2	2	32.09	30.8	5.62e+006
Methanol dehydrogenase regulatory protein	AFK18978.1	2	2	32.07	7.7	8.26e+005
Malate dehydrogenase (oxaloacetate-decarboxylating)(NADP+)	AFK20129.1	3	2	32.03	4.6	6.87e+005
Ribose-1,5-bisphosphate isomerase (ribulose-bisphosphate forming)	AFK18682.1	3	3	31.95	9.7	5.21e+005
NADPH2:quinone reductase	AFK20343.1	2	2	31.86	7.5	8.86e+005
Ribose 5-phosphate isomerase	AFK17935.1	2	2	31.62	11.7	2.71e+005
Thioredoxin	AFK18964.1	2	2	31.32	10.4	1.13e+006
Heat shock protein HtpX	AFK17854.2	3	2	31.31	9.5	1.52e+006
Hypothetical protein HFX_0813	AFK18535.1	3	2	31.25	24.4	6.76e+005
Methionine aminopeptidase	AFK20296.1	3	2	31.07	5.7	4.07e+006
Serine protease inhibitor family protein	AFK20013.1	2	2	30.71	4.8	1.24e+006
Hypothetical protein HFX_0694	AFK18417.1	2	2	30.67	36.4	3.81e+005
Hypothetical protein HFX_1182	AFK18895.1	2	2	30.59	16.6	1.11e+006
PLP-dependent aminotransferase (aspartate aminotransferase)	AFK19365.1	2	2	30.48	7.2	5.33e+005
Glycine dehydrogenase subunit 2	AFK20092.1	2	2	30.43	8.8	2.40e+005
Endoribonuclease L-PSP	AFK18161.1	2	2	30.31	25	6.46e+005
Na+/Ca2+-exchanging protein	AFK18397.1	2	2	30.27	6.6	5.76e+005
Halocyanin precursor-like protein	AFK18843.1	2	2	30.11	15.6	2.93e+006
Cytochrome b/b6 (plasmid)	AFK20941.1	2	2	30.00	3.9	1.36e+006

Table S4. Representative proteins identified in the micelles with Nar and Nir activities obtained after the use of DEAE-Sepharose CL-6B from 3 LC-MS/MS runs.

Protein name	Database Accession	Spectra	Distinct Peptides	Distinct Summed MS/MS Search Score	% AA Coverage	Total Protein Spectral Intensity
NADH dehydrogenase, subunit CD (ubiquinone)	AFK18696.1	40	28	473.42	63.7	2.23e+008
NADH dehydrogenase, subunit D (ubiquinone)	AFK18684.1	6	5	86.21	7.7	6.07e+007
A-type ATP synthase subunit A	AFK18041.1	34	22	410.90	47	1.49e+008
Nitrous-oxide reductase (plasmid)	AFK20926.1	29	23	381.40	38.6	3.24e+008
Succinate dehydrogenase, subunit A (flavoprotein)	AFK20495.1	28	19	361.17	48.9	1.19e+008
A-type ATP synthase subunit B	AFK18042.1	30	19	352.32	59.8	2.35e+008
Poly(3-hydroxyalkanoate) synthase subunit PhaC (plasmid)	AFK21054.1	27	17	331.66	54.8	7.84e+007
Dipeptide ABC transporter dipeptide-binding protein	AFK17806.1	23	18	316.83	42.6	9.91e+007
Dipeptide ABC transporter ATP-binding protein	AFK18330.2	24	17	313.78	51	1.47e+008
Thermosome, beta subunit	AFK18158.2	24	19	306.80	48.3	3.79e+007
Nucleoside-binding protein	AFK19185.1	22	17	298.10	64.4	1.05e+008
A-type ATP synthase subunit C	AFK18039.1	21	16	291.58	65.5	9.91e+007
Periplasmic solute binding protein	AFK20085.1	19	16	290.21	58.9	5.40e+007
A-type ATP synthase subunit I	AFK18036.1	22	15	282.21	28.1	1.24e+008
SPFH domain, Band 7 family protein	AFK18490.1	23	15	274.67	49	9.63e+007
SPFH domain, Band 7 family protein	AFK17777.1	5	4	63.54	10.8	6.38e+006
Nitrate reductase alpha chain (plasmid)	AFK20939.1	17	17	269.39	24.7	2.09e+007
Thermosome, alpha subunit	AFK17883.2	18	15	268.32	44.4	2.54e+007
Gas-vesicle operon protein gvpC	AFK19401.1	23	13	263.40	49	7.05e+007
Sugar ABC transporter substrate binding protein	AFK20386.1	20	14	248.53	44	9.18e+007
Poly(3-hydroxyalkanoate) synthase subunit PhaE (plasmid)	AFK21053.1	30	11	238.40	71.4	4.58e+008
Iron-sulfur protein (4Fe-4S)	AFK17960.2	18	14	237.96	30.2	3.69e+007
PBS lyase HEAT-like repeat protein	AFK18736.1	17	13	233.77	39	1.04e+008
Serine protease (plasmid)	AFK21203.1	17	15	233.41	37.6	5.11e+007
Halocyanin hcpG	AFK18949.1	15	13	224.11	31.2	1.96e+007
Dimethylsulfoxide reductase	AFK19896.1	14	13	217.75	21.3	1.14e+007
Dimethylsulfoxide reductase	AFK19898.1	6	6	88.59	7.9	4.19e+006
Dipeptide/oligopeptide/nickel ABC transporter periplasmic substrate-binding protein	AFK18790.1	14	13	212.68	29.7	1.59e+007

Oxidoreductase	AFK18898.2	12	12	194.49	66.2	1.71e+007
Aconitate hydratase	AFK18238.1	13	12	185.41	18.2	1.82e+007
Proline dehydrogenase	AFK18055.1	14	11	185.22	53.7	3.65e+007
Proline dehydrogenase	AFK18914.1	5	5	66.54	25.4	3.23e+006
Catalase (including: peroxidase)	AFK19564.1	14	12	185.15	22.8	1.91e+007
ABC-type iron(III) transport system,substrate-binding protein	AFK19499.1	14	9	181.55	48.5	5.63e+007
Thermosome alpha subunit	AFK18461.1	14	11	181.45	30.7	1.02e+007
A-type ATP synthase subunit D	AFK18044.1	18	11	179.68	54.8	2.88e+007
Hypothetical protein HFX_1776	AFK19481.1	11	11	176.84	34.5	1.56e+007
Electron transfer flavoprotein alpha subunit	AFK20418.1	11	11	175.20	27.9	1.22e+007
A-type ATP synthase subunit E	AFK18038.1	17	9	174.26	68.5	6.89e+007
Phenylacetic acid degradation protein PaaC (plasmid)	AFK21497.1	11	9	172.21	57.3	1.18e+007
Succinate dehydrogenase, subunit B (iron-sulfur protein)	AFK20496.1	12	11	171.19	37.8	2.43e+007
Hypothetical protein HFX_1777	AFK19482.1	12	9	168.49	73	1.35e+008
A-type ATP synthase subunit H	AFK18035.1	11	9	166.35	69	4.47e+007
ABC-type dipeptide/oligopeptide/nickel transport system, substrate binding protein	AFK20131.1	10	9	163.61	31.9	1.96e+007
Glutamate dehydrogenase (NAD(P)+)	AFK19225.1	12	9	161.60	39.3	1.34e+007
Branched-chain-amino-acid aminotransferase	AFK18053.1	12	10	159.45	49.6	1.29e+007
Glycerol kinase	AFK19308.1	11	11	156.84	26.3	6.56e+006
Flavin-dependent dehydrogenase	AFK20419.1	10	9	150.52	26.3	1.01e+007
Dihydrolipoamide S-acyltransferase (pyruvate dehydrogenase E2 component)	AFK20618.1	11	10	149.87	24.2	1.38e+007
Immunogenic protein	AFK20638.1	13	8	149.49	48.8	1.25e+008
Acyl-CoA synthetase	AFK18591.1	10	10	149.37	19	6.95e+006
Acyl-CoA synthetase (plasmid)	AFK20963.1	3	3	44.68	4.9	3.28e+006
Acyl-CoA synthetase (plasmid)	AFK20965.1	5	5	73.25	8.1	3.77e+006
Phosphohexomutase (phosphoglucomutase, phosphomannomutase)	AFK17941.1	10	10	145.64	35.2	4.71e+006
2-methylcitrate dehydratase (plasmid)	AFK21002.1	9	9	142.00	34.7	7.44e+006
Molecular chaperone DnaK	AFK19355.1	9	8	141.80	19.8	1.00e+007
Aldehyde dehydrogenase (NAD+)	AFK18912.1	10	10	141.17	26.6	6.16e+006
Phosphoserine phosphatase	AFK20621.1	9	8	141.02	66.6	5.40e+006
Molybdate transport protein	AFK19675.1	9	8	137.84	30.4	8.38e+006
Stress response protein	AFK20336.2	12	7	137.45	37	1.74e+007
Potassium transport protein kefC	AFK19701.1	11	9	133.58	16	7.24e+006

AAA-type ATPase (transitional ATPase-like protein)	AFK20074.1	11	10	132.85	15.9	3.33e+006
Phosphopyruvate hydratase	AFK20460.1	10	8	132.49	30.8	1.18e+007
Hypothetical protein HFX_1529	AFK19236.1	10	8	131.14	29.9	7.64e+006
ABC-type transport system ATP-binding protein	AFK18720.1	7	7	127.73	49.5	7.35e+006
Hypothetical protein HFX_0491	AFK18222.1	10	7	126.94	53	2.54e+007
Hypothetical protein HFX_1590	AFK19296.1	9	8	126.77	27.7	9.75e+006
RecJ-like exonuclease	AFK20553.1	9	9	124.89	19.5	3.45e+006
Putative phosphonate ABC transporter, periplasmic phosphonate-binding protein	AFK19847.1	8	7	123.69	26.1	2.01e+007
Nitrite reductase copper containing protein	AFK19882.1	12	8	123.51	25.1	3.91e+007
Hypothetical protein HFX_6060 (plasmid)	AFK21187.1	10	7	123.04	25.9	9.06e+006
Arylsulfatase	AFK18199.1	8	8	122.75	29	6.84e+006
Geranylgeranyl hydrogenase-like protein / electron-transferring-flavoprotein dehydrogenase	AFK19181.1	8	8	122.66	27.1	1.25e+007
Molybdopterin oxidoreductase	AFK19899.1	10	7	122.34	30.7	2.38e+007
S-adenosylmethionine-dependent methyltransferase-like protein	AFK18456.1	9	8	121.45	38	1.39e+007
Enoyl-CoA hydratase (plasmid)	AFK21050.1	11	7	119.95	48.4	4.85e+007
Pyruvate--ferredoxin oxidoreductase, beta subunit	AFK19080.1	7	7	119.89	37.8	5.55e+006
Phytoene dehydrogenase (phytoene desaturase)	AFK18509.1	9	8	119.81	26.7	6.29e+006
Poly(3-hydroxyalkanoate) granule-associated 12 kDa protein (plasmid)	AFK21051.1	8	6	118.95	77.2	4.68e+007
CBS domain-containing protein	AFK17996.1	8	7	117.73	21.2	9.08e+006
Glutamine synthetase	AFK17986.2	7	7	115.36	25.2	2.90e+006
Glycosyl transferase	AFK19287.1	9	8	114.33	30.7	2.54e+006
IMP dehydrogenase	AFK18995.1	8	7	113.34	17.4	5.52e+006
Nitrite reductase (NO-forming)	AFK19872.1	10	6	112.23	20.8	1.53e+008
Pyruvate--ferredoxin oxidoreductase, alpha subunit	AFK19081.1	7	6	111.45	16.1	7.90e+006
FAD dependent oxidoreductase	AFK19621.1	7	7	110.91	22.7	4.49e+006
ABC-type glutamine/glutamate/polar amino acids transport system, substrate-binding protein	AFK20126.1	7	6	109.41	38.8	6.38e+006
Halocyanin precursor-like protein	AFK19879.1	7	6	107.30	35.7	3.41e+007
Sulfatase arylsulfatase A-like protein	AFK18425.2	8	7	106.95	18.9	1.74e+007
Sulfatase arylsulfatase A-like protein	AFK19826.1	2	2	33.86	4.2	1.03e+007
Hypothetical protein HFX_2807	AFK20480.1	8	6	106.04	71.6	2.92e+007
Gluconate dehydratase	AFK19260.1	9	7	104.63	26.9	1.46e+007
Aldehyde reductase	AFK18579.1	6	6	103.73	35.5	5.50e+006
Putative hydrolase or acyltransferase of alpha/beta superfamily	AFK18525.1	7	7	102.61	40.2	1.19e+007

Hypothetical protein HFX_1575	AFK19282.2	8	6	102.03	39.9	1.34e+007
Hypothetical protein HFX_1766	AFK19471.1	7	7	101.15	47.2	2.31e+007
Cytochrome b subunit of nitric oxide reductase	AFK19877.1	8	5	99.58	14.3	8.25e+006
AAA-type ATPase (transitional ATPase-like protein)	AFK20391.1	7	7	98.29	11.1	3.34e+006
Hypothetical protein HFX_2555	AFK20236.1	7	7	98.17	22.3	8.84e+006
UpsA domain-containing protein	AFK19975.2	6	6	97.58	47.1	6.91e+006
Phosphate ABC transporter periplasmic substrate-binding protein	AFK20069.1	7	6	96.28	26.7	7.18e+006
Tryptophanase	AFK17753.2	6	6	96.25	23.6	7.72e+006
Nitrate reductase beta chain (plasmid)	AFK20938.1	7	7	95.18	19.3	9.26e+006
Dihydrolipoamide dehydrogenase	AFK20619.1	8	6	94.77	20	3.66e+006
Putative cation-transporting ATPase	AFK18658.2	6	6	94.76	11.6	1.76e+006
NADH dehydrogenase	AFK19343.1	6	5	94.27	27.4	2.88e+006
ABC-type dipeptide/oligopeptide/nickel transport system, substrate binding protein (plasmid)	AFK20740.1	8	6	92.84	14.8	4.71e+006
Hypothetical protein HFX_1586	AFK19292.1	7	7	92.08	20.1	5.20e+006
Putative mechanosensitive ion channel	AFK19964.1	9	5	91.95	31.6	1.11e+007
Hypothetical protein HFX_2088	AFK19779.1	7	6	91.57	23.3	3.04e+006
Hypothetical protein HFX_1589	AFK19295.1	5	5	91.00	17.5	6.28e+006
NADH dehydrogenase, subunit B (ubiquinone)	AFK18695.1	9	6	90.67	35.1	3.53e+007
3-hydroxyacyl-CoA dehydrogenase	AFK19216.2	7	5	90.66	24.8	2.17e+007
Hypothetical protein HFX_6278 (plasmid)	AFK21400.1	7	5	89.96	41.7	2.25e+007
Hypothetical protein HFX_2509	AFK20191.2	6	6	87.81	17.7	8.85e+006
Phosphonates ABC transporter ATP-binding protein	AFK19846.1	6	5	86.33	32.5	5.34e+006
Hypothetical protein HFX_6053 (plasmid)	AFK21180.1	7	6	86.27	25.2	4.00e+006
Electron transfer flavoprotein beta subunit	AFK20417.2	6	5	85.13	28.6	4.98e+006
Hemerythrin HHE cation binding region (plasmid)	AFK20978.1	6	5	84.41	34.4	8.25e+006
NADH dehydrogenase-like complex, subunit I	AFK18698.1	5	5	83.72	50.9	9.82e+006
NADH dehydrogenase 32K chain-like protein	AFK17846.1	6	6	83.69	25.4	4.83e+006
Branched-chain/neutral amino acids amide ABC transporter periplasmic substrate-binding protein	AFK19529.1	6	6	83.51	19.4	1.09e+007
NADH dehydrogenase, subunit H (ubiquinone)	AFK18697.1	6	5	83.45	13.1	1.45e+007
Isocitrate dehydrogenase (NADP+)	AFK20291.1	6	6	83.09	18.1	3.30e+006
Electron transfer flavoprotein alpha-subunit	AFK18029.1	6	5	82.38	38.4	5.84e+006
ABC transporter ATP-binding protein	AFK18549.1	5	5	82.38	21.2	3.55e+006
Hypothetical protein HFX_5226 (plasmid)	AFK21058.1	11	4	81.77	71.2	1.52e+008

Stress response protein (plasmid)	AFK21518.1	5	5	80.51	22.4	1.10e+007
Hypothetical protein HFX_0671	AFK18394.1	6	5	80.04	24.8	5.61e+006
Transmembrane oligosaccharyl transferase / dolichyl-diphosphooligosaccharide--protein glycosyltransferase	AFK19298.1	6	6	79.58	7.3	1.17e+006
Naphthoate synthase	AFK19237.1	6	6	78.55	22.6	4.68e+006
Ferredoxin (2Fe-2S)	AFK20674.1	5	4	78.17	37.2	2.37e+007
Orotate phosphoribosyltransferase-like protein/conserved Entner-Douderoff pathway protein	AFK18805.1	6	5	77.81	29	4.82e+006
Prefoldin beta subunit	AFK18347.1	6	4	76.90	48.3	5.17e+006
Thiosulfate sulfurtransferase	AFK17767.2	6	5	76.79	25.8	8.27e+006
S-adenosyl-L-homocysteine hydrolase	AFK17910.1	5	5	76.77	22.4	1.96e+006
Membrane protease subunit, stomatin/prohibitin	AFK17891.1	6	5	76.04	20.4	6.48e+006
Putative hydrolase or acyltransferase of alpha/beta superfamily	AFK19333.1	5	5	75.96	29.2	2.99e+006
Halocyanin precursor-like protein	AFK18843.1	4	4	74.56	46.3	2.06e+007
Metalloprotease	AFK18012.1	7	5	74.25	16.1	6.03e+006
Phosphate ABC transporter ATP-binding protein	AFK20072.1	5	5	73.78	15.2	3.03e+006
Putative iron transport protein	AFK19393.1	5	4	73.39	18.8	4.80e+006
Gas-vesicle operon protein gvpA	AFK19402.1	6	4	73.29	57.6	2.80e+007
Superoxide dismutase, Fe-Mn family	AFK20579.1	5	4	72.85	26.6	2.17e+007
Superoxide dismutase, Fe-Mn family (plasmid)	AFK21528.1	4	3	56.81	20.5	1.65e+007
4-aminobutyrate aminotransferase	AFK19853.1	5	5	72.71	16.7	4.83e+006
4-aminobutyrate aminotransferase	AFK20535.2	2	2	27.87	4.2	4.02e+006
Protein-disulfide isomerase	AFK18965.1	6	4	71.66	29.7	1.21e+007
NADH dehydrogenase/oxidoreductase-like protein	AFK19950.1	7	4	71.52	28.5	6.92e+006
Hypothetical protein HFX_1239	AFK18952.1	5	4	70.80	26.9	4.78e+006
Serine protein kinase	AFK20509.1	5	5	70.78	8.9	1.45e+006
Thioredoxin	AFK18964.1	6	4	70.55	34.8	8.22e+006
Electron transfer flavoprotein alpha subunit	AFK19622.1	6	4	70.55	16.3	4.73e+006
Xaa-Pro aminopeptidase	AFK19088.1	5	5	70.30	25.8	1.76e+006
Putative phosphate acetyltransferase	AFK18715.1	4	4	70.09	15.6	4.19e+006
Aspartate aminotransferase	AFK18689.1	5	4	69.88	17.7	3.35e+006
S-adenosylmethionine synthetase	AFK19445.1	4	4	69.62	14.1	1.30e+006
Acetyl-CoA acetyltransferase (plasmid)	AFK21178.1	5	5	69.01	24.2	3.85e+006
Ornithine cyclodeaminase	AFK18155.1	5	4	68.51	21	4.16e+006
Dolichyl-phosphate beta-D-mannosyltransferase	AFK19835.1	4	4	67.92	18.4	2.58e+006

Acyl-CoA dehydrogenase	AFK20404.1	4	4	67.87	17.3	2.87e+006
Phosphoenolpyruvate synthase / pyruvate, water dikinase	AFK18505.1	5	5	67.61	7.6	7.54e+005
Dipeptide/oligopeptide/nickel ABC transporter ATP-binding protein	AFK17802.1	5	5	66.63	13.6	4.03e+006
Carbohydrate ABC transporter substrate-binding protein, CUT1 family	AFK20566.1	3	3	66.12	13.6	1.15e+007
Hypothetical protein HFX_5081 (plasmid)	AFK20916.2	5	4	66.01	16.2	1.33e+007
Hypothetical protein HFX_2220	AFK19909.2	4	4	65.81	2.6	1.90e+006
Hypothetical protein HFX_0728	AFK18451.1	5	5	65.54	37.3	7.86e+006
Hypothetical protein HFX_2616	AFK20294.1	5	5	65.50	27.2	1.84e+006
Inorganic pyrophosphatase	AFK18410.1	5	5	65.44	31.6	7.54e+006
Hypothetical protein HFX_0661	AFK18385.1	5	4	64.54	64.3	1.61e+007
3-oxoacyl-[acyl-carrier protein] reductase	AFK19230.1	6	4	64.27	20.6	7.49e+006
FKBP-type peptidylprolyl isomerase 2	AFK19430.2	4	4	63.44	15.4	1.03e+007
Electron transfer flavoprotein beta subunit	AFK18030.1	5	3	63.23	22.7	5.91e+006
Cell division protein FtsZ	AFK18399.1	4	4	63.22	18.5	1.72e+006
2-oxoglutarate ferredoxin oxidoreductase, subunit alpha	AFK18583.1	4	4	62.88	11.6	1.61e+006
A-type ATP synthase subunit F	AFK18040.1	7	3	62.42	57.5	1.81e+007
Sulfatase-like protein	AFK19290.1	4	4	62.39	18.7	1.98e+006
Hypothetical protein HFX_0940	AFK18659.1	4	4	62.27	15.9	4.22e+006
Citrate (si)-synthase	AFK18167.1	4	4	62.11	12.9	6.02e+006
Poly(3-hydroxyalkanoate) granule-associated protein(phasin) (plasmid)	AFK21052.1	8	4	62.01	24.6	1.88e+008
Proteasome subunit alpha	AFK18815.1	4	4	61.97	18.2	4.41e+006
Serine protease inhibitor family protein	AFK20013.1	4	4	61.64	13.6	6.76e+006
Copper-binding plastocyanin like protein (plasmid)	AFK20927.1	5	3	61.54	36.9	1.08e+007
Glycine dehydrogenase subunit 1	AFK20093.1	4	4	61.36	12.7	4.87e+006
Putative sulfatase	AFK19294.1	4	4	61.01	12.7	1.02e+006
Phospho-adenylyl-sulfate reductase	AFK18802.1	4	4	60.91	19.8	5.26e+006
CBS domain-containing protein	AFK20079.1	4	4	60.73	14.4	3.35e+006
Prefoldin alpha subunit	AFK17872.1	5	4	60.56	47.7	6.94e+006
NADH dehydrogenase, subunit M (ubiquinone)	AFK18703.1	4	4	60.07	11.9	6.33e+006
ABC transporter ATP-binding protein	AFK20685.1	4	4	60.06	14.9	1.55e+006
Adenylosuccinate synthetase	AFK18856.1	4	4	60.03	13	2.18e+006
Hypothetical protein HFX_0292	AFK18031.1	5	4	59.98	13.1	5.08e+006
Hypothetical protein HFX_1249	AFK18962.1	4	4	58.90	10.1	2.83e+006

Hypothetical protein HFX_2289	AFK19976.1	5	4	58.90	75	3.89e+006
Hypothetical protein HFX_6434 (plasmid)	AFK21553.1	5	4	58.69	13.9	4.24e+006
Enoyl-CoA hydratase	AFK19171.2	5	4	58.18	17.8	4.33e+006
ABC transporter ATP-binding protein (plasmid)	AFK20923.1	4	4	57.86	15.1	1.22e+007
Phosphate transport system regulatory protein PhoU	AFK20073.1	5	3	57.56	30.5	2.51e+006
Ferredoxin (2Fe-2S)	AFK19572.1	7	3	57.27	22.1	2.07e+007
Endoglucanase	AFK18519.1	4	4	57.08	17.5	1.72e+006
Succinate--CoA ligase, alpha subunit (ADP-forming)	AFK20154.1	4	4	56.98	22.4	2.87e+006
Uracil phosphoribosyltransferase	AFK20636.1	5	4	56.62	30.9	2.16e+006
Imidazolonepropionase (plasmid)	AFK21452.1	4	4	56.62	13.3	8.40e+005
Haloalkane dehalogenase	AFK20076.1	4	4	56.54	18.5	1.34e+006
Malate dehydrogenase	AFK20690.2	3	3	56.32	11.8	2.42e+006
Short chain dehydrogenase/ reductase	AFK18407.1	4	4	55.95	20.2	1.67e+006
Hypothetical protein HFX_2459	AFK20144.2	3	3	55.35	4.5	8.39e+006
N-acyl-L-amino acid amidohydrolase	AFK19179.1	4	4	55.32	14.5	1.66e+006
Oxidoreductase	AFK20381.1	3	3	55.22	11.6	8.42e+005
Hypothetical protein HFX_2343	AFK20030.1	4	4	55.18	13.6	2.27e+006
Sugar ABC transporter ATP-binding protein	AFK20383.1	6	3	54.78	12.9	1.03e+007
Glycine dehydrogenase subunit 2	AFK20092.1	3	3	54.59	14.1	1.30e+006
Anthranilate phosphoribosyltransferase	AFK19965.1	3	3	54.32	13.2	3.40e+006
Hypothetical protein HFX_2260	AFK19948.1	3	3	53.19	23.4	1.81e+006
Hypothetical protein HFX_1464	AFK19172.1	4	4	52.98	22.8	1.81e+006
Putative inosine monophosphate dehydrogenase	AFK17799.1	4	4	52.75	16.5	1.02e+006
Nucleoside diphosphate kinase	AFK20428.1	3	3	52.65	26.6	6.24e+006
Universal stress protein	AFK18810.1	4	3	52.32	26	1.18e+006
Hypothetical protein HFX_0482	AFK18214.1	6	3	52.29	32.8	5.29e+006
Glutamate dehydrogenase (NAD(P)+)	AFK19867.1	4	4	52.21	9.7	3.00e+006
Putative signal transduction protein with CBS domains (plasmid)	AFK21146.1	4	4	51.85	11.3	1.15e+006
Menaquinol--cytochrome-c reductase	AFK20314.1	4	3	51.84	13.5	1.05e+007
Ribulose-bisphosphate carboxylase large chain	AFK18685.1	4	4	51.73	14.2	7.28e+005
Putative intracellular protease	AFK19063.1	3	3	51.14	21.7	1.10e+007
Hypothetical protein HFX_2180	AFK19869.1	4	3	51.09	8.7	2.99e+006
Thioredoxin	AFK18139.1	3	3	50.82	51.1	1.94e+006

Ferredoxin:NAD+ oxidoreductase	AFK20041.1	3	3	50.28	16.2	1.38e+006
Dihydroxyacetone kinase, DhaK subunit	AFK19313.1	3	3	49.81	17.8	1.90e+006
Gas-vesicle operon protein gvpH	AFK19407.1	3	3	49.59	17.1	5.81e+006
Proteasome subunit alpha	AFK20587.1	3	3	49.53	12.2	2.05e+006
Adenylate kinase	AFK20192.2	3	3	49.35	21.1	2.36e+006
Protein of unknown function DUF1486	AFK20429.1	4	3	49.32	22.4	2.38e+006
FAD-dependent pyridine nucleotide-disulfide oxidoreductase	AFK17859.1	3	3	49.27	11.5	1.04e+006
Phenylacetate-CoA oxygenase subunit PaaA (plasmid)	AFK21499.2	3	3	49.27	11.4	1.94e+006
Aminopeptidase (leucyl aminopeptidase, aminopeptidase T)	AFK18178.1	4	3	48.95	14.1	1.00e+006
Hypothetical protein HFX_0970	AFK18688.1	3	3	48.74	7.9	1.24e+006
Monoamine oxidase regulatory protein (plasmid)	AFK21482.1	3	3	48.52	26.9	1.31e+006
Proteasome beta subunit	AFK19329.1	4	3	48.01	20.8	2.82e+006
NADH dehydrogenase, subunit L (ubiquinone)	AFK18702.1	5	3	47.62	7.8	2.22e+006
Hypothetical protein HFX_2780	AFK20456.1	3	3	47.62	12.8	9.52e+005
Oxidoreductase	AFK18724.1	3	3	47.41	12.6	8.85e+005
Ribose-1,5-bisphosphate isomerase (ribulose-bisphosphate forming)	AFK18682.1	4	4	47.31	17.9	1.43e+006
DMSO reductase family type II enzyme, heme b subunit (plasmid)	AFK20937.1	3	3	47.03	13.4	1.43e+006
Hypothetical protein HFX_2647	AFK20325.1	3	3	46.86	11.7	2.06e+006
Hypothetical protein HFX_0016	AFK17760.1	3	3	46.79	19.7	2.50e+006
ABC-type transport system ATP-binding protein	AFK20086.1	4	3	46.69	16.5	2.86e+006
Putative X-Pro dipeptidase	AFK18714.1	3	3	46.66	14.9	7.20e+005
Dodecin	AFK20375.1	3	3	46.57	69.1	1.38e+007
Succinate--CoA ligase beta subunit (ADP-forming)	AFK20155.1	3	3	46.33	11	1.41e+006
Acetyl-CoA C-ac(et)yltransferase	AFK19698.1	3	3	46.30	14.8	9.25e+005
Zinc-transporting ATPase (plasmid)	AFK21399.1	4	4	46.27	4.3	9.77e+005
Signal sequence peptidase	AFK17747.2	3	3	45.98	14.4	2.20e+006
Hypothetical protein HFX_1684	AFK19390.1	4	2	45.97	21.6	1.29e+007
D-3-phosphoglycerate dehydrogenase	AFK19716.1	3	3	45.94	10	1.33e+006
Ca2+-transporting ATPase	AFK18654.1	3	3	45.62	4.3	1.24e+006
Arylsulfatase, choline-sulfatase	AFK19291.1	4	4	45.56	12.4	2.45e+006
ABC-type branched-chain amino acid transport systems, substrate-binding protein	AFK20482.1	3	3	45.02	13.4	2.02e+006
Urocanate hydratase (plasmid)	AFK21450.1	3	3	44.92	7.5	1.44e+006
Oligopeptide ABC transporter ATPase component	AFK17803.1	3	3	44.53	9.4	1.36e+006

Hypothetical protein HFX_1141	AFK18857.1	5	3	44.53	37.6	1.97e+007
Hsp20-type chaperone	AFK18151.1	3	3	44.52	25.1	6.39e+006
Sialidase-1	AFK20474.1	3	3	44.47	6.6	2.21e+006
Hypothetical protein HFX_0293	AFK18032.2	3	3	44.28	10.8	1.43e+006
Serine hydroxymethyltransferase	AFK20524.1	3	3	44.17	7.9	2.22e+006
Putative monovalent cation/H+ antiporter subunit E	AFK18782.1	3	3	44.04	25.7	1.08e+006
Short-chain dehydrogenase / reductase SDR / glucose 1-dehydrogenase	AFK20158.1	3	3	43.63	17.4	8.78e+005
Carbonic anhydrase	AFK18667.1	3	3	43.24	14.7	3.54e+006
Putative acetyltransferase (plasmid)	AFK21133.1	3	3	43.18	23.5	1.51e+006
Cation efflux protein	AFK17990.1	3	3	43.14	10.8	2.78e+006
RecJ like exonuclease	AFK18734.2	3	3	43.00	4.8	1.17e+006
Hypothetical protein HFX_1679	AFK19385.1	3	3	41.95	7.9	1.89e+006
ABC-type dipeptide/oligopeptide/nickel transport system, substrate-binding protein	AFK19559.1	3	3	41.82	6.3	1.64e+006
Methionine aminopeptidase	AFK20296.1	3	3	41.67	8.4	3.94e+006
Circadian regulator	AFK18935.1	3	3	41.66	14.6	1.29e+006
Biotin carboxylase	AFK20173.1	3	3	41.32	5.4	2.71e+006
Halocyanin precursor-like protein	AFK18536.1	2	2	41.30	15.8	4.16e+006
Halocyanin precursor-like protein	AFK18518.1	2	2	41.30	16.5	4.16e+006
Hypothetical protein HFX_2662	AFK20340.1	3	3	41.19	14.6	1.24e+006
Hypothetical protein HFX_0588	AFK18313.1	3	3	41.18	11.3	1.49e+006
Molybdopterin oxidoreductase	AFK19900.1	3	3	41.16	8.4	1.83e+006
Putative acylaminoacyl-peptidase	AFK18673.1	3	3	41.15	3.8	6.18e+005
ABC-type dipeptide/oligopeptide/nickel transport system, substrate-binding protein (plasmid)	AFK21027.1	4	3	41.09	5.9	5.34e+006
Cytochrome b/b6 (plasmid)	AFK20941.1	3	3	40.50	10.9	9.75e+006
Hypothetical protein HFX_0697	AFK18420.1	4	2	40.36	38.7	2.47e+007
Hypothetical protein HFX_5167 (plasmid)	AFK21001.1	4	3	40.26	19.2	3.09e+006
Dipeptidyl aminopeptidase/acylaminoacyl peptidase	AFK18522.1	3	3	40.01	5.4	1.18e+006
Lysophospholipase	AFK20242.1	3	3	40.01	13	9.96e+005
Hypothetical protein HFX_0457	AFK18192.2	3	3	39.92	20.9	1.54e+006
Zn-dependent hydrolase, glyoxylase	AFK19254.1	3	3	39.59	16.1	5.31e+005
Glutamate/aspartate transport protein	AFK19350.1	3	3	39.48	6.2	1.67e+006
Riboflavin synthase beta subunit (6,7-dimethyl-8-ribityllumazine synthase)	AFK18690.1	3	3	39.26	36.5	7.25e+005
Glutamate-1-semialdehyde aminotransferase	AFK17832.1	3	3	39.03	9.4	1.07e+006

Methylmalonyl-CoA decarboxylase alpha chain	AFK20161.1	3	3	38.69	7.9	1.60e+006
Hypothetical protein HFX_6351 (plasmid)	AFK21472.1	3	3	38.08	26.4	1.64e+006
Putative patatin-like phospholipase (plasmid)	AFK21580.1	3	3	38.06	13.7	2.64e+006
Sugar ABC transporter ATP-binding protein (UGPC)	AFK20563.1	3	2	37.96	10.2	2.18e+006
Hypothetical protein HFX_0936	AFK18655.1	2	2	37.90	27.2	6.09e+005
Cytochrome c oxidase subunit II / ba3-type terminal oxidase subunit II	AFK18662.1	2	2	37.86	14.2	1.85e+007
Hypothetical protein HFX_1268	AFK18981.1	3	3	37.66	4.1	9.24e+005
Acetyl transferase	AFK20422.1	2	2	37.45	16.8	3.54e+006
Aconitate hydratase	AFK19741.1	3	3	37.10	6.5	1.05e+006
Hypothetical protein HFX_2772	AFK20448.1	4	2	36.82	20.5	1.37e+007
Hypothetical protein HFX_2513	AFK20195.1	3	3	36.73	19	1.69e+006
PLP-dependent aminotransferase (aspartate aminotransferase)	AFK19365.1	3	3	36.72	9.9	9.76e+005
Hypothetical protein HFX_6273 (plasmid)	AFK21396.2	3	3	36.30	8.7	1.11e+006
3-ketoacyl-acyl carrier protein reductase (PhaB) (plasmid)	AFK21048.1	3	3	36.05	12	8.54e+006
Gas-vesicle operon protein gvpF	AFK19405.1	2	2	36.04	15	6.30e+005
Phosphoribosylaminoimidazole synthetase	AFK19325.1	2	2	35.83	6.1	1.63e+006
Molybdopterin biosynthesis protein moeA	AFK20001.1	3	3	35.75	11	8.82e+005
NAD synthetase	AFK19658.1	3	3	35.74	10.1	4.85e+006
Carboxypeptidase	AFK18120.1	3	3	35.64	8.7	1.27e+006
Poly(3-hydroxyalkanoate) synthase subunit PhaC	AFK20356.1	3	3	35.63	9.7	1.40e+006
Acyl-CoA dehydrogenase	AFK18868.1	3	3	35.47	9.4	8.14e+005
Amino acid-binding protein (plasmid)	AFK21485.1	2	2	35.02	6.9	4.86e+005
Peptidyl-prolyl cis-trans isomerase B (cyclophilin B)	AFK19961.1	4	2	34.67	16.2	8.27e+006
Acyl-CoA synthetase	AFK18955.2	3	3	34.45	5.4	9.33e+005
Hypothetical protein HFX_2532	AFK20214.1	3	3	33.88	10.2	1.01e+006
Mechanosensitive ion channel	AFK19459.1	2	2	33.73	7.7	2.40e+006
Ribose ABC transporter ATP-binding protein	AFK19184.1	3	3	33.64	5.2	2.33e+006
Stress response protein	AFK18130.1	2	2	33.63	20.8	5.42e+005
ABC-type dipeptide/oligopeptide/nickel transport systems, ATP-binding protein I & II	AFK18329.1	2	2	33.59	2.8	5.39e+005
Preprotein translocase subunit SecF	AFK19760.1	2	2	33.31	11.1	5.02e+005
Arginase	AFK19340.1	2	2	33.26	14.3	1.38e+007
Glycerol-3-phosphate dehydrogenase subunit B	AFK19306.1	2	2	33.21	9	2.10e+005
NADPH-dependent FMN reductase	AFK20556.2	2	2	33.16	24.4	1.52e+006

Hypothetical protein HFX_6067 (plasmid)	AFK21194.1	2	2	32.86	6.2	8.23e+005
Universal stress protein (plasmid)	AFK21282.1	2	2	32.83	15.6	1.53e+006
Methylmalonyl-CoA mutase, N-terminal domain protein	AFK18588.1	2	2	32.62	6.3	5.58e+005
Cell division protein ftsZ	AFK19949.2	2	2	32.57	7.3	7.45e+005
Halocyanin hcpH	AFK18872.1	2	2	32.43	28.3	3.30e+006
Universal stress protein UspA-like protein	AFK18989.1	2	2	32.41	26.2	6.82e+006
Hypothetical protein HFX_2853	AFK20523.1	3	2	32.40	16.3	5.59e+005
Oligopeptide ABC transporter permease protein	AFK17804.1	2	2	32.32	4.8	1.56e+006
Ubiquinone/menaquinone biosynthesis methyltransferase	AFK18034.2	2	2	32.21	12.9	2.92e+006
Hsp20-type chaperone (plasmid)	AFK20982.1	2	2	31.89	17.6	5.58e+005
Hypothetical protein HFX_1448	AFK19156.1	3	2	31.81	12.7	4.23e+006
Acyl-CoA dehydrogenase	AFK19198.1	2	2	31.71	9.1	7.48e+005
Endoribonuclease L-PSP	AFK18161.1	2	2	31.70	25	9.98e+005
Thioesterase (plasmid)	AFK21493.1	2	2	31.17	28.3	9.94e+005
Hypothetical protein HFX_1622	AFK19328.1	2	2	30.96	23.7	2.25e+006
OsmC family protein	AFK19097.2	2	2	30.92	20.5	3.88e+006
Hsp20 type chaperone	AFK18447.1	2	2	30.79	21.6	7.06e+005
Uridine phosphorylase	AFK20307.1	2	2	30.78	10.3	2.71e+006
Hypothetical protein HFX_1243	AFK18956.1	2	2	30.71	7.9	6.01e+006
Hypothetical protein HFX_5285 (plasmid)	AFK21116.1	2	2	30.59	18.7	1.65e+006
Hypothetical protein HFX_1139	AFK18855.1	2	2	30.47	31.1	1.11e+006
Pyridoxal biosynthesis lyase PdxS	AFK20032.1	2	2	30.41	6.2	6.92e+005
Phosphonates ABC transporter permease protein	AFK19844.1	2	2	30.25	9.7	6.86e+005

Table S5. Representative proteins identified in the micelles with Nar and Nir activities obtained after the use of HiPrep™ Q-Sepharose 16/10 FF from 3 LC-MS/MS runs.

Protein name	Database Accession	Spectra	Distinct Peptides	Distinct Summed MS/MS Search Score	% AA Coverage	Total Protein Spectral Intensity
nitrate reductase alpha chain (plasmid)	AFK20939.1	28	22	380.05	34.4	3.88e+007
dipeptide ABC transporter ATP-binding protein	AFK18330.2	34	18	354.37	50.1	3.10e+008
nitrous-oxide reductase (plasmid)	AFK20926.1	25	23	349.62	38.2	1.90e+008
nucleoside-binding protein	AFK19185.1	23	16	297.84	59.3	3.03e+008
succinate dehydrogenase, subunit A (flavoprotein)	AFK20495.1	19	15	278.01	36.4	7.91e+007
proline dehydrogenase	AFK18055.1	21	15	271.67	67	5.92e+007
proline dehydrogenase	AFK18914.1	9	7	112.84	34.4	1.21e+007
A-type ATP synthase subunit E	AFK18038.1	32	12	245.46	72.1	3.81e+008
sugar ABC transporter substrate binding protein	AFK20386.1	14	12	216.60	38.5	3.85e+007
A-type ATP synthase subunit C	AFK18039.1	17	12	215.91	43.3	7.89e+007
A-type ATP synthase subunit I	AFK18036.1	15	11	214.94	16.1	8.48e+007
NADH dehydrogenase, subunit CD (ubiquinone)	AFK18696.1	18	13	214.59	30.7	3.52e+007
NADH dehydrogenase, subunit D (ubiquinone)	AFK18684.1	6	4	66.43	6.6	1.84e+007
A-type ATP synthase subunit H	AFK18035.1	18	12	212.54	80.9	1.95e+008
ABC-type dipeptide/oligopeptide/nickel transport system, substrate binding protein	AFK20131.1	16	11	204.37	36.4	4.70e+007
A-type ATP synthase subunit A	AFK18041.1	16	11	197.16	28.8	1.94e+007
poly(3-hydroxyalkanoate) synthase subunit PhaE (plasmid)	AFK21053.1	19	9	188.11	71.4	1.74e+008
iron-sulfur protein (4Fe-4S)	AFK17960.2	13	11	187.43	26.5	3.63e+007
nitrite reductase copper containing protein	AFK19882.1	17	12	182.42	46.3	5.32e+007
serine protease (plasmid)	AFK21203.1	12	11	181.73	28.1	1.84e+007
immunogenic protein	AFK20638.1	16	8	174.36	41.9	3.71e+008
poly(3-hydroxyalkanoate) synthase subunit PhaC (plasmid)	AFK21054.1	12	10	170.53	31	1.59e+007
SPFH domain, Band 7 family protein	AFK18490.1	12	11	169.54	32.3	1.47e+007
PBS lyase HEAT-like repeat protein	AFK18736.1	11	9	166.11	23	9.36e+007
nitrite reductase (NO-forming)	AFK19872.1	11	12	161.07	32.8	2.40e+008
dipeptide ABC transporter dipeptide-binding protein	AFK17806.1	10	10	151.07	21.1	1.43e+007
dihydroorotase	AFK19587.1	9	8	145.79	32.1	3.36e+006
periplasmic solute binding protein	AFK20085.1	8	8	144.87	31.5	1.37e+007

catalase (including: peroxidase)	AFK19564.1	12	8	141.07	14.5	2.77e+007
A-type ATP synthase subunit B	AFK18042.1	11	8	136.27	22	2.13e+007
halocyanin precursor-like protein	AFK19879.1	9	8	136.09	42.3	1.16e+007
nitrate reductase beta chain (plasmid)	AFK20938.1	11	9	136.08	27.5	2.12e+007
hypothetical protein HFX_6060 (plasmid)	AFK21187.1	9	8	133.28	30.3	9.87e+006
oxidoreductase	AFK18898.2	8	8	131.22	34.7	5.65e+006
hypothetical protein HFX_1575	AFK19282.2	10	7	129.06	47.8	4.61e+007
carbohydrate ABC transporter substrate-binding protein, CUT1 family	AFK20566.1	10	6	126.05	26.2	2.69e+007
hypothetical protein HFX_1144	AFK18860.1	8	8	122.77	45.1	3.65e+006
stress response protein (plasmid)	AFK21518.1	8	7	121.34	36.3	3.14e+007
dipeptide/oligopeptide/nickel ABC transporter periplasmic substrate-binding protein	AFK18790.1	8	8	120.96	17.6	5.93e+006
hypothetical protein HFX_0491	AFK18222.1	10	6	117.31	52.4	4.89e+007
hypothetical protein HFX_2343	AFK20030.1	8	7	116.90	32.1	6.63e+006
sulfatase arylsulfatase A-like protein	AFK18425.2	9	8	115.50	15.3	1.22e+007
hypothetical protein HFX_1589	AFK19295.1	7	7	112.25	17.4	7.26e+006
acetyl transferase	AFK20422.1	9	6	110.63	36.8	1.55e+007
naphthoate synthase	AFK19237.1	7	7	110.00	27.8	7.35e+006
hypothetical protein HFX_1586	AFK19292.1	8	7	108.80	19.5	6.32e+006
ferredoxin (2Fe-2S)	AFK19572.1	6	6	106.51	39.1	2.25e+007
cytochrome b subunit of nitric oxide reductase	AFK19877.1	9	6	106.03	15.6	4.20e+006
molybdate transport protein	AFK19675.1	8	7	106.01	30.1	4.63e+006
thioredoxin	AFK18964.1	9	6	103.10	49.4	4.30e+007
hypothetical protein HFX_6278 (plasmid)	AFK21400.1	6	6	101.55	48.8	3.29e+007
acetyl-CoA C-acetyltransferase (plasmid)	AFK21477.1	7	7	100.56	28	4.90e+006
acetyl-CoA C-ac(et)yltransferase	AFK19698.1	4	4	60.33	16.9	1.96e+006
2-methylcitrate dehydratase (plasmid)	AFK21002.1	7	6	94.97	22.9	3.02e+006
aldehyde reductase	AFK18579.1	6	6	93.57	37.3	2.35e+006
electron transfer flavoprotein alpha subunit	AFK20418.1	6	6	91.97	13.6	4.73e+006
hypothetical protein HFX_2807	AFK20480.1	5	5	91.34	54.7	1.63e+007
dihydrolipoamide dehydrogenase (plasmid)	AFK21581.1	7	6	90.72	20.9	4.26e+006
NADPH-dependent FMN reductase	AFK20556.2	6	4	86.29	46.8	1.32e+007
ABC-type iron(III) transport system,substrate-binding protein	AFK19499.1	7	5	85.78	27.1	4.53e+007
gas-vesicle operon protein gvpC	AFK19401.1	7	5	85.02	18.6	2.92e+007

protein-disulfide isomerase	AFK18965.1	6	4	84.04	29.7	1.43e+007
ferredoxin (2Fe-2S)	AFK20674.1	10	4	84.01	37.2	1.03e+008
phosphate ABC transporter ATP-binding protein	AFK20072.1	6	6	82.61	23.3	2.05e+006
nucleoside diphosphate kinase	AFK20428.1	7	5	81.52	40.2	1.55e+007
thermosome, beta subunit	AFK18158.2	6	5	81.10	17.1	1.30e+006
gas-vesicle operon protein gvpA	AFK19402.1	4	4	79.01	57.6	1.43e+007
3-hydroxyacyl-CoA dehydrogenase	AFK19216.2	5	4	70.08	22.7	9.44e+006
hypothetical protein HFX_2509	AFK20191.2	5	5	67.93	17	4.53e+006
hypothetical protein HFX_0016	AFK17760.1	5	5	67.77	29.1	3.50e+006
glycine dehydrogenase subunit 1	AFK20093.1	5	5	67.52	15.4	3.89e+006
ABC-type dipeptide/oligopeptide/nickel transport system, substrate binding protein (plasmid)	AFK20740.1	4	4	66.15	10	9.16e+005
halocyanin precursor-like protein	AFK18843.1	6	4	63.83	40.3	9.09e+007
pterin-4-alpha-carbinolamine dehydratase	AFK20006.1	4	3	63.15	59.3	4.90e+006
acetyl-CoA acetyltransferase (plasmid)	AFK21178.1	5	4	63.14	19.8	6.26e+006
gluconate dehydratase	AFK19260.1	4	4	62.53	10.6	2.42e+006
Hemerythrin HHE cation binding region (plasmid)	AFK20978.1	5	4	62.30	24.4	9.90e+006
molybdopterin biosynthesis protein moeA	AFK20001.1	4	4	59.57	17.4	1.69e+006
copper-binding plastocyanin like protein (plasmid)	AFK20927.1	4	3	59.55	36.9	1.25e+007
glutamate dehydrogenase (NAD(P)+)	AFK19225.1	4	4	58.56	12.4	1.77e+006
putative NAD(P)H-dependent xylose reductase	AFK18957.2	4	4	57.78	13.8	2.52e+006
succinate dehydrogenase, subunit B (iron-sulfur protein)	AFK20496.1	4	4	56.65	17.4	3.76e+006
metallo-beta-lactamase superfamily protein	AFK18753.1	4	3	56.43	28.1	4.41e+006
hsp20-type chaperone	AFK18151.1	4	4	56.42	38.5	6.95e+006
short-chain dehydrogenase / reductase SDR / glucose 1-dehydrogenase	AFK20158.1	5	4	56.05	21.2	4.26e+006
hypothetical protein HFX_0694	AFK18417.1	3	3	55.83	46.3	3.57e+006
CBS domain-containing protein	AFK17996.1	3	3	54.45	8.8	1.04e+006
dTMP kinase	AFK19952.1	4	4	54.12	23.8	2.55e+006
poly(3-hydroxyalkanoate) granule-associated 12 kDa protein (plasmid)	AFK21051.1	3	3	54.09	34.5	1.27e+007
monoamine oxidase regulatory protein (plasmid)	AFK21482.1	3	3	53.89	26.9	8.42e+006
hypothetical protein HFX_1141	AFK18857.1	5	4	53.70	48.5	1.71e+007
enoyl-CoA hydratase (plasmid)	AFK21050.1	4	3	53.66	15.5	9.72e+006
cobalamin adenosyltransferase	AFK20083.1	4	3	53.52	22	2.73e+006
citrate (si)-synthase	AFK18167.1	3	3	53.24	12.4	1.54e+006

poly(3-hydroxyalkanoate) granule-associated protein(phasin) (plasmid)	AFK21052.1	7	3	51.48	20.1	1.24e+008
UpsA domain-containing protein	AFK19975.2	3	3	50.09	15.4	4.68e+006
phosphonates ABC transporter ATP-binding protein	AFK19846.1	4	3	49.64	19.3	2.05e+006
halocyanin hcpG	AFK18949.1	4	4	48.68	5.1	1.39e+006
flavin-dependent dehydrogenase	AFK20419.1	3	3	48.68	8.6	9.74e+005
hypothetical protein HFX_1777	AFK19482.1	4	3	47.63	26.2	2.01e+007
protein of unknown function DUF1486	AFK20429.1	3	3	47.38	22.4	1.34e+006
geranylgeranyl hydrogenase-like protein / electron-transferring-flavoprotein dehydrogenase	AFK19181.1	3	3	47.03	8.1	1.56e+006
ribose-1,5-bisphosphate isomerase (ribulose-bisphosphate forming)	AFK18682.1	4	4	46.44	13.2	1.50e+006
stress response protein	AFK20336.2	3	3	45.54	15.6	1.68e+006
hypothetical protein HFX_5226 (plasmid)	AFK21058.1	3	3	45.49	48.5	9.32e+005
thiamine-binding periplasmic protein precursor-like protein	AFK17765.2	4	3	45.35	14.2	1.80e+006
putative phosphonate ABC transporter, periplasmic phosphonate-binding protein	AFK19847.1	3	2	45.07	10.1	1.13e+006
hypothetical protein HFX_2088	AFK19779.1	3	3	44.78	11.4	6.54e+005
NAD synthetase	AFK19658.1	4	3	44.15	10.1	1.62e+006
serine protease inhibitor family protein	AFK20013.1	3	3	44.03	7.5	4.08e+006
4-alpha-glucanotransferase	AFK19479.2	3	3	43.94	5.4	1.84e+006
hypothetical protein HFX_2910	AFK20580.2	3	3	43.42	36	6.96e+005
S-adenosylmethionine-dependent methyltransferase-like protein	AFK18456.1	3	3	43.13	11.9	1.48e+006
ubiquinone/menaquinone biosynthesis methyltransferase	AFK18034.2	3	2	41.83	16.3	1.65e+006
hypothetical protein HFX_2082	AFK19774.1	3	3	41.64	21.2	7.43e+005
gas-vesicle operon protein gvpF	AFK19405.1	3	3	41.53	18.3	1.31e+006
hypothetical protein HFX_0141	AFK17882.2	2	2	40.97	37.3	2.71e+006
aconitate hydratase	AFK18238.1	3	3	40.92	3.5	1.22e+006
thymidylate synthase	AFK20583.1	3	3	40.76	14.5	1.00e+006
molecular chaperone DnaK	AFK19355.1	2	2	40.67	5.1	7.73e+005
hypothetical protein HFX_1239	AFK18952.1	2	2	40.38	17.6	1.08e+006
NADH dehydrogenase/oxidoreductase-like protein	AFK19950.1	2	2	40.00	10.2	8.02e+005
phosphate ABC transporter periplasmic substrate-binding protein	AFK20069.1	3	3	39.24	7.5	2.98e+006
acyl-CoA dehydrogenase	AFK20404.1	3	3	39.11	13.1	7.59e+005
hypothetical protein HFX_0940	AFK18659.1	2	2	38.79	9.4	1.19e+006
dihydrolipoamide S-acyltransferase (pyruvate dehydrogenase E2 component)	AFK20618.1	3	3	38.71	7.4	6.64e+005
thermosome, alpha subunit	AFK17883.2	3	3	38.58	5.7	1.44e+006

hypothetical protein HFX_0080	AFK17822.1	2	2	38.21	26.6	3.30e+005
hypothetical protein HFX_6434 (plasmid)	AFK21553.1	3	3	38.04	10.3	1.87e+006
hsp20-type chaperone (plasmid)	AFK20982.1	2	2	37.79	19	7.72e+005
hypothetical protein HFX_2289	AFK19976.1	2	2	37.43	35.2	1.53e+006
oxidoreductase (thioredoxin-disulfide reductase-like protein)	AFK19539.2	3	3	36.92	10.5	9.46e+005
dnaJ/dnaK ATPase stimulator grpE	AFK19357.1	2	2	35.99	19.4	8.83e+005
NADH dehydrogenase, subunit H (ubiquinone)	AFK18697.1	3	2	35.68	7.1	3.62e+006
phytoene dehydrogenase (phytoene desaturase)	AFK18509.1	3	3	35.56	8.4	1.18e+006
glutamate dehydrogenase (NAD(P)+)	AFK19867.1	3	3	35.54	7.5	5.63e+005
glycerol kinase	AFK19308.1	2	2	35.49	5.6	4.37e+006
dipeptide/oligopeptide/nickel ABC transporter ATP-binding protein	AFK17802.1	3	3	35.47	5.7	1.14e+006
1-(5-phosphoribosyl)-5-[(5- phosphoribosylamino)methylideneamino] imidazole-4-carboxamide isomerase	AFK20645.1	2	2	35.11	13.8	4.19e+005
putative mechanosensitive ion channel	AFK19964.1	2	2	34.97	10.3	1.07e+006
NADH dehydrogenase, subunit B (ubiquinone)	AFK18695.1	4	2	34.69	11.5	5.15e+006
anthranilate phosphoribosyltransferase	AFK19965.1	2	2	33.87	7.3	6.55e+005
superoxide dismutase, Fe-Mn family (plasmid)	AFK21142.1	2	2	33.25	14	8.31e+005
halocyanin hcpH	AFK18872.1	2	2	33.03	28.3	5.49e+006
branched-chain-amino-acid aminotransferase	AFK18053.1	3	2	32.88	8.9	1.19e+006
putative iron transport protein	AFK19393.1	2	2	32.87	6.6	1.21e+006
mechanosensitive ion channel	AFK19459.1	2	2	32.77	7.7	5.11e+006
hypothetical protein HFX_1529	AFK19236.1	2	2	32.70	6.1	8.22e+005
hypothetical protein HFX_2772	AFK20448.1	3	2	32.53	20.5	4.39e+006
membrane protein Pan1	AFK18234.1	2	2	32.33	6.1	2.90e+005
riboflavin synthase beta subunit (6,7-dimethyl-8-ribityllumazine synthase)	AFK18690.1	2	2	32.21	29.8	1.16e+006
ferredoxin: NAD+ oxidoreductase	AFK20041.1	2	2	32.18	11.3	7.57e+005
phosphate transport system regulatory protein PhoU	AFK20073.1	2	2	32.13	15	9.19e+005
aspartate aminotransferase	AFK18689.1	2	2	32.00	8.8	3.61e+005
hypothetical protein HFX_1590	AFK19296.1	2	2	31.95	6.4	3.11e+006
hypothetical protein HFX_5081 (plasmid)	AFK20916.2	2	2	31.79	8.5	4.94e+005
NAD-dependent epimerase/dehydratase	AFK18563.1	2	2	31.36	10.3	2.81e+005
3-oxoacyl-[acyl-carrier protein] reductase	AFK19230.1	3	2	31.22	9.9	1.98e+006
glutamine synthetase	AFK17986.2	2	2	30.77	7.6	3.23e+005
triphosphoribosyl-dephospho-CoA synthase	AFK20166.1	2	2	30.25	13.6	4.43e+005

hypothetical protein HFX_2180	AFK19869.1	2	2	30.95	3.5	8.84e+005
cytochrome b/b6 (plasmid)	AFK20941.1	2	2	30.23	8.6	7.00e+005

A

MEL**KRK**TIA**K**VIAVVFIFNLVVMGAGAWFAYQEAPPIPE**K**VVGPDGEVIVNGEEI**R**DG**KK**VFQQNGLMNHGSILGNGAYYGVDYT
ADALEL**K**VQYM**R**DYYAQE**R**HGESYSALDSATQAAIADVVE**K**DLDGTYEGGAIEYSEAE**R**YAHEQV**R**QEYVQ**R**YHEGDHE**R**GVPV
GMIDSEAEAEQFADFAMWTAWFSHTD**R**PGSTHSYTNDWPYQPGAGNDATAASMTWSVIAMVLLVAGAGLGIWLY**K**SVELPEP
SAEGISVPEPGEVSIFPSQ**R**AAL**R**FIPVAAGLFVAQVLLGGLLAHFYIE**R**AGFFGIETLFGIHILQLLPFSIA**K**TWHIDLAILWIAATWLG
AGLFLPPLLTGYEP**RK**QSTYINGLLGAIVVVTLGGLGGIWLGANGYIDGPLWWILGNEGLEYLEVG**K**LWQFGILAGFLIWAGLAV**R**G
L**K**PLLD**K**EPVYGLAHMILYAGGSIALLFTAGFLFTPDTNIAVTEFW**R**WWVVHMWVEGAFEFFIVAIVGLTLVSMNLLS**RR**SAE**K**AV
MLQALLVMGTGIIGVSHHYWWVGMPDMWVPLGSVFSTLELIPLVFILYEALGQY**R**TMSTGENFPY**R**LPFMFIIASGVWNFVGAG
VLGFFINLPLINYYEHGTYLTVGHAHAAMFGAFGFLALGMVTYMLQLSIDPA**R**WDGSWL**R**AAFWCWNVGLVLMVFVSVLPVGFL
QLETAFTGSYAAA**R**SLAFYNQPIIQTLFWA**R**LPGDTLMILGTVIYAADLV**RKR**FVL**R**ESSDDPSVEDMAVAEGILGDD

B

Sequence	MH^+ Matched (Da)	Spectra	Spectral intensity
(K)DLDGTYEGGAIEYSEAER(Y)	1974.86	2	4.32E5
(R)FIPVAAGLFVAQVLLGGLLAHFYIER(A)	2814.61	1	4.71E5
(R)HGESYSALDSATQAAIADVVEK(D)	2262.09	1	4.51E5
(R)LPGDTLMILGTVIYAADLVR(K)	2131.18	3	1.35E6
SLAFYNQPIIQTLFWAR(L)	2068.10	1	4.27E5
(K)VVGPDGEVIVNGEEIR(D)	1681.88	1	1.07E6

Figure S1. Panel A: aminoacid sequence of *Haloferax mediterranei* qNor. Lysine residues (K) and arginine residues (R) are shown in bold letters. The 14 transmembrane segments are shown in grey. Panel B: sequence of the six different peptides detected by LC-MS/MS after tripsine digestion of qNor in micelles of the last step of enrichment.

Figure S2. Amino acid sequence alignments between nitrite reductase-NO forming (Nir-NO) and copper-containing nitrite reductase (Nir-Copper) using the bioinformatic tool Clustal Omega (Sievers, F., Wilm, A., Dineen, D., Gibson, T.J., Karplus, K., Li, W., et al., 2011). The percentage of identity was 23.30%.

CONCLUSIONS

- Based on the haloarchaeal genomes analysed, the genes involved in denitrification are grouped into three gene clusters (*nar, nir-nor, nos*) coding for denitrification enzymes NarGHI, NirK, qNor and NosZ. In case of incomplete denitrifiers, some of the genes (or clusters) are absent.
- The respiratory Nor of *H. mediterranei* is a qNor related to bacterial qNors. In fact, the vast majority of haloarchaeal genomes studied (141) reveal the presence of a single *norZ* orthologue. The evidences show that Nor-coding genes in haloarchaea are incorrectly annotated.
- *H. volcanii* is unable to reduce NO_3^- to NO_2^- and N_2O to N_2. Although it denitrifies *sensu stricto* as it reduces NO_2^- to gaseous products, this strain is not a good candidate for controlling N-oxide emissions.
- *H. denitrificans* can act as source of N_2O under some culture conditions and shows a dramatic transition to denitrification, mainly due to a low induction by O_2-sensors which implies a slow and late Nar expression.
- *H. mediterranei* displays a reproducible and robust phenotype in terms of accumulation of N-oxide intermediates, reducing all NO_3^-/NO_2^- available to N_2. It reflects a well-orchestrated denitrification apparatus.
- *H. mediterranei* requires the presence of low micromolar concentrations of O_2 for the *novo* synthesis of denitrification enzymes (Nar and Nir).
- In *H.* mediterranei, O_2 is the superordinate controller of denitrification, being Nar and Nos, both transcriptionally activated by hypoxia (and probably NO_3^-), while Nir and Nor expression require the presence of NO (and possibly NO_2^-) as well as Nos.

- The use of lipid micelles and proteomic analysis allows the identification of the components of the machinery of dentrification in *H. mediterranei*: the four N-reductases, their potential electron donors (as halocyanins or azurins) and the elements that sustain the proton motive force (NADH dehydrogenase, menaquinone and ATP synthase A-type).